

APOSR 70-2892TR

8071-33-F-2

712673

**AN ESTIMATE OF THE CONFIGURATION OF
THE SURFACE OF THE EARTH'S CORE FROM
THE CONSIDERATION OF SURFACE FOCUS
PcP TRAVEL TIMES**

**Supplement to Final Report
1 June 1966 Through 30 May 1970**

**Prepared For
Geophysics Division
Air Force Office of Scientific Research
Arlington, Virginia 22209**

By CHARLES G. BUFE

SEPTEMBER 1970



GEOPHYSICS LABORATORY
Willow Run Laboratories
INSTITUTE OF SCIENCE AND TECHNOLOGY

**Sponsored By
Advanced Research Projects Agency
Nuclear Monitoring Research Office
Project VELA UNIFORM
ARPA Order No. 292, Amendments 32 and 37
Contract AF 49(638)-1759**

This document has been approved for public release and sale; its distribution is unlimited.

111

**BEST
AVAILABLE COPY**

8071-33-F₂

**AN ESTIMATE OF THE CONFIGURATION OF
THE SURFACE OF THE EARTH'S CORE FROM
THE CONSIDERATION OF SURFACE FOCUS
PcP TRAVEL TIMES**

**Supplement to Final Report
1 June 1966 Through 30 May 1970**

**Prepared For
Geophysics Division
Air Force Office of Scientific Research
Arlington, Virginia 22209**

By CHARLES G. BUFE

**Sponsored By
Advanced Research Projects Agency
Nuclear Monitoring Research Office
Project VELA UNIFORM
ARPA Order No. 292, Amendments 32 and 37**

GEOPHYSICS LABORATORY
Willow Run Laboratories
INSTITUTE OF SCIENCE AND TECHNOLOGY
THE UNIVERSITY OF MICHIGAN
Ann Arbor, Michigan

FOREWORD

The research described in this report was conducted by the Geophysics Laboratory of Willow Run Laboratories, a unit of The University of Michigan's Institute of Science and Technology. The work was performed as part of Project VELA UNIFORM, sponsored by the Advanced Research Projects Agency and monitored by the Air Force Office of Scientific Research under Contract No. AF 49(638)-1759. The research extended from 1 June 1966 through 30 May 1970; the Project Scientist is Mr. William J. Best.

The principal investigators for this project were P. Jackson, R. Turpening, and D. Willis. This report was submitted for publication in July 1970. The Willow Run Laboratories' report number is 8071-33-F₂.

PREFACE

The research reported in this paper was conducted at the Geophysics Laboratory of the Institute of Science and Technology, The University of Michigan, under the direction of Dr. James T. Wilson and Dr. David E. Willis.

The unselfish communication of ideas and data by researchers of the Environmental Science Services Administration at San Francisco, Boulder, and Rockville, and of the Lamont-Doherty Geological Observatory is gratefully acknowledged.

The author would also like to thank Professor Henry N. Pollack for his harmonic analysis program and Dr. Philip L. Jackson for the ray traces used in this paper.

This research was supported by the Advanced Research Projects Agency as a part of Project VELA UNIFORM and was monitored by the Air Force Office of Scientific Research under Contract AF49(638)-1759.

ABSTRACT

Travel times of PcP and P phases from nuclear and high explosive sources are interpreted in terms of variations in the radius of the earth's outer core. Travel-time residuals from the Taggart-Engdahl [1968] tables are determined for the PcP-P time interval and for PcP travel times, corrected for station and source terms. The travel times are also corrected for elevation of source and station and ellipticity, excluding the core ellipticity term. This interpretation favors a core which is slightly larger than that of the reference model of Taggart and Engdahl [1968] and which has less ellipticity than estimated by Bullen [1936]. Other interpretations in terms of lateral variation in mantle velocity are also possible.

Because all of the events and most of the stations whose data are used lie in the northern hemisphere, the description of core shape is incomplete and is representative only of regions of the core surface in the vicinity of the PcP reflection points.

The distribution of data does not permit a conventional spherical harmonic analysis of the inferred variation in core radius. A modified spherical harmonic analysis method is devised to smooth the data and to estimate the shape of the core. The variation of core radius determined from this representation is approximately ± 10 kilometers on the basis of terms to degree and order 5. The standard deviation of the data is approximately ± 20 kilometers, indicating the presence of variations of higher degree and order, many of which are probably due to factors other than undulation of the mantle-core boundary. Variations in geoid height resulting from the inferred variation in core radius do not correlate with, but are of the same order of magnitude as, those determined from satellite observations.

Analysis of a limited number of short-period PcP amplitudes shows no significant variation of the PcP amplitude/period ratio with epicentral

distance and an estimated scatter of data on the same order as that found for P in the distance range 70° to 90° . The PcP phase is generally shorter in apparent period than the P phase. This relationship is reversed, however, for arrivals from the Novaya Zemlya event of October 27, 1966.

The PcP amplitude and travel-time variance can be explained, for the most part, in terms of lateral variations in thickness and distribution of crustal and upper mantle velocity zones consistent with the model proposed by Nuttli and Bolt [1969] for northern California.

CONTENTS

	Page
Abstract	iii
Preface	v
List of Tables	vii
List of Figures	viii
List of Appendices	x
Introduction	1
PcP Observations from Zero-Focus Sources	2
Correction for the Earth's Ellipticity	5
Determination of Travel-Time Residuals	11
Estimate of Travel-Time Error	13
Possible Interpretations of Residuals	24
Conversion of Time Residuals to Variations of Outer Core Radius	26
Distribution of PcP Reflection Points	26
Presentation of δr Data	27
Statistical Distribution of $\overline{\delta r}$ Data	33
Harmonic Representation of the $\overline{\delta r}$ Data	33
An Estimate of the Shape of the Core	39
Computation of Geoid Heights	42
Presentation of Amplitude Data	47
A Model Study of Crust and Upper Mantle Effects	49
Summary and Conclusions	57
Recommendations	58
References	60
Appendix 1: Basic Data Listed by Event	63
Appendix 2: Sample Output of Distance Program with Reflection Point and Ellipticity Parameters	82
Appendix 3: Residuals and Reflection Point Coordinates	83

FIGURES

	Page
1. Distribution of zero-focus sources.	4
2. Ray path geometry in an elliptically stratified earth.	6
3. Delay factor, ellipticity correction, and effects.	9
4. Delay factor, elevation correction.	10
5. Delay factor, ellipticity correction, internal.	12
6. P ₂ and PcP arrivals at PG-BC (Longshot) and TRN (Sahara).	14
7. PcP residuals from Taggart-Engdahl tables, United States events.	15
8. PcP residuals from Taggart-Engdahl tables, foreign events.	16
9. PcP residuals after application of source and station corrections, United States events.	17
10. PcP residuals after application of source and station corrections, foreign events.	18
11. PcP-P residuals, United States events.	19
12. PcP-P residuals, foreign events.	20
13. Surface focus events recorded at North American stations on vertical short-period instruments.	23
14. Inverse delay factor, core-mantle boundary.	25
15. Distribution of PcP reflection points, $\Delta \leq 70^\circ$.	28
16. Sectorially averaged δr of core based upon PcP travel times.	29
17. Sectorially averaged δr of core based upon PcP travel times, station and source corrections applied.	30
18. Sectorially averaged δr of core based upon the PcP-P travel-time interval.	31
19. δr based upon PcP-P data, 40° to 90° North Latitude.	32
20. Sectorially averaged $\overline{\delta r}$ of core.	34
21. Histogram of δr of core (1 km intervals).	35
22. $\overline{\delta r}$ from harmonic expansion using coefficient set number 1.	40

	Page
23. $\overline{\delta r}$ from harmonic expansion using coefficient set number 2.	41
24. Geoid heights computed from $\overline{\delta r}$ distribution of Figure 22.	43
25. Geoid heights computed from $\overline{\delta r}$ distribution of Figure 23.	44
26. Geoid heights computed from satellite observations (after Kaula [1966]).	46
27. Variation of vertical A/T of PcP with epicentral distance.	48
28. Variation of vertical A/T of P in the distance range 70° to 105°.	50
29. Vertical PcP/P ratio A/T as a function of epicentral distance.	51
30. Variation of period ratio T_p/T_{pCP} with epicentral distance.	52
31. PcP A/T ratio as a function of $\overline{\delta r}$.	53
32. PcP/P residual of A/T as a function of the PcP-P travel time residual.	54
33. Effect of variations in crust and upper mantle structure on the PcP-P travel time difference.	55
34. Effect of variations in crust and upper mantle structure on the PcP/P vertical component A/T ratio.	56

TABLES

	Page
1. Description of Surface-Focus Events	3
2. Error Estimation, PcP Residuals	21
3. PcP-P Estimate of Error in Travel-Time Residual	21
4. Harmonic Coefficients	38

Introduction

The purpose of this study is to examine the variation in PcP travel times and the PcP-P time interval from zero-focus sources and to estimate on this basis the shape of the core. Because of the distribution of zero-focus sources, the results apply only to the northern hemisphere. The contributions of crust and upper mantle velocity variations to the PcP and PcP-P scatter are assessed, and appropriate corrections applied whenever possible.

Background

A. Vogel [1960] considered the travel time dispersions of the PcP, ScS, PcS, and ScP waves as consequences of a non-uniform reflection depth. Using data from earthquake sources, he interpreted travel time anomalies as corresponding to variations of more than ± 200 kilometers in the depth to the core-mantle boundary. The geographical pattern of core depths was found to differ for the periods 1948-1954, and 1930-1936. He also found correlation of the core depth anomalies with those of the earth's gravity and magnetic fields. Egyed [1964] accounted for the amplitude of the undulations of Izsak's [1964] satellite geoid in terms of the density contrast of a sphere of 200 km diameter situated at the core-mantle boundary.

The present study differs from that of Vogel in several important ways:

1. Only surface-focus (nuclear or high explosive) events are used.
2. In each case the zero time is either known or is assumed by adjusting the computed zero times based on the Jeffreys-Bullen surface-focus times by a regional correction. The adjusted times indicate that the shots were fired on or within a fraction of a second of an exact minute; hence in most cases the unknown origin times are assumed to be exactly on the minute.
3. Epicenter locations used in this study are either known a priori or have been determined with an accuracy unattainable a few years ago.
4. Depth phases are not present, eliminating a number of

arrivals which, at certain distances, could be confused with core phases.

5. Only PcP and P travel times from short-period instruments are used.

PcP Observations from Zero-Focus Sources

The data used in this study represent all available PcP readings from zero-focus events that are known to the author. To avoid the redundancy inherent in using all available data from NTS sources, only the Bilby and Faultless data are included. The source regions and events used are described in Table 1 and shown in Figure 1. Data are included from many recording sites, including U.S.C.&G.S., U.S.G.S., AFTAC stations, LASA, and a number of independent university or foreign government-operated stations. Epicentral distances for the PcP observations range from 15° to 85°. Published, bulletin, or listed arrivals identified as PcP have been accepted as such and included in the analysis unless inspection of the record by the author or others has shown this to be incorrect. In some cases unidentified arrivals or misidentified arrivals are included when the travel time indicates the phase should be PcP.

Data from western Pacific sources were obtained from Kogan [1960], Carder [1964], Carder [1968], and Doyle and Webb [1958]. Buchbinder [1965] and Jordan [1968] supplied the Bilby and Faultless data respectively. Longshot data were from Carder, et al. [1967], Buchbinder [1968a], Taggart and Engdahl [1968], Clark [1966a], Bufe and Willis [1969], and others. CHASE III and IV arrivals are from Buchbinder [1969], Clark [1965], Clark [1966b], and from the ESSA Earthquake Data Reports. The travel times for the Sahara event were read by the author from records of the ESSA worldwide net. Semipalatinsk and Novaya Zemlya data are from Jordan [1968], from B.C.I.S., ESSA, and LASA bulletins, and from the author's readings. All PcP travel times used are tabulated in Appendix 1, where the sources of data are referenced in detail. Readings made or verified by the author are indicated by an asterisk. Arrivals determined by the author have been subjected to several criteria, which follow.

1. Arrival should be distinct from surrounding microseismic background and P coda.
2. Generally PcP will be equal to or higher than P in frequency

Table 1. Description of Surface-Focus Events

<u>Source Region</u>	<u>Event</u>	<u>Date</u>	<u>Zero Time</u>	<u>Latitude</u>	<u>Longitude</u>
Western Pacific	Bravo	02/28/54	18:45:00.0	11°41'28"N	165°16'23"E
	Romeo	03/26/54	18:30:00.4	11°41'28"N	165°16'23"E
	Navajo	07/10/56	17:56:00.3	11°39'48"N	165°23'14"E
	Koa	05/12/58	18:30:00.1	11°40'30"N	162°12'20"E
	Oak	06/28/58	19:30:00.1	11°36'28"N	162°06'28"E
	Poplar	07/12/58	03:30:00.1	11°41'17"N	165°15'52"E
Nevada Test Site	Bilby	09/13/63	17:00:00.1	37°03'38"N	116°01'18"W
	Faultless	01/19/68	18:15:00.0	38°38'02"N	116°12'54"W
Aleutian Chain	Long Shot	10/29/65	21:00:00.1	51°26'17.3"N	179°10'57.2"E
East Coast U.S.	CHASE III	07/15/65	14:16:08.1	37°11'48"N	74°21'06"W
	CHASE IV	09/16/65	19:51:10.2	37°11'34"N	74°26'34"W
Sahara		02/27/65	11:30:00.0*	24.04°N	05.01°E
Novaya Zemlya ¹		10/27/66	05:58:00.0*	73.40°N	54.87°E
		11/07/68	10:02:07.1*	73.40°N	54.87°E
Semipalatinsk		01/15/65	06:00:00.0*	49.92°N	78.92°E
		02/13/66	04:58:00.0*	49.83°N	78.09°E
		02/26/67	03:58:00.0*	49.84°N	78.05°E

*Time is estimated.

¹The Novaya Zemlya events were apparently not fired on the exact minute. The zero time for the event of 11/07/68 was determined from P wave travel times to stations which also recorded the event of 10/27/66. Computation of a +0.5 second travel time residual for P waves in a region characterized by negative residuals indicates zero times nearly one second later than those shown above for the Novaya Zemlya events.

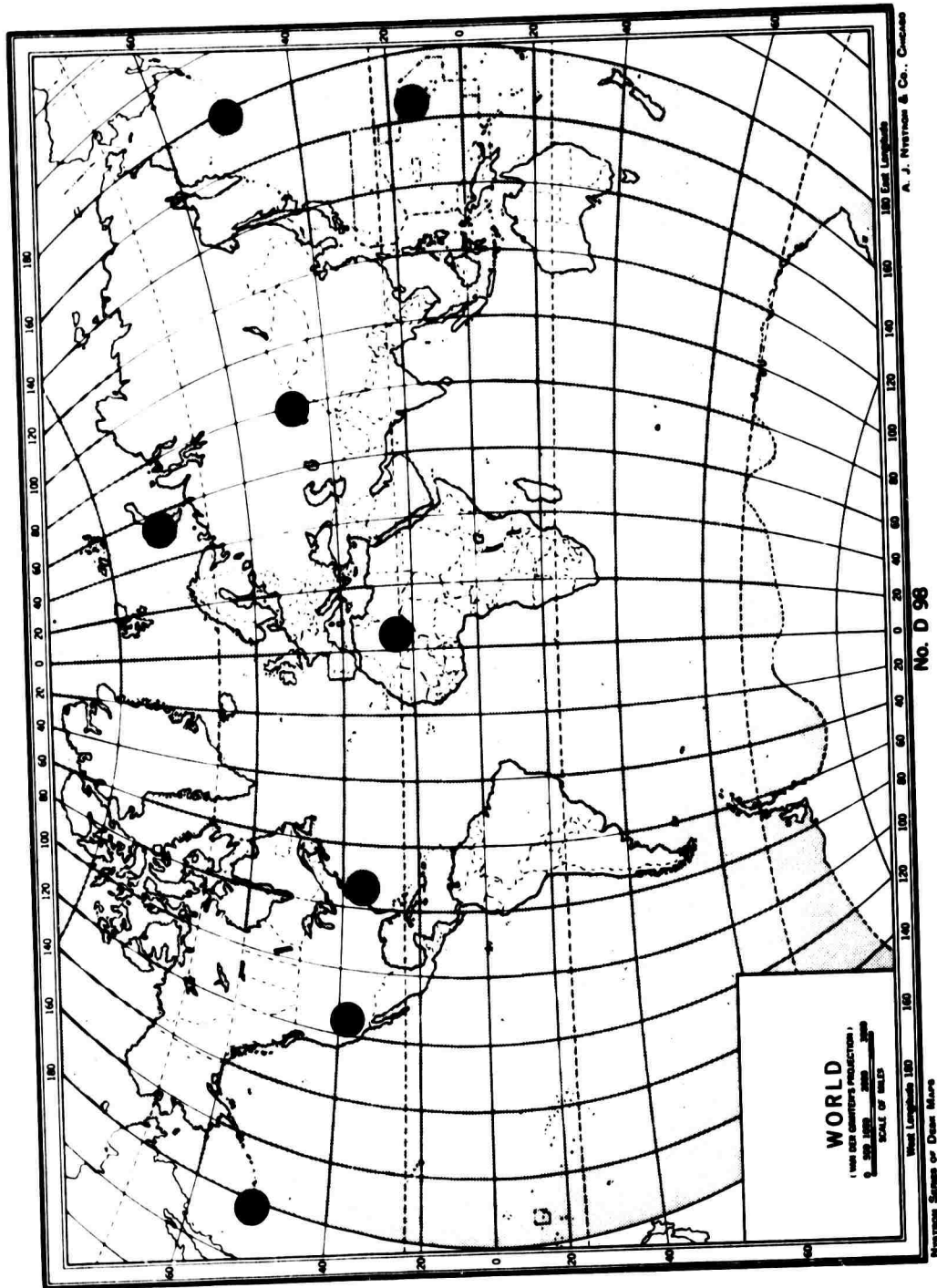


FIGURE 1. DISTRIBUTION OF ZERO-FOCUS SOURCES.

at distances greater than 30° . This relationship has been noted by Kogan [1968] and is explained by Kanamori [1967] in terms of attenuation characteristics in the mantle. Arrivals from the Novaya Zemlya event of 10/27/66 are exceptions to this rule.

3. At epicentral distances greater than about 30° , the waveforms of PcP and P should be similar, such that the PcP-P time interval could be determined by auto-correlation. Spectral analyses by Kanamori [1967] and Buchbinder [1969] have shown this to be true.

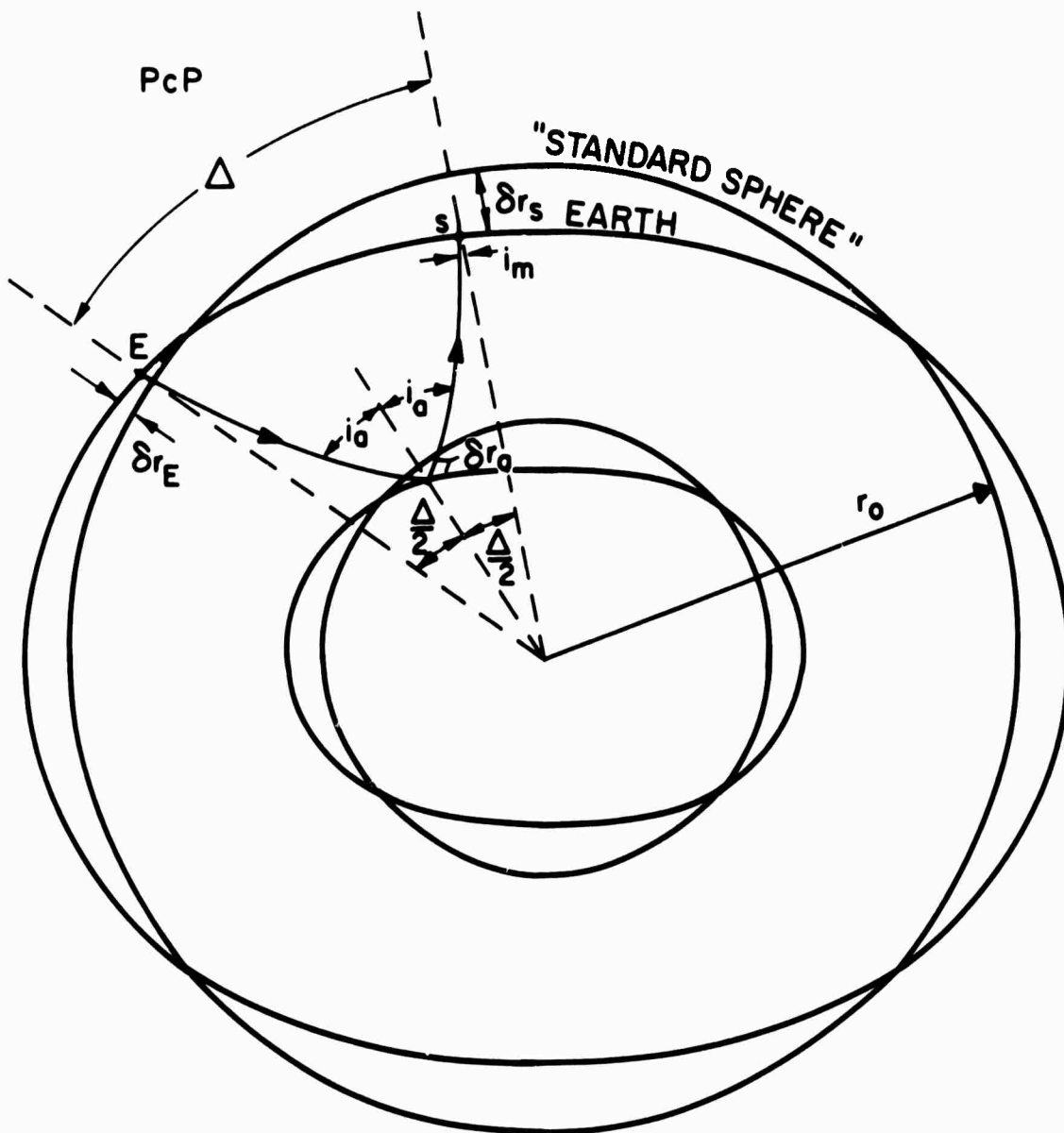
4. In many instances for stations at the shorter epicentral distances both horizontal and vertical component seismograms were scanned. The ratio of vertical to horizontal amplitudes should be larger for PcP than for P.

Since many of the arrivals selected by the author did not meet all of these criteria and the reliability of the bulletin data in this respect is unknown, no attempt was made to assign weights to readings on this basis.

Correction for the Earth's Ellipticity

Jeffreys [1935] described the effect of the earth's ellipticity on the travel times of seismic body waves. The ellipticity correction for P or S waves involves terms dependent upon the ellipticity of the earth's outer surface and the latitudes of source and station and upon the ellipticities of internal strata of equal velocity along the ray path. Bullen [1936] assumed hydrostatic conditions to apply within the earth and calculated the variation of density with depth on the basis of the velocities of P and S waves. The ellipticities of internal strata of equal density were then computed, ranging from 0.00337 at the earth's surface to 0.00256 at its center.

The ellipticity correction to the PcP travel time can be considered as four separate terms with geometry as illustrated in Figure 2. Jeffreys [1935] has shown that, to the first order in $\frac{\delta r}{r}$, the difference between the actual travel time of the P or S ray between source and station and the time between the two corresponding points on the surface of the standard sphere, is given by



NOTE: Ellipticity Greatly Exaggerated.

FIGURE 2. RAY PATH GEOMETRY IN AN ELLIPTICALLY STRATIFIED EARTH.

$$(T'-T)_{P \text{ or } S} = p \left[\frac{1}{r^2} \frac{dr}{d\theta} \delta r \right]_0^{\Delta} + p \int_0^{\Delta} \delta r \left[\frac{d^2 \frac{1}{r}}{d\theta^2} + \frac{1}{r} \right] d\theta \quad (1)$$

where p is the ray parameter defined at any point on the ray path as

$$p = \frac{r^2}{v} \frac{d\theta}{ds}, \quad v \text{ is the local wave velocity, and} \quad (2)$$

r is the distance of the point from the center of the earth. Considering the PcP ray path in two segments, source to core and core to station, each segment subtending a central angle $\Delta/2$, the above expression becomes

$$(T'-T) = p \left[\frac{1}{r^2} \frac{dr}{d\theta} \delta r \right]_0^{\frac{\Delta}{2}} + p \left[\frac{1}{r^2} \frac{dr}{d\theta} \delta r \right]_{\frac{\Delta}{2}}^{\Delta} + p \int_0^{\frac{\Delta}{2}} r \left[\frac{d^2 \frac{1}{r}}{d\theta^2} + \frac{1}{r} \right] d\theta + p \int_{\frac{\Delta}{2}}^{\Delta} \delta r \left[\frac{d^2 \frac{1}{r}}{d\theta^2} + \frac{1}{r} \right] d\theta. \quad (3)$$

The first two terms of (3) represent the "end effects" portion of the ellipticity correction. By (2), they can be written

$$\left[\frac{1}{v} \frac{dr}{ds} \delta r \right]_0^{\frac{\Delta}{2}} + \left[\frac{1}{v} \frac{dr}{ds} \delta r \right]_{\frac{\Delta}{2}}^{\Delta}. \quad (4)$$

Since $\frac{dr}{ds}$ is negative on the down path (source to core), (4) can be written

$$\left[\frac{1}{v} \left| \frac{dr}{ds} \right| \delta r \right]_{\Delta} - 2 \left[\frac{1}{v} \left| \frac{dr}{ds} \right| \delta r \right]_{\frac{\Delta}{2}} + \left[\frac{1}{v} \left| \frac{dr}{ds} \right| \delta r \right]_0 \quad (5)$$

or

$$\left[\frac{\cos i}{v} \delta r \right]_{\text{station}} - 2 \left[\frac{\cos i}{v} \delta r \right]_{\text{mantle-core boundary}} + \left[\frac{\cos i}{v} \delta r \right]_{\text{source}}. \quad (6)$$

This is the standard "delay time" format often used in refraction studies and in applying elevation corrections to seismic travel times. The second term of (6) has been excluded from the ellipticity corrections applied in this work, since it is δr at the core-mantle boundary which we wish to determine, i.e., for the purpose of computing ellipticity corrections, the core is assumed to be spherical.

Thus the "end effects" portion of the ellipticity correction is reduced to the source and station terms of (6), which can be simplified to

$$\left[\frac{\cos i}{v} \right]_{\text{base of crust}} \cdot (\delta r_{\text{source}} + \delta r_{\text{station}}), \text{ assuming} \quad (7)$$

similar conditions at opposite ends of the ray path.

The path difference is assumed to occur in the upper mantle. The factor $\cos i/v$ at the base of the crust has been evaluated as a function of epicentral distance for PcP and is plotted in Figure 3. Angle of incidence was determined from the relationship

$$\sin i = \frac{v}{r} \frac{\delta t}{\delta \theta} \quad (8)$$

assuming a sub-crustal velocity of 8.1 km/sec. The values of $\delta t/\delta \theta$ were taken from Taggart and Engdahl's [1968] PcP travel-time tables.

The δr values in equation (7) are functions of the latitude of the source or station and the ellipticity of the earth's surface. In general, from the definition of the standard sphere

$$\delta r = \epsilon r S_2 \quad (9)$$

where ϵ is the ellipticity and S_2 is the surface harmonic, $S_2 = \frac{1}{3} - \cos^2 \phi$, where ϕ is the geocentric colatitude. The δr sum was computed for each source-station combination and used in conjunction with Figure 3 and Eq. (7) to compute the "end effects" portion of the ellipticity correction. Elevation corrections were applied in the same manner, assuming a crustal velocity of 6.0 km/sec and $\cos i/v$ versus epicentral distance as plotted in Figure 4.

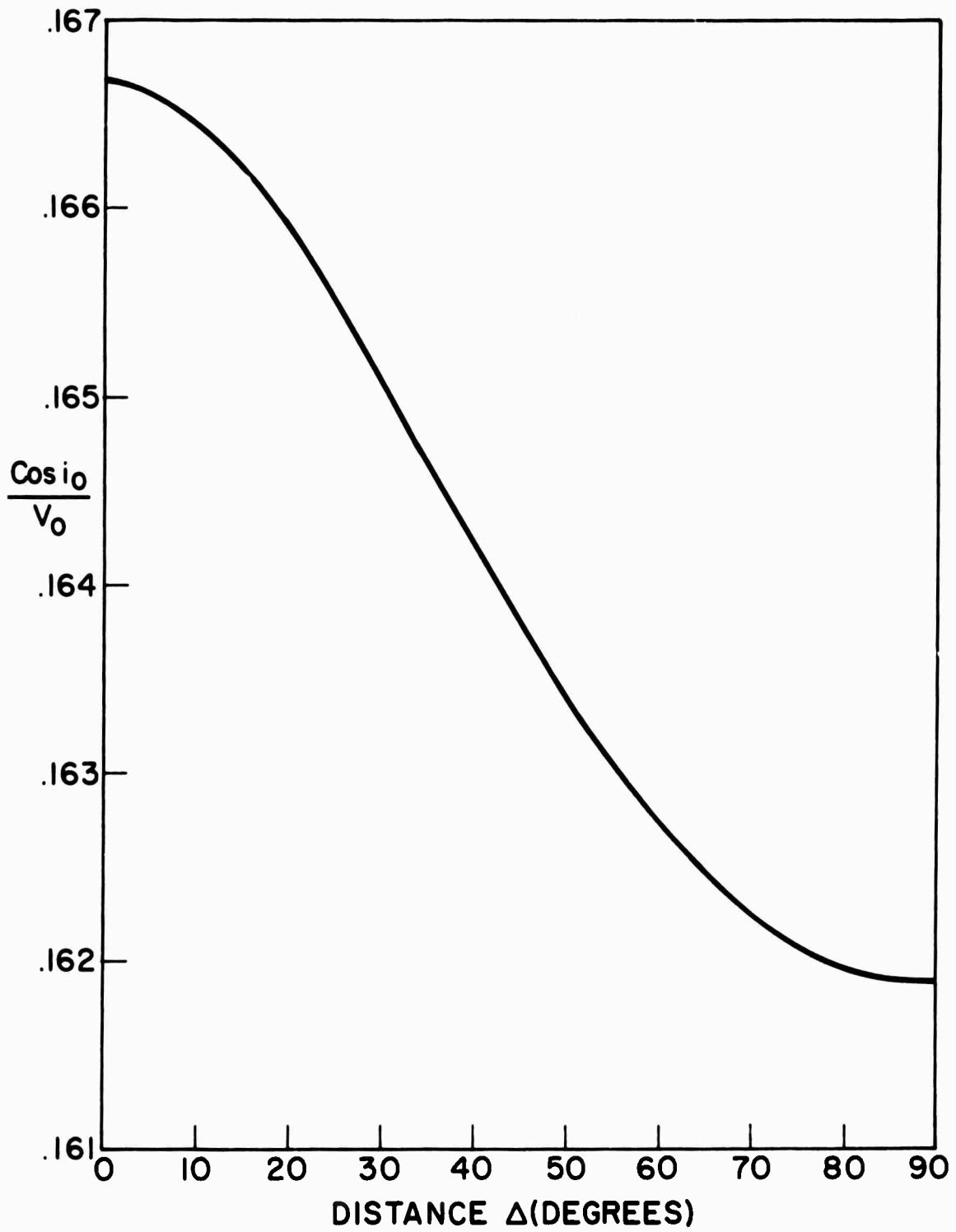


FIGURE 3. DELAY FACTOR, ELLIPTICITY CORRECTION, END EFFECTS.

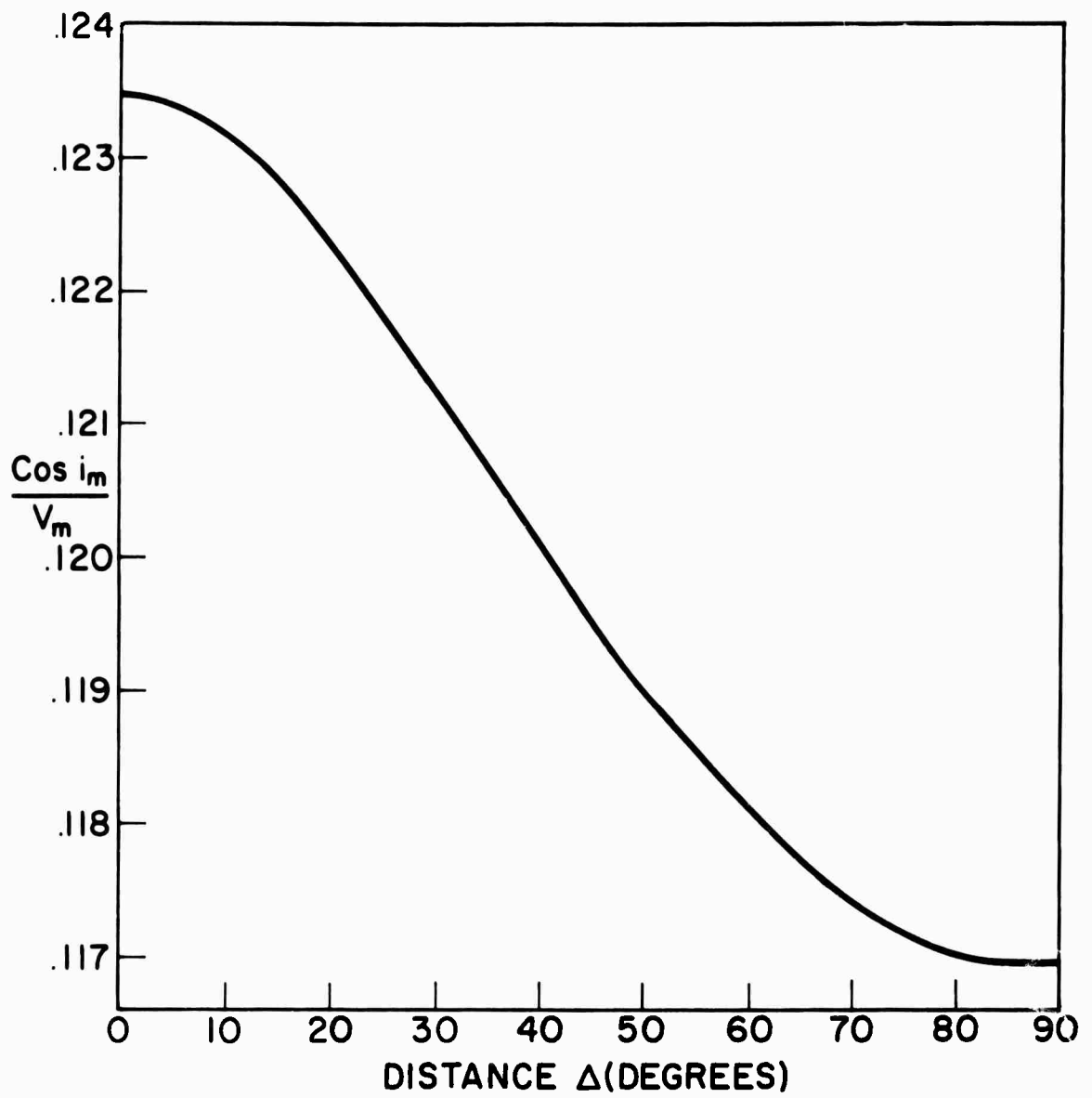


FIGURE 4. DELAY FACTOR, ELEVATION CORRECTION.

The integral terms of (3) represent the part of the correction due to the ellipticity of internal strata along the ray path. Bullen [1938], using his [1936] values of ellipticity of internal strata, has shown that this expression can, subject to errors not exceeding 0.1 second, be put in the form $f_1(\frac{\Delta}{2})(S_0 + \frac{2}{5} S_a + S_1)$, where S_0 and S_1 are the values of the surface harmonic S_2 at the epicenter and observatory respectively, and S_a the value at the point of reflection on the core-mantle boundary. Bullen's computed values of $f_1(\frac{\Delta}{2})$ are plotted as a function of Δ in Figure 5.

Bullen's [1936] values of core radius and core ellipticity are involved in this approximation, but because of the integral nature of this term, perturbations of the core radius and ellipticity of the order encountered in this study would not significantly change the correction. The term $(S_0 + \frac{2}{5} S_a + S_1)$ was computed for each epicenter and station combination and used in conjunction with the curve of Figure 5 to compute the correction due to the ellipticity of internal strata. The summed ellipticity corrections were then combined with elevation corrections for each source and station combination, applied to the observed travel times, and the resulting corrected travel times compiled in Appendix 1. Care was taken in computing the ellipticity correction to avoid the introduction of systematic errors which would affect the determination of the core's shape.

Determination of Travel-Time Residuals

The datum chosen for this study is that of Taggart and Engdahl [1968], whose curve is based on the model of Herrin, et al. [1968] and a core depth determined from zero-focus PcP travel times. Residuals from the Taggart-Engdahl tables were determined for the corrected travel times. Another set of residuals was determined by applying station and source corrections. These were applied in the same manner used by Taggart and Engdahl [1968], assuming nearly vertical incidence and neglecting azimuthal terms. Station and source corrections with appropriate datum adjustments were taken from Herrin and Taggart [1968], Cleary and Hales [1966], Carder, Gordon, and Jordan [1966], estimated from Figure 2 of Toksöz and Arkani Hamed [1967], or determined by the writer. It was hoped that the

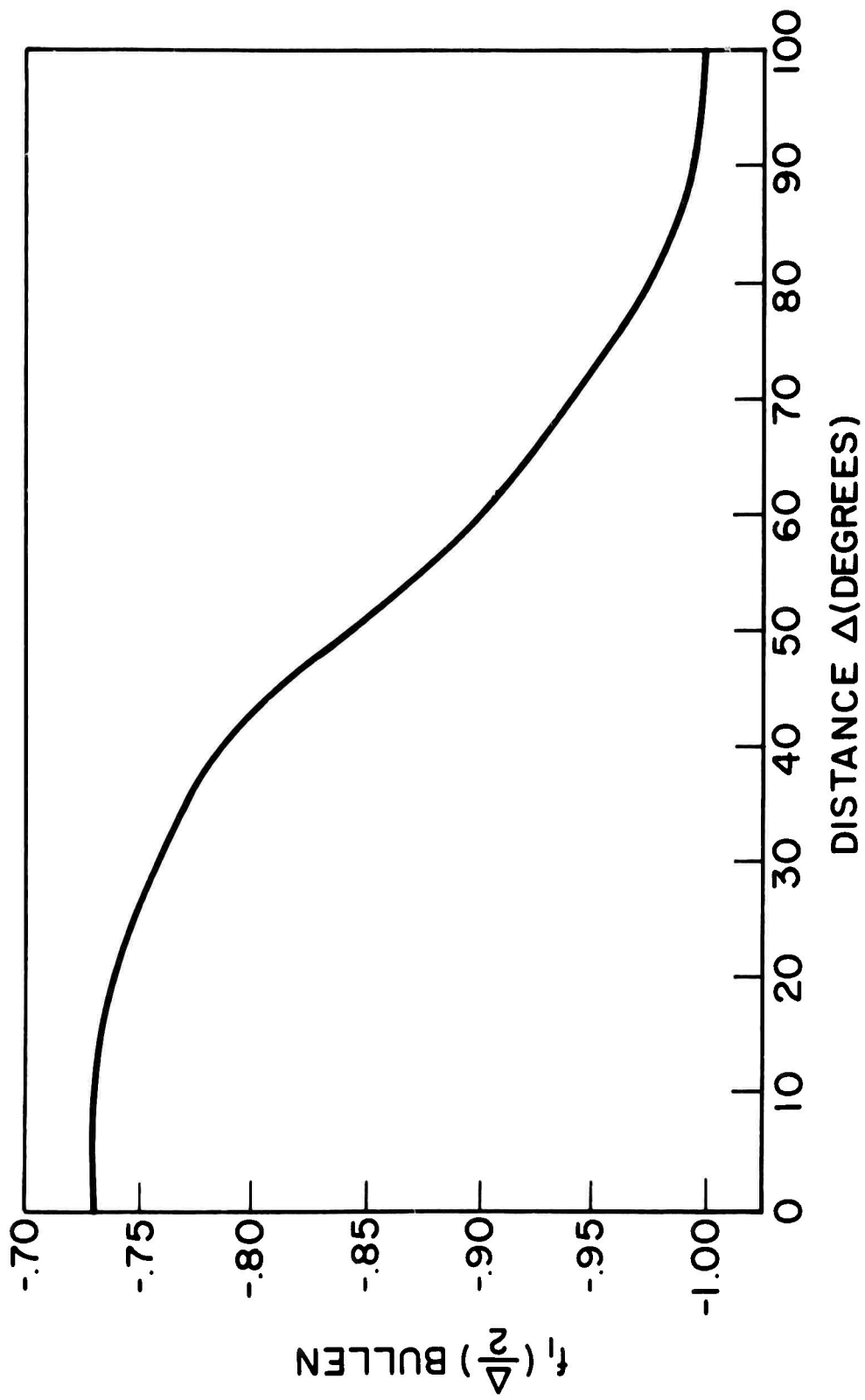


FIGURE 5. DELAY FACTOR, ELLIPTICITY CORRECTION, INTERNAL.

scatter due to heterogeneity of the crust and upper mantle would be reduced by the application of these corrections. Another possible method of accomplishing this is by the use of the PcP-P time interval, the method used by Vogel [1960]. The use of PcP-P has many advantages and a few disadvantages. At distances beyond about 35° the paths of P and PcP through the crust and upper mantle are close enough together to produce near cancellation of station and source effects for the two phases in most cases. Errors in station time or origin time will not affect PcP-P. On the negative side, variations in compressional wave velocity near the "bottom" of the P ray path would produce P-wave travel-time anomalies but would have little effect on PcP, thus changing the PcP-P interval. In addition, while P is normally a stronger phase than PcP, there are some instances where the onset of PcP is more sharply defined than that of P. Two such examples are shown in Figure 6.

In order to determine the PcP-P arrival-time interval, P-wave travel times as read and corrected for ellipticity and elevation, have been tabulated with the PcP times and are included in Appendix 1. Residuals from the Taggart-Engdahl [1968] PcP-P table have been calculated, with corrections applied for ellipticity and elevation.

The three sets of residuals described above are tabulated in Appendix 3 and are shown as functions of epicentral distance in Figures 7 through 12. Figures 7 and 8 show PcP residuals, corrected for ellipticity and elevation only, for U. S. events and for foreign events, respectively. Figures 9 and 10 are the same presentations with additional source and station corrections applied to the residuals. PcP-P residuals are shown in Figure 11 for U.S. explosive sources, and in Figure 12 for foreign events.

Estimate of Travel-Time Error

There are several sources of errors which will affect the PcP travel-time residual determinations. These errors are of two types; those which can be estimated, and those which cannot. The first class are listed below in Tables 2 for PcP residuals and 3 for PcP-P, with estimates of their magnitudes. Error estimates are considered for two ranges of epicentral distance ($<45^\circ$ and $>45^\circ$) and source areas are classified according to the believed accuracy of zero time and epicenter location.

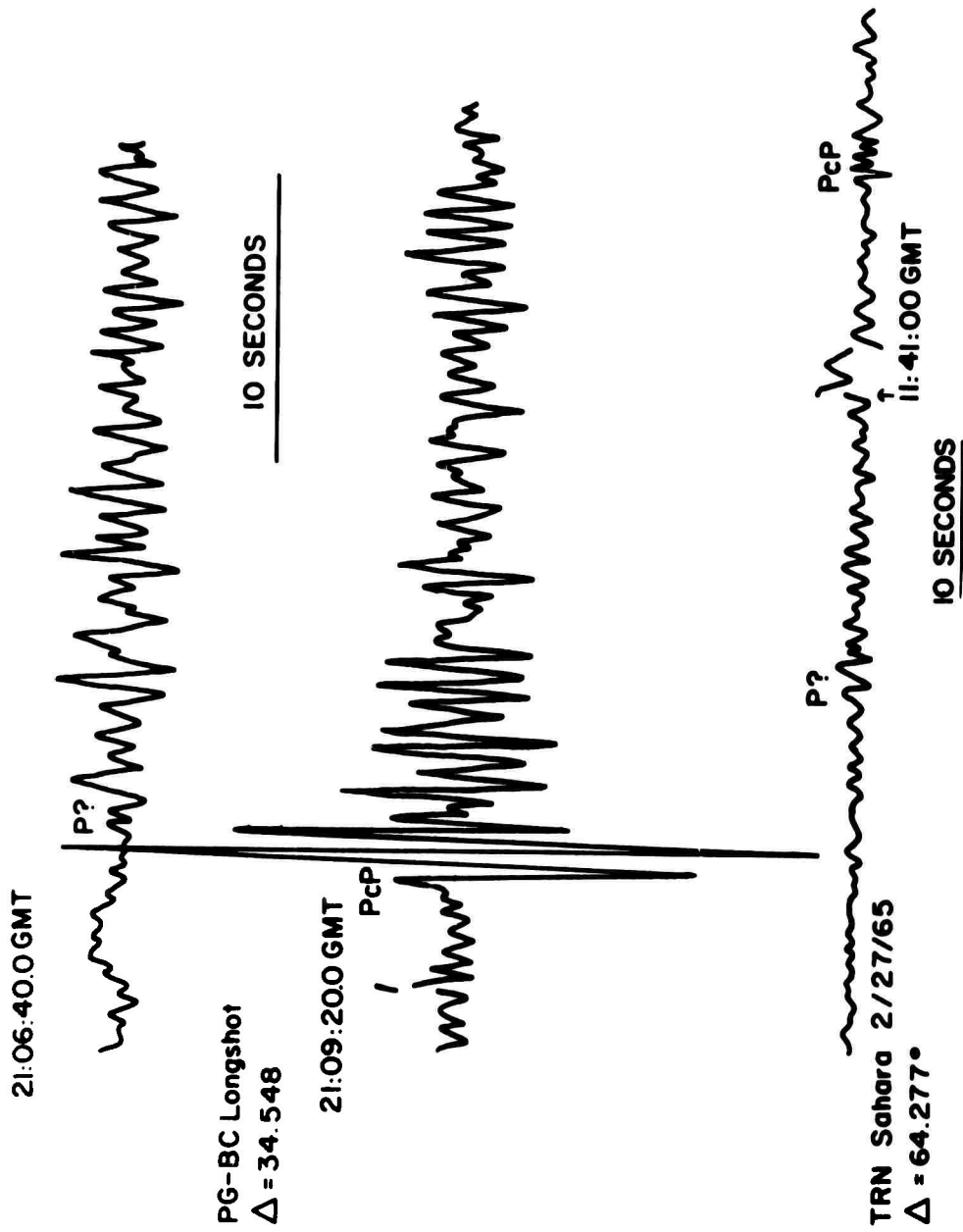


FIGURE 6. P? AND PcP ARRIVALS AT PG-BC (LONGSHOT) AND TRN (SAHARA).

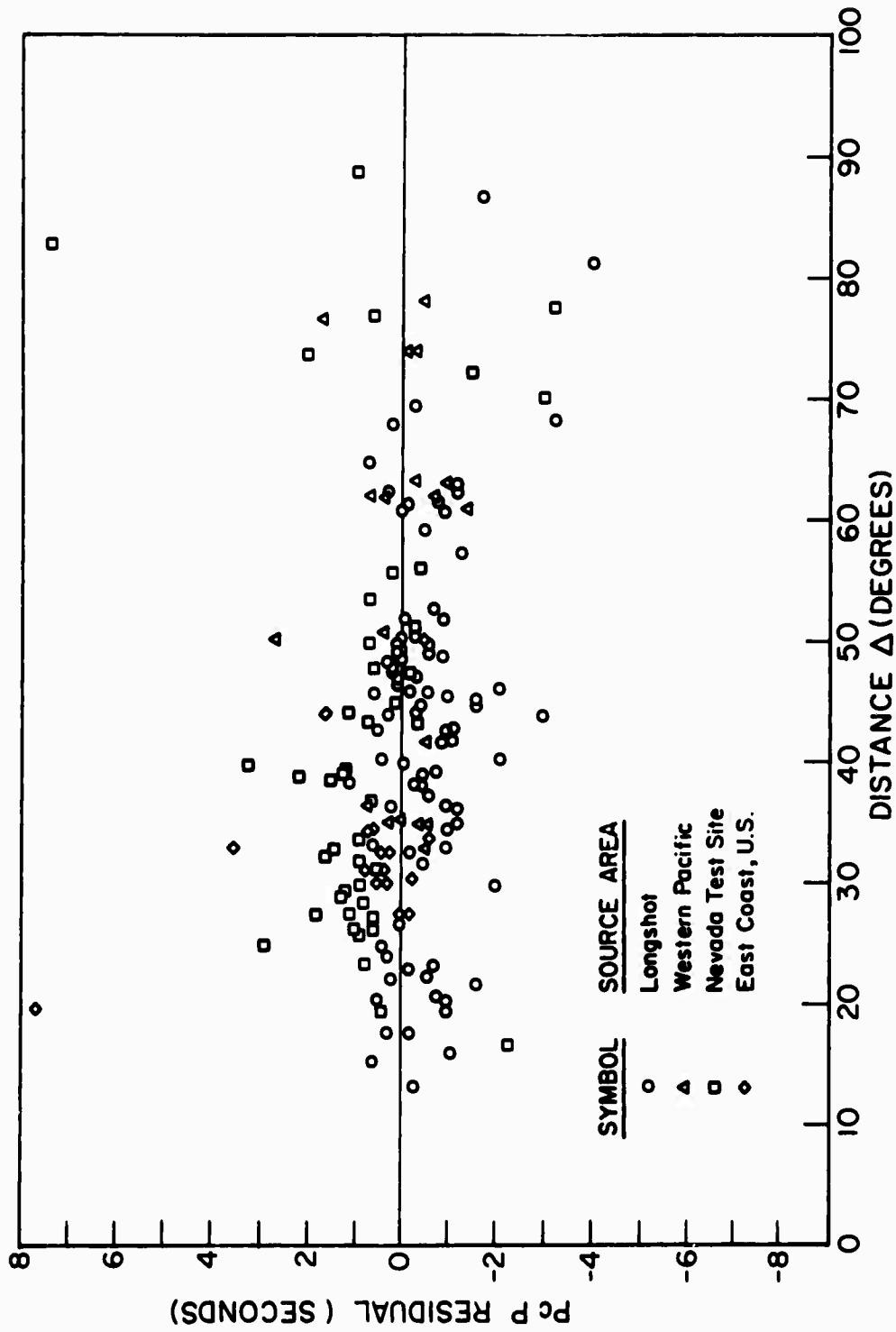


FIGURE 7. PcP RESIDUALS FROM TAGGART-ENGDAHL TABLES, UNITED STATES EVENTS.

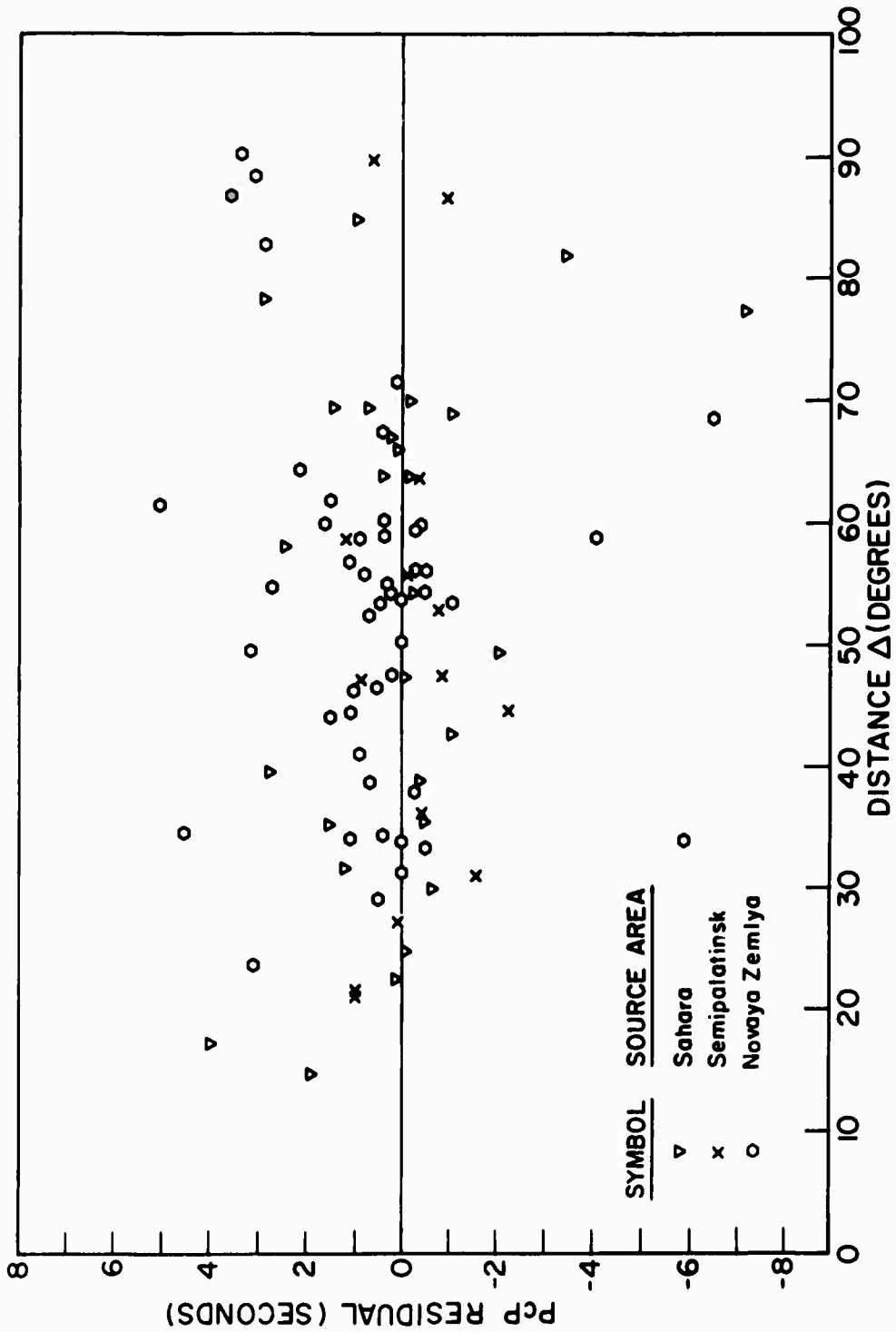


FIGURE 8. PcP RESIDUALS FROM TAGGART-ENGDahl TABLES, FOREIGN EVENTS.

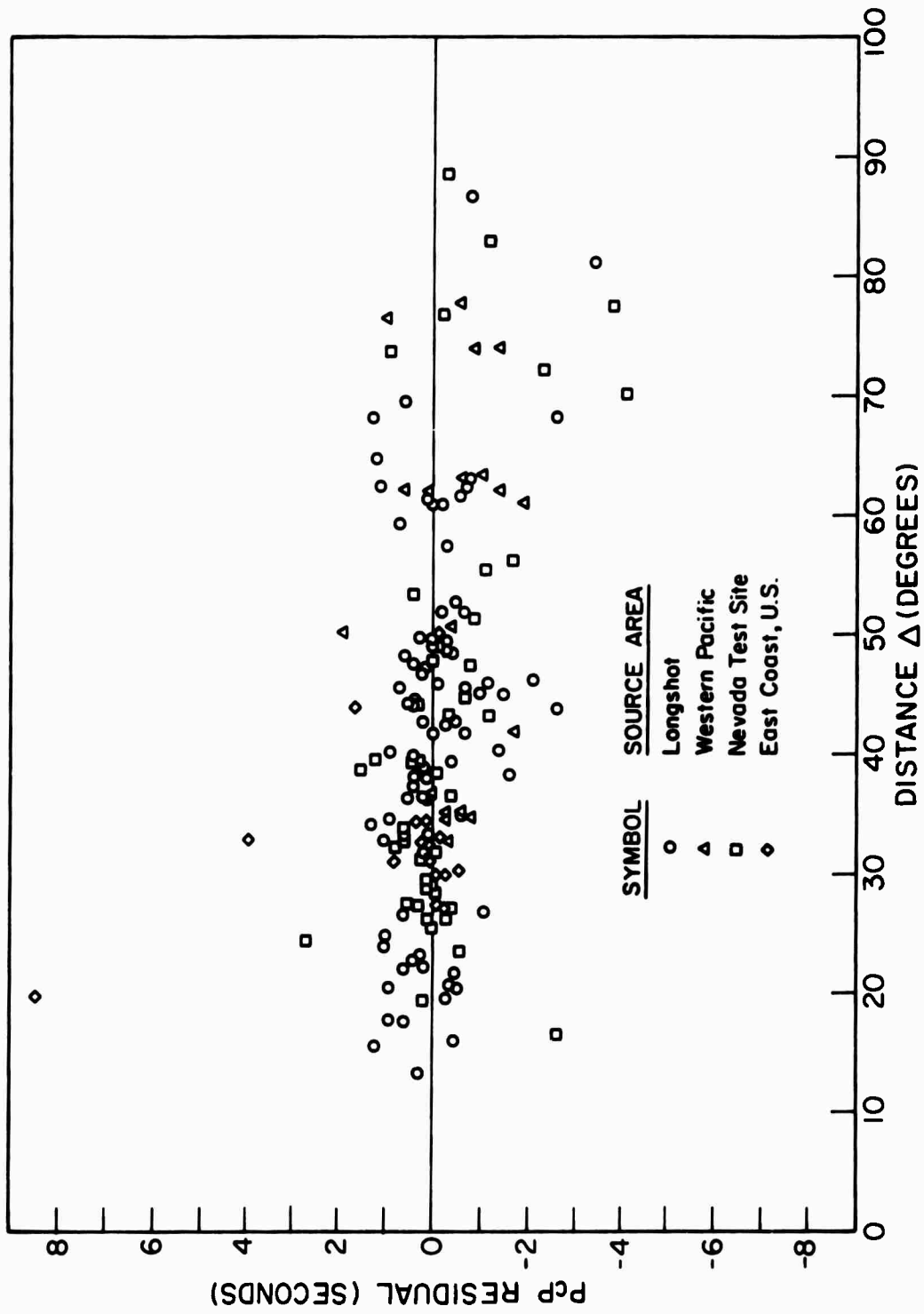


FIGURE 9. PcP RESIDUALS AFTER APPLICATION OF SOURCE AND STATION CORRECTIONS, UNITED STATES EVENTS.

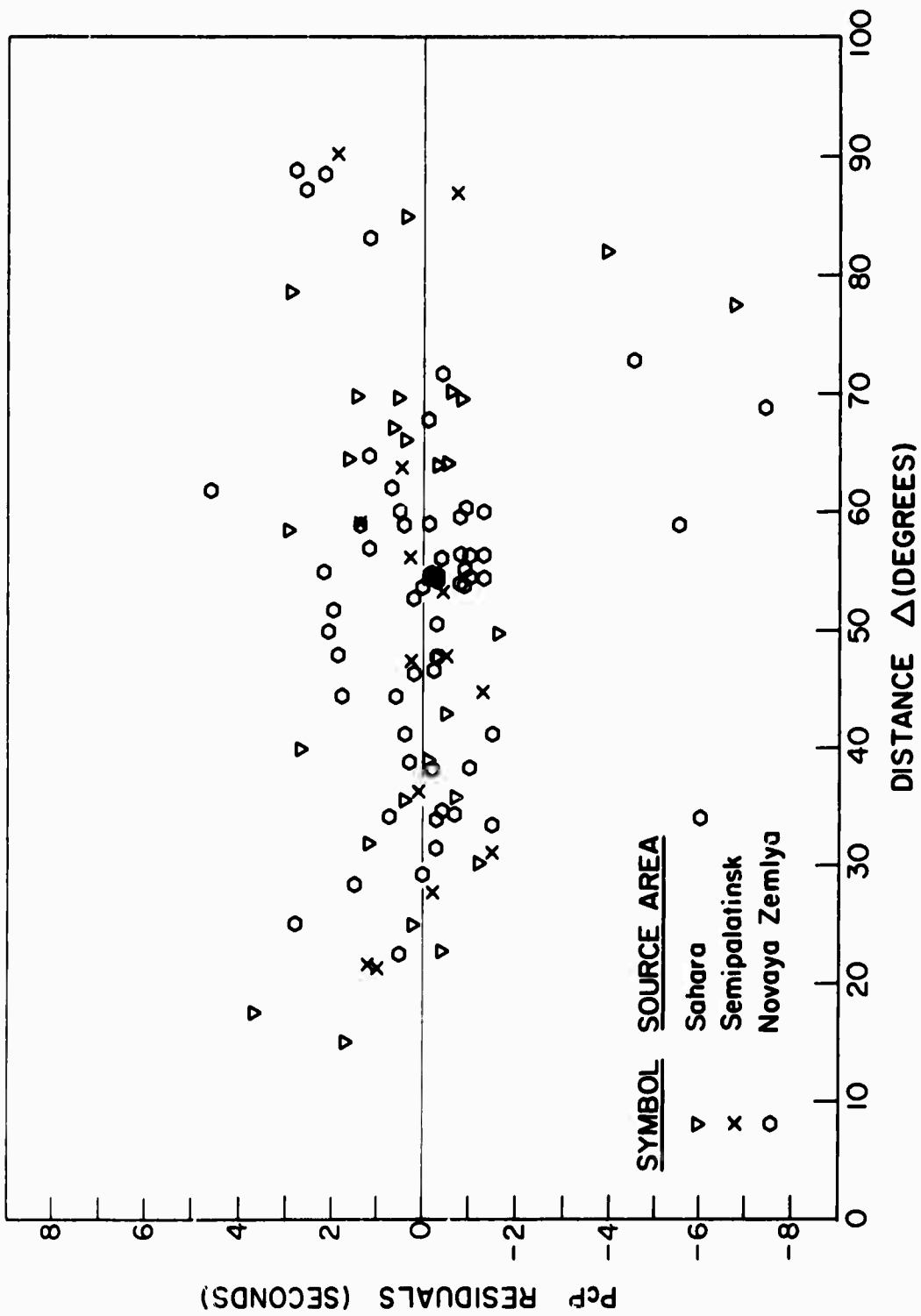


FIGURE 10. PcP RESIDUALS AFTER APPLICATION OF SOURCE AND STATION CORRECTIONS, FOREIGN EVENT

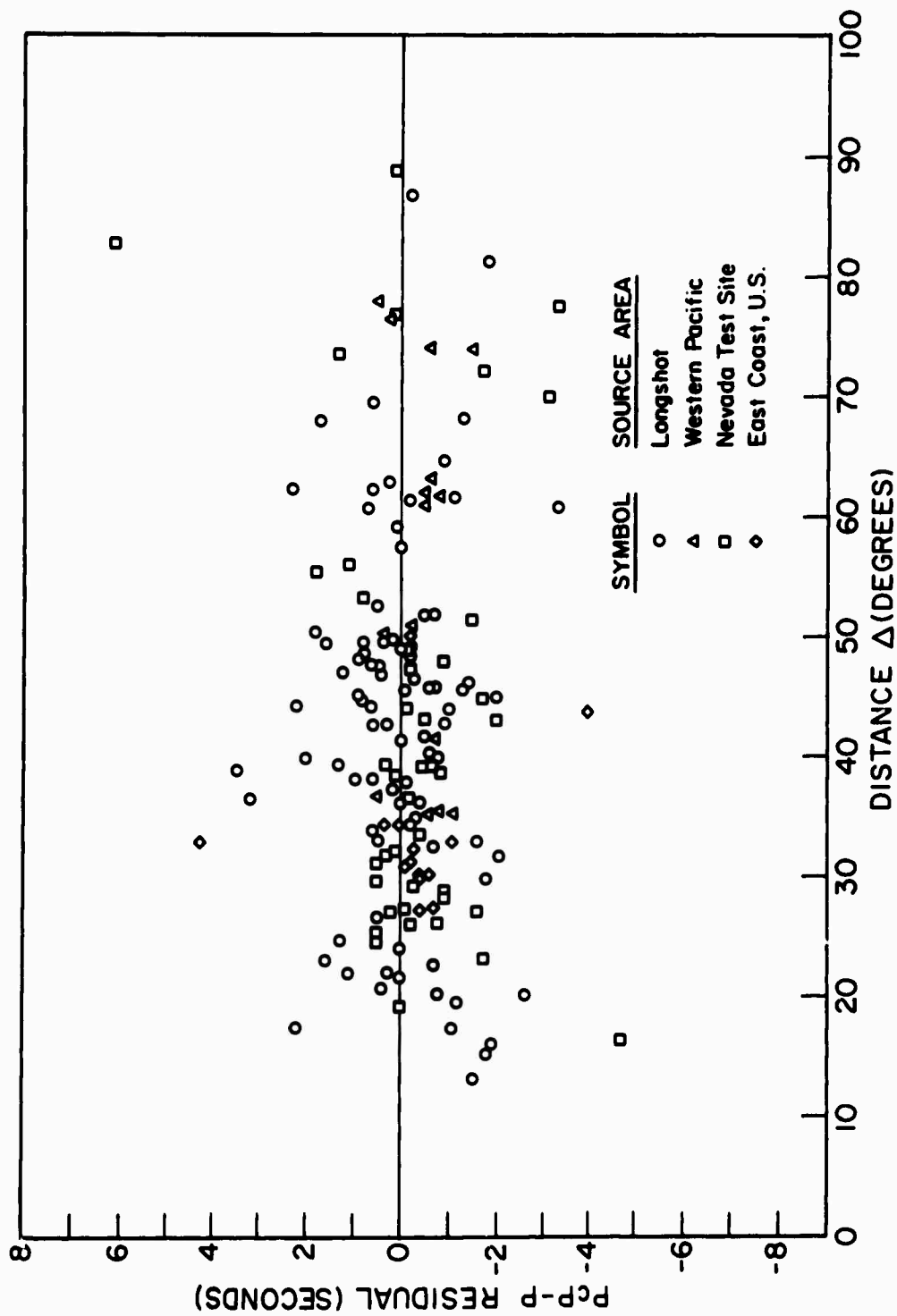


FIGURE 11. PcP-P RESIDUALS, UNITED STATES EVENTS.

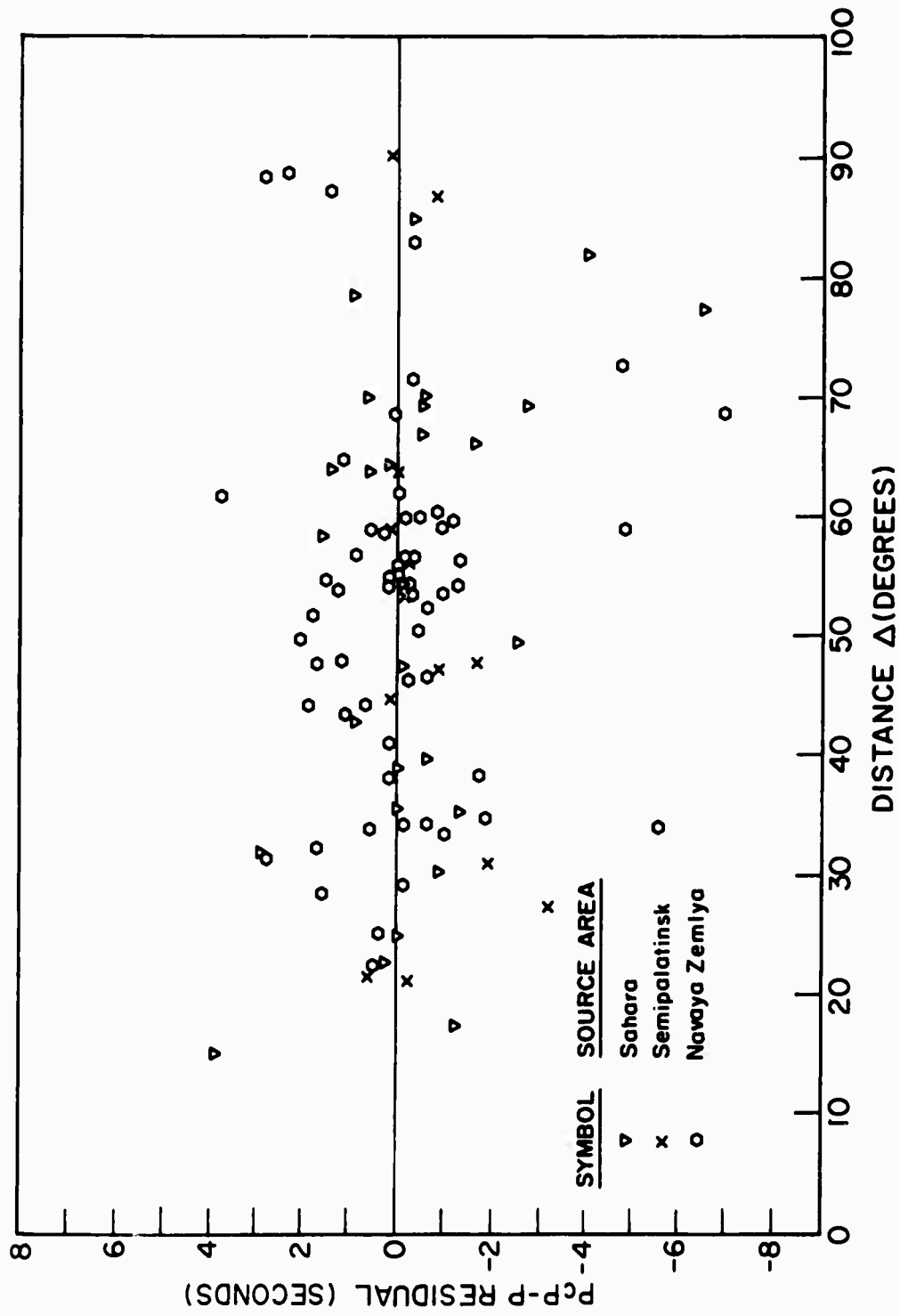


FIGURE 12. PcP-P RESIDUALS, FOREIGN EVENTS.

Table 2. Error Estimation, PcP Residuals

<u>Type of Error</u>	<u>Distance Range</u>	<u>Error in Seconds for Event</u>		
		<u>U.S.</u>	<u>French</u>	<u>Russian</u>
1. Epicenter Location	$\Delta < 45^\circ$	--	$\pm .1$	$\pm .2$
	$\Delta > 45^\circ$	--	$\pm .2$	$\pm .4$
2. Zero Time		--	$\pm .2$	$\pm .3$
3. Station Time		± 0.1	± 0.1	± 0.1
4. Error in Scaling Time of PcP from Record		± 0.2	± 0.2	± 0.2
Estimate of Mean	$\Delta < 45^\circ$	± 0.2	± 0.3	± 0.4
Error Sum	$\Delta > 45^\circ$	± 0.2	± 0.4	± 0.5

Table 3. PcP-P

Estimate of Error in Travel-Time Residual

<u>Type of Error</u>	<u>Distance Range</u>	<u>Error in Seconds for Event</u>		
		<u>U.S.</u>	<u>French</u>	<u>Russian</u>
1. Epicenter Location	$\Delta < 45^\circ$	negligible	$\pm .3$	$\pm .5$
	$\Delta > 45^\circ$	negligible	$\pm .1$	$\pm .2$
2. Zero Time	All	no effect	-----	
3. Station Time	All	no effect	-----	
4. Error in Scaling Time of PcP from Record		± 0.2	± 0.2	± 0.2
5. Error in Scaling Time of P from Record		± 0.1	± 0.1	± 0.1
Estimate of Mean	$\Delta < 45^\circ$	± 0.2	± 0.4	± 0.5
Error Sum	$\Delta > 45^\circ$	± 0.2	± 0.2	± 0.3

Estimates of mean error sum are determined using the method of random vector addition:

$$\text{Mean Error Sum} = \sqrt{E_1^2 + E_2^2 + E_3^2 + E_4^2 + E_5^2}$$

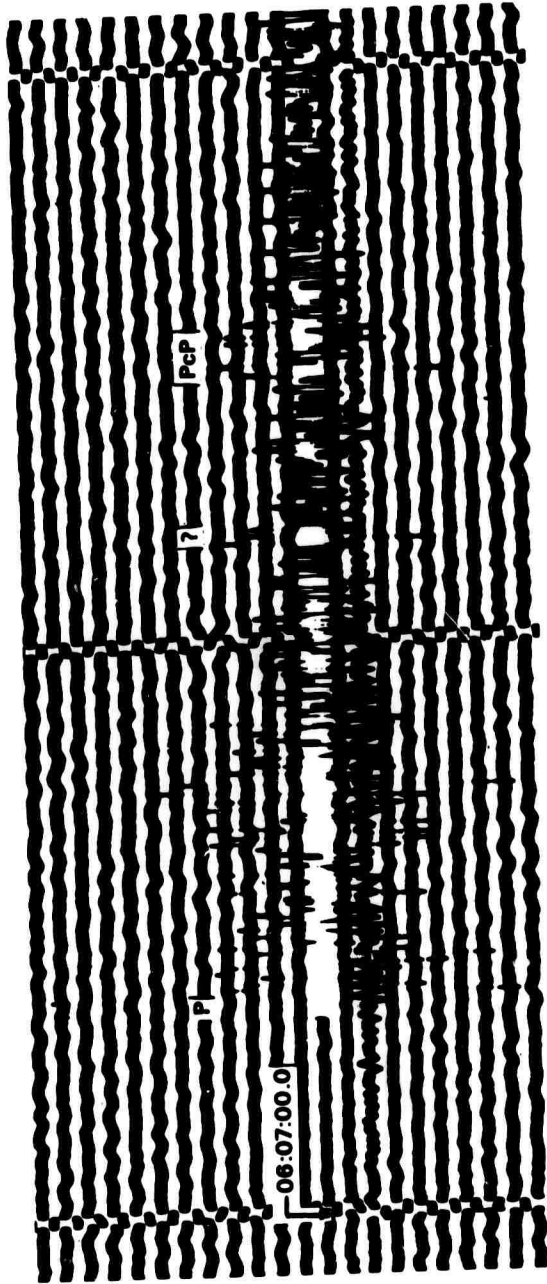
From Tables 2 and 3 it is seen that the sources of error in the PcP residuals are somewhat different from those involving PcP-P residuals. For instance, the error due to an incorrect epicenter location will be more pronounced at short distances for PcP-P and at long distances for PcP residuals

The second class of error cannot be measured or predicted with any degree of certainty, and involves mis-identification of arrivals or failure to select the "first break" of PcP.

In regard to the first possibility, there is often a tendency to "seek out" a PcP by selecting the strongest arrival nearest the predicted PcP time. If the author's criteria for PcP discussed earlier are not heeded, and sometimes even if they are heeded, mis-identification is a distinct possibility. The primary problem here is that the assumption that a readable PcP phase must be present somewhere on the seismogram is incorrect. It has been shown (see Carder, 1964) that PcP is a "will of the wisp" which may appear or disappear with a slight shift of epicenter or recording station. The wide scatter of PcP amplitudes from Longshot (Carder, et al., 1967 and Clark, 1966a) is further evidence of this phenomenon. Amplitudes of some of the arrivals whose travel times are used here are discussed in a later section of this paper.

At distances near 45°, PP and PcP are sometimes confused, although examination of the horizontal component records will usually resolve this difficulty. In a narrow distance range near 60° there appears to be a series of arrivals preceding PcP and having an apparent velocity between those of first P and PcP. One possible such phase is the "B" phase of Gutenberg and Richter [1935] whose travel-time curve parallels that of PcP and is 9 to 18 seconds earlier. The unidentified arrival shown at the top of Figure 13 could be taken as PcP were it not for the "on time" PcP arrival 18 seconds later. At distances beyond 70 degrees, crustal reverberations may produce pseudo PcP's. Longshot and Novaya Zemlya events show a complex P coda at most distances. Arrivals from separate events are also possible sources of a coincidental error.

Event: Novaya Zemlya 10/27/66 recorded at Edmonton, Alberta (EDM), $\Delta = 53.413^\circ$



Event: Sahara 2/27/65 recorded at State College, Pennsylvania (SCP), $\Delta = 69.530^\circ$

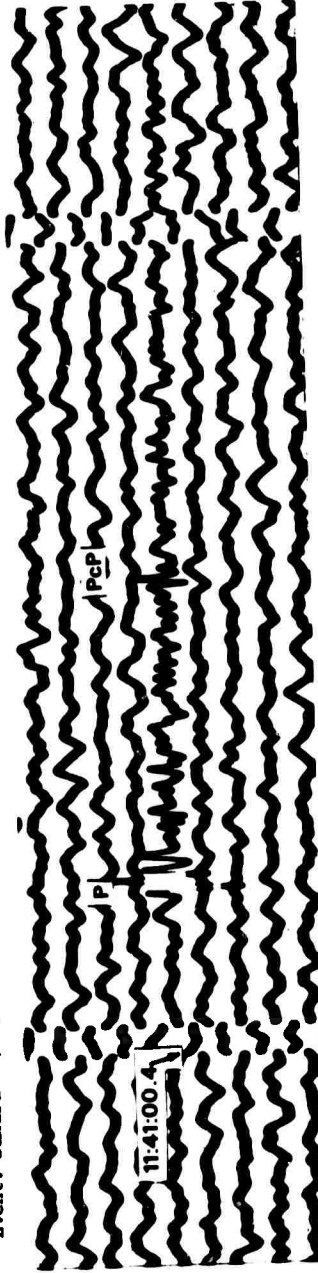


FIGURE 13. SURFACE-FOCUS EVENTS RECORDED AT NORTH AMERICAN STATIONS ON VERTICAL SHORT-PERIOD INSTRUMENTS.

Estimates of mean error sum are determined using the method of random vector addition:

$$\text{Mean Error Sum} = \sqrt{E_1^2 + E_2^2 + E_3^2 + E_4^2 + E_5^2}$$

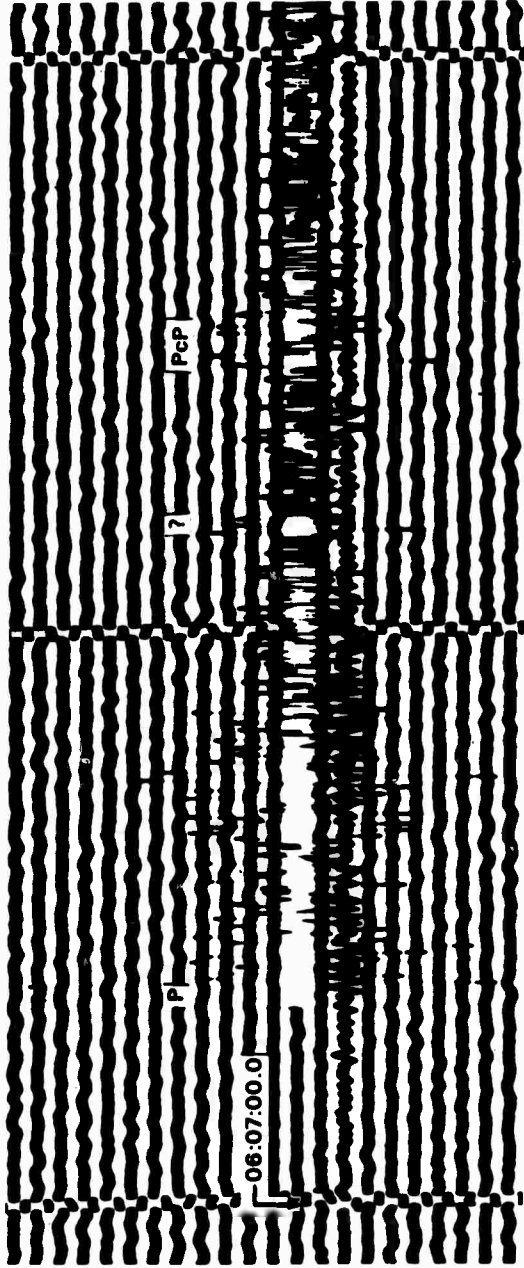
From Tables 2 and 3 it is seen that the sources of error in the PcP residuals are somewhat different from those involving PcP-P residuals. For instance, the error due to an incorrect epicenter location will be more pronounced at short distances for PcP-P and at long distances for PcP residuals

The second class of error cannot be measured or predicted with any degree of certainty, and involves mis-identification of arrivals or failure to select the "first break" of PcP.

In regard to the first possibility, there is often a tendency to "seek out" a PcP by selecting the strongest arrival nearest the predicted PcP time. If the author's criteria for PcP discussed earlier are not heeded, and sometimes even if they are heeded, mis-identification is a distinct possibility. The primary problem here is that the assumption that a readable PcP phase must be present somewhere on the seismogram is incorrect. It has been shown (see Carder, 1964) that PcP is a "will of the wisp" which may appear or disappear with a slight shift of epicenter or recording station. The wide scatter of PcP amplitudes from Longshot (Carder, et al., 1967 and Clark, 1966a) is further evidence of this phenomenon. Amplitudes of some of the arrivals whose travel times are used here are discussed in a later section of this paper.

At distances near 45°, PP and PcP are sometimes confused, although examination of the horizontal component records will usually resolve this difficulty. In a narrow distance range near 60° there appears to be a series of arrivals preceding PcP and having an apparent velocity between those of first P and PcP. One possible such phase is the "B" phase of Gutenberg and Richter [1935] whose travel-time curve parallels that of PcP and is 9 to 18 seconds earlier. The unidentified arrival shown at the top of Figure 13 could be taken as PcP were it not for the "on time" PcP arrival 18 seconds later. At distances beyond 70 degrees, crustal reverberations may produce pseudo PcP's. Longshot and Novaya Zemlya events show a complex P coda at most distances. Arrivals from separate events are also possible sources of a coincidental error.

Event: Novaya Zemlya 10/27/66 recorded at Edmonton, Alberta (EDM), $\Delta = 53.413^\circ$



Event: Sahara 2/27/65 recorded at State College, Pennsylvania (SCF), $\Delta = 69.530^\circ$

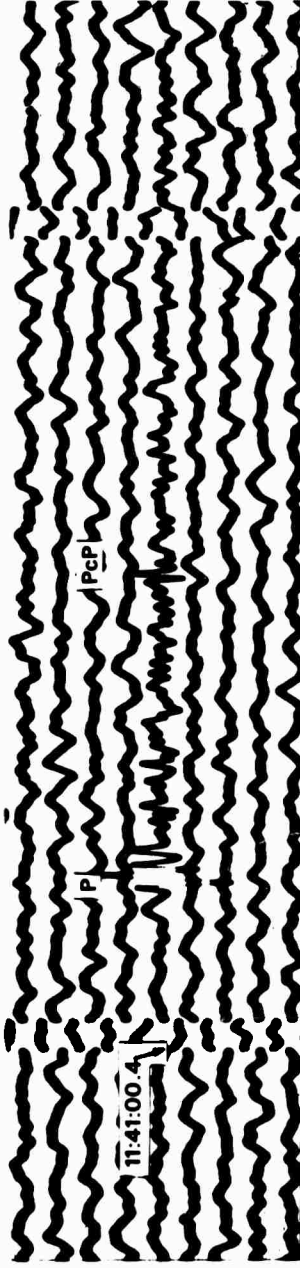


FIGURE 13. SURFACE-FOCUS EVENTS RECORDED AT NORTH AMERICAN STATIONS ON VERTICAL SHORT-PERIOD INSTRUMENTS.

In selecting the "first break" of PcP, the author generally found the relationship of Buchbinder [1968a] to hold true, with like polarity for PcP and P at distances greater than about 30 degrees and opposite polarity at shorter distances. "Visual cross-correlation" was used to determine the PcP-P interval, and hence the PcP arrival time, at distances larger than about 30 degrees. At shorter distances the first distinct motion was selected, and was generally a dilation.

Possible Interpretations of Residuals

The travel-time residuals described in the previous section can be interpreted, within the limitations of their probable errors, as due to several factors:

1. Anomalous crust and upper mantle velocities near epicenter or station.
2. Anomalous lower mantle velocities.
3. Variations in depth to the core-mantle boundary.
4. Slope or "dip" of the core-mantle interface.

Factor 1 is certainly significant; station and source anomalies do exist as shown by Carder, Gordon, and Jordan [1966], and may be highly directional as demonstrated by Cleary and Hales [1966], Cleary [1967], and Herrin and Taggart [1968]. These effects serve to increase the scatter of the data and may also produce systematic errors. It is believed that such errors will be reduced by: 1) the application of source and station corrections or by (2) the use of PcP-P times in the analysis.

Anomalous lower mantle velocities would produce residuals very difficult to eliminate or distinguish from those due to variations in core depth. The velocity structure in the lower four hundred kilometers is not known (Taggart and Engdahl, 1968) with any degree of certainty and may vary with latitude and longitude.

The residuals for epicentral distances less than 70 degrees will be interpreted in terms of variations in depth to the core-mantle boundary. Such data should permit a determination of the gross features of the northern hemisphere of the core's outer surface. The presence of slope or dip on the core-mantle boundary would presuppose the existence of signifi-

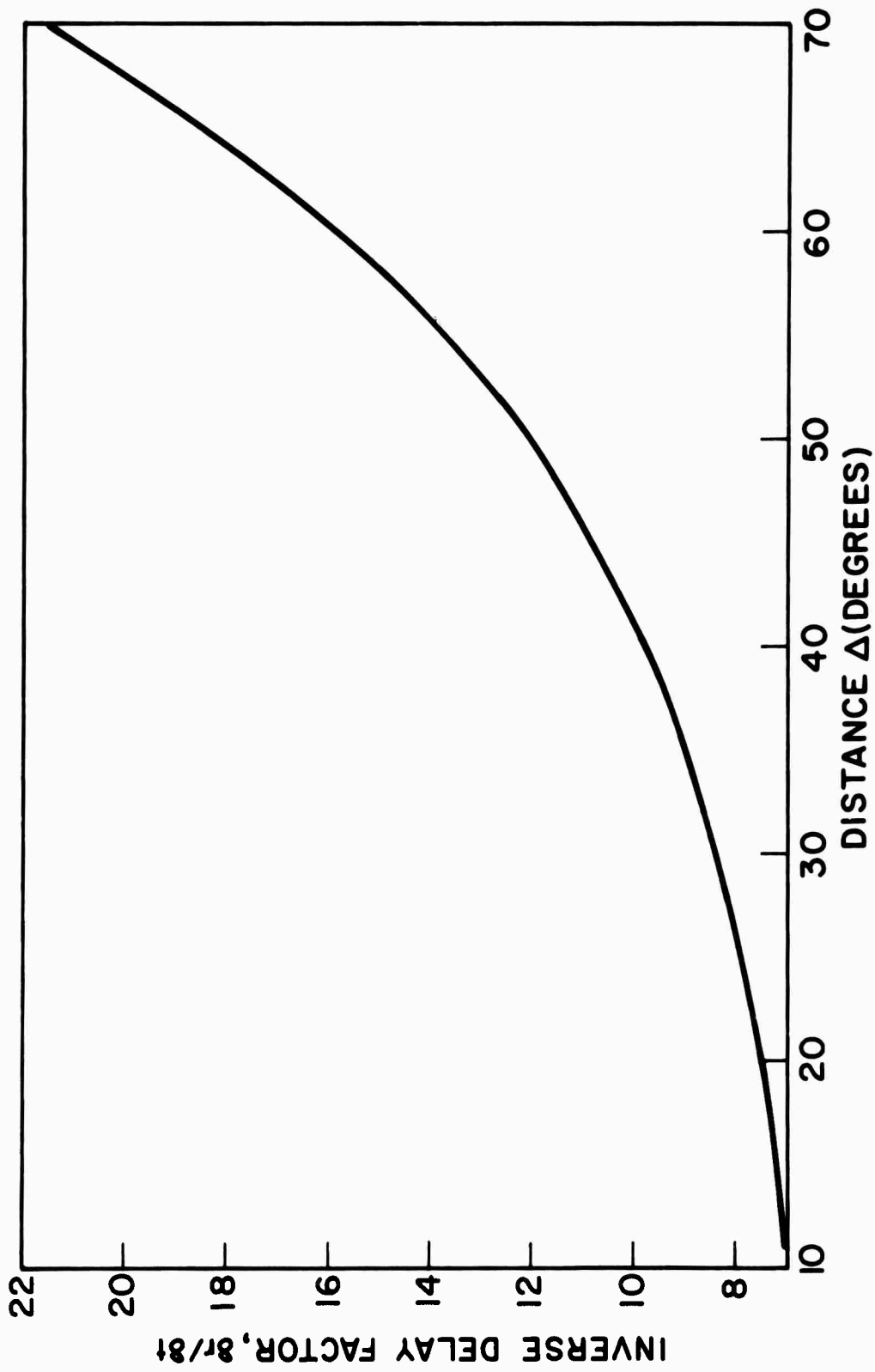


FIGURE 14. INVERSE DELAY FACTOR, CORE-MANTLE BOUNDARY.

cant variations in core radius, unless the interface consisted of a large number of angular reflecting blocks of relatively small dimensions.

Conversion of Time Residuals to Variations in Outer Core Radius

In consideration of the ellipticity correction, equation (6), the term due to δr at the core-mantle boundary was deliberately omitted. The travel-time residuals will now be equated to this term and expressed in terms of variation in core radius. The proportionality factor,

$\frac{V_a}{2 \cos i_a}$, is plotted as a function of epicentral distance in Figure 14.

The angle of incidence at the core, i_a , is determined by the relationship

$\sin i_a = \frac{V_a}{r_a} \frac{\delta t}{\delta \theta}$, where $\frac{\delta t}{\delta \theta}$ is derived from the Taggart-Engdahl PcP travel

time tables, r_a is the core radius (3477 km), and V_a is the velocity (13.67 km/sec) in the mantle just above the core. These values are from model 4 of Taggart and Engdahl [1968]. The inverse delay factor of Figure 14, $\frac{\delta r}{\delta t}$, increases exponentially with distance and would be infinite at grazing incidence. The decision to restrict the δr interpretation to epicentral distances less than 70 degrees was determined in part by this consideration and in part by the fact that some of the better PcP arrivals seem to be found near this distance. This is illustrated in the bottom half of Figure 13 where PcP from the Sahara event recorded at State College, Pennsylvania, at a distance of 70 degrees is shown.

Distribution of PcP Reflection Points

A computer program was written to compute the point of reflection for PcP, assuming that reflection occurs at the projection on the core of the midpoint of the geocentric great circle path from epicenter to station. The program consists of a standard geocentric distance and azimuth algorithm modified to accept a subroutine which calculates longitude and geocentric latitude of reflection point, azimuth of the ray at the reflection point, the sum (HSUM) of $\delta r_{\text{epicenter}}$ plus $\delta r_{\text{station}}$ due to the ellipticity of the earth's surface, the harmonic S_2 defined in conjunction with equation (9) as a function of the latitude of the reflection point, and

the sum $S_0 + \frac{2}{5} S_a + S_1$ which involves S_2 harmonics at the epicenter, reflection point and station and is used in the calculation of the correction for the ellipticities of internal strata of equal velocity. A print-out displaying the output of the Fortran program as modified is included in Appendix 2.

PcP reflection points corresponding to data used for determination of δr_{core} are plotted on an azimuthal equidistant polar projection, and is shown in Figure 15. Coverage of the northern hemisphere is by no means complete, but should be sufficient to detect broad trends. Coverage of the north polar region is better than that near the equator, and the majority of the reflection points fall at mid-latitudes.

Presentation of δr Data

The density of reflection points in some regions precludes the inclusion of each point on a global residual map. Consequently the data are represented by sector means, all values being averaged within zones 10° of latitude by 10° of longitude. This method allows the minimum dilution of a large percentage of the data, since the smaller areas enclosed by zones at higher latitudes are compensated by the greater density of reflection points there.

The sectorially averaged variations in core radius presented in Figure 16 are based upon PcP travel times at distances less than 70° , corrected for elevation and ellipticity only. Averages determined in the same manner for residuals based upon PcP travel times with station and source corrections applied are shown in Figure 17. A similar presentation for δr based upon PcP-P times is shown in Figure 18.

To show some of the individual data points, the δr based upon PcP-P at reflection points north of 40° north latitude have been plotted on the larger scale polar projection of Figure 19. Note the general agreement of δr at neighboring reflection points from different events.

The agreement of the values in Figures 17 and 18 is not as great as had been anticipated. As indicated earlier, the two data sets should be equivalent, since the crust and upper mantle travel-time anomalies have, hopefully, been largely compensated in each case. However, since the error dependence was shown to be different for the two sets of data, the best

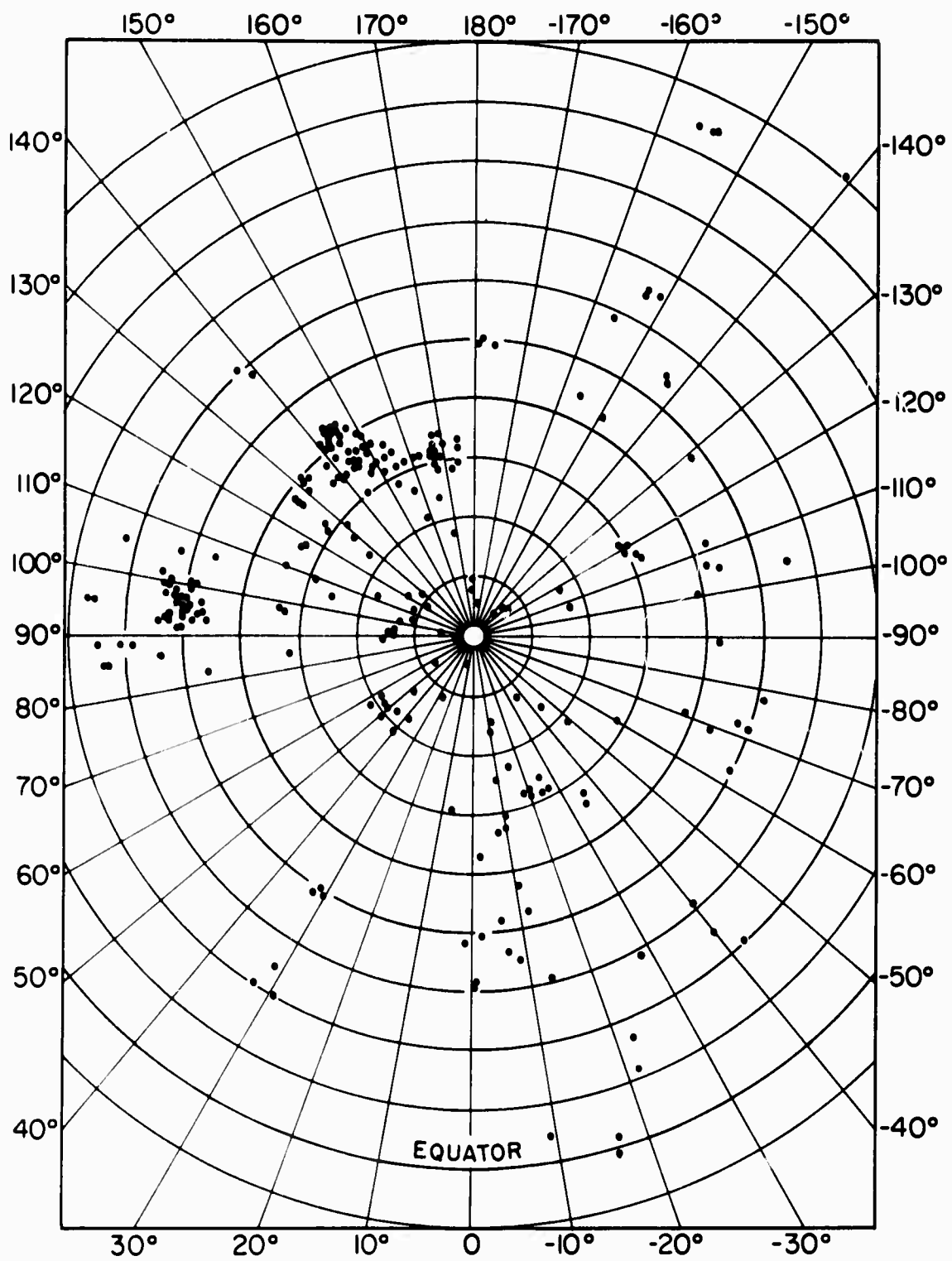


FIGURE 15. DISTRIBUTION OF PcP REFLECTION POINTS, $\Delta \leq 70^\circ$.

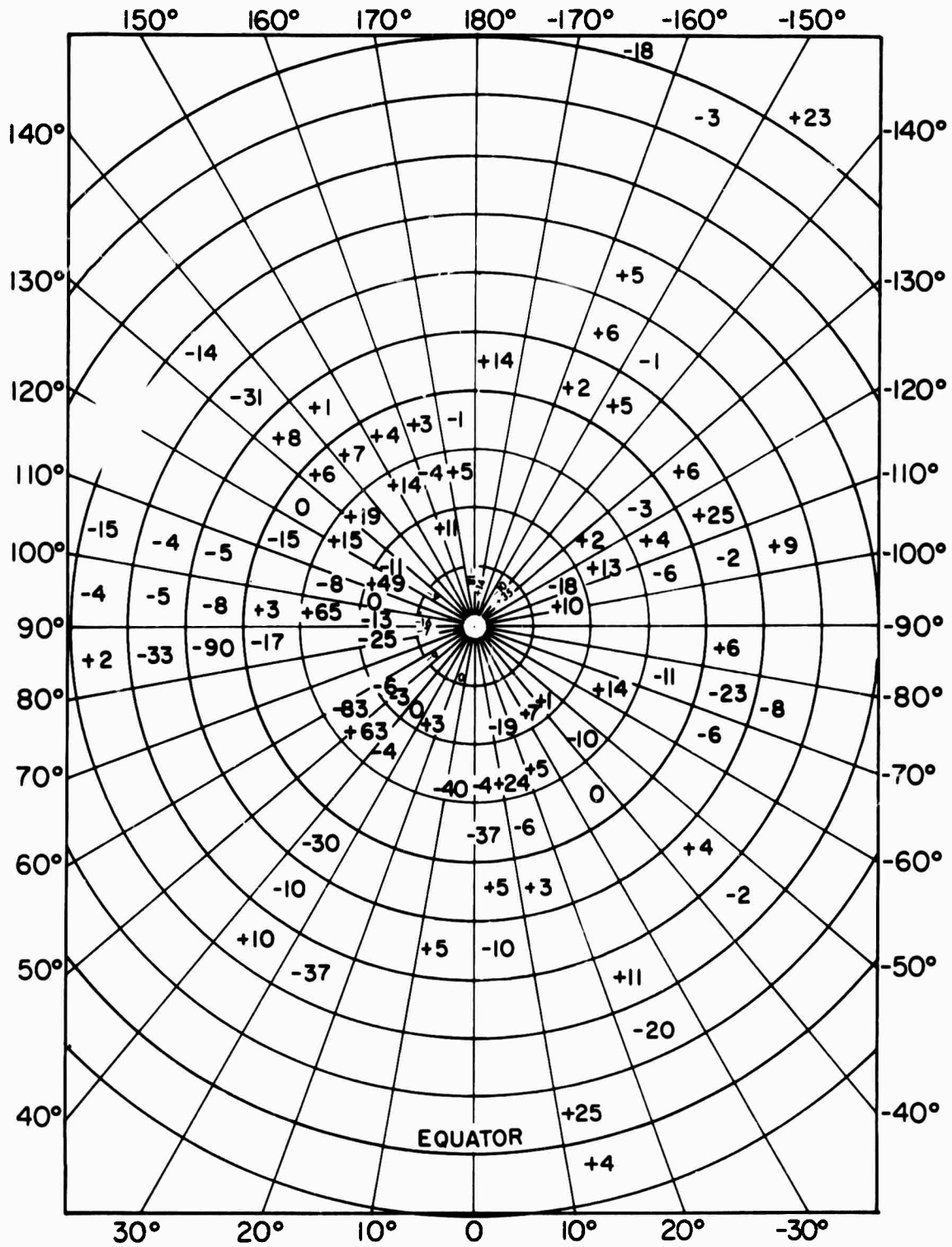


FIGURE 16. SECTORIALLY AVERAGED δr OF CORE BASED UPON PcP TRAVEL TIMES.

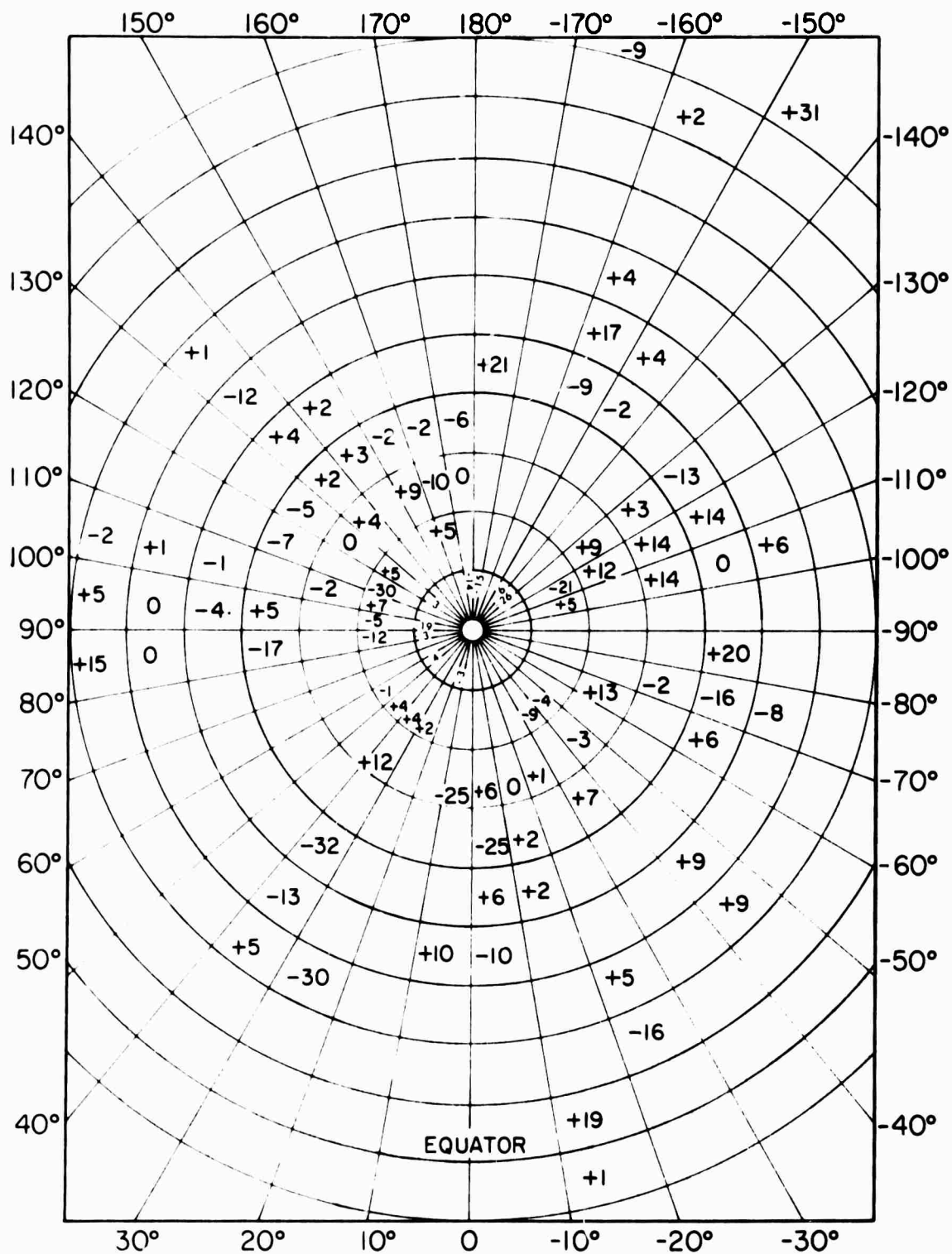


FIGURE 17. SECTORIALLY AVERAGED δr OF CORE BASED UPON PcP TRAVEL TIMES, STATION AND SOURCE CORRECTIONS APPLIED.

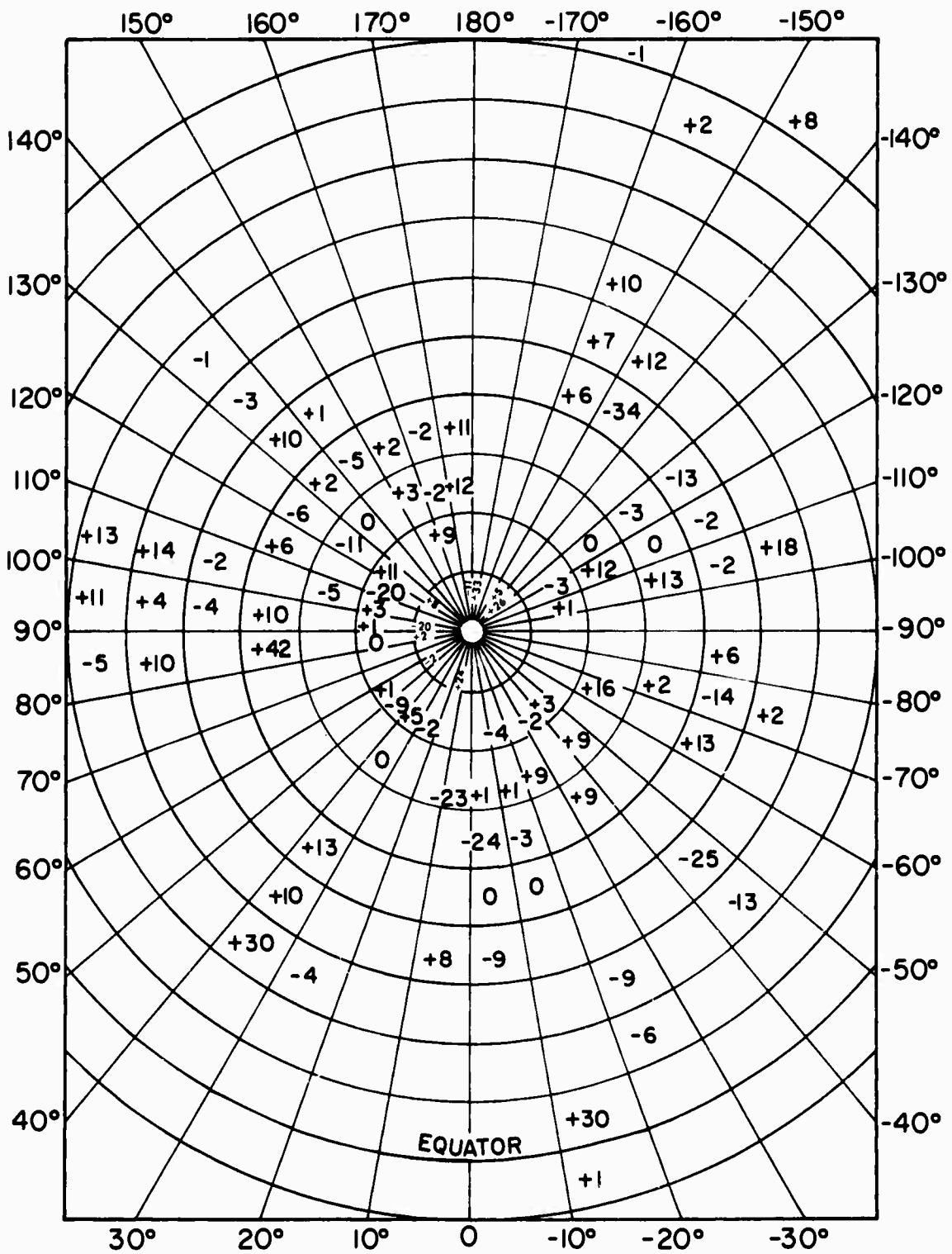


FIGURE 18. SECTORIALLY AVERAGED $\delta\tau$ OF CORE BASED UPON THE PcP-P TRAVEL TIME INTERVAL.

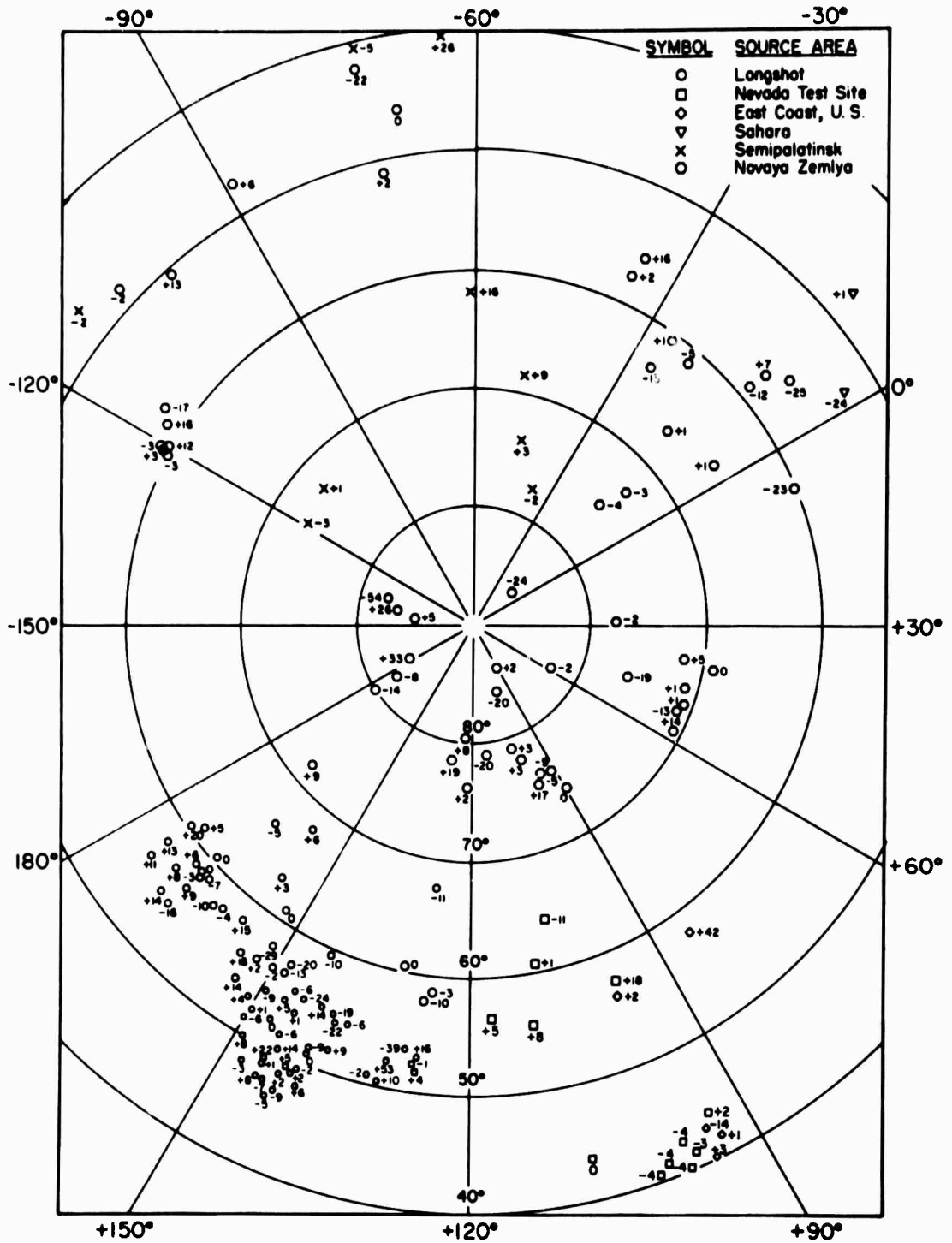


FIGURE 19. δr BASED UPON PcP-P DATA, 40° - 90° NORTH LATITUDE.

estimate of core radius is obtained by averaging the sets, producing a new set, $\overline{\delta r}$. The $\overline{\delta r}$ was obtained at each reflection point by averaging the δr determined from PcP times corrected for station and source travel-time anomalies and the δr obtained from the PcP-P times, except in the few cases where station time was not known or no P arrival time was available. Further data analysis will utilize primarily the $\overline{\delta r}$ set, sectoral averages of which are displayed in Figure 20.

Statistical Distribution of the $\overline{\delta r}$ Data

A histogram (Figure 21) of the $\overline{\delta r}$ data was prepared, showing the number of data points in each one kilometer interval. The data mean is +0.75 kilometers, with a standard deviation of 20.58 kilometers. A few scattered data points more than two standard deviations from the mean fall beyond the scale limits of the abscissa of Figure 21 and hence are not shown. The distribution is nearly Gaussian, with little evidence of bi- or multimodality which might indicate a layered structure consisting of more than one reflector. The distribution of $\overline{\delta r}$ is, of course, dependent upon the spatial distribution of the reflection points, especially with regard to latitude. Any layered structure of the mantle-core boundary which might exist would be quite "blurred" by the variation of core radius with latitude. The value of the mean of $\overline{\delta r}$ reflects the preponderance of data on the flattened portion of the core spheroid, north of 35° north latitude. It will be shown that the data indicate a somewhat larger increase in the core radius of Taggart and Engdahl's [1968] model 4.

Harmonic Representation of the $\overline{\delta r}$ Data

The distribution and scatter of the data of Figures 16 through 20 makes contouring difficult, if not impossible. A method of smoothing and interpolation is needed to present the data as a function of latitude and longitude, to extract significant trends, and to describe the gross shape of the core. This has been achieved by expressing the $\overline{\delta r}$ in a series of spherical harmonics.

Such an arbitrary function of colatitude (ϕ) and longitude (θ) on the surface of the unit sphere can be represented by a series of surface harmonics,

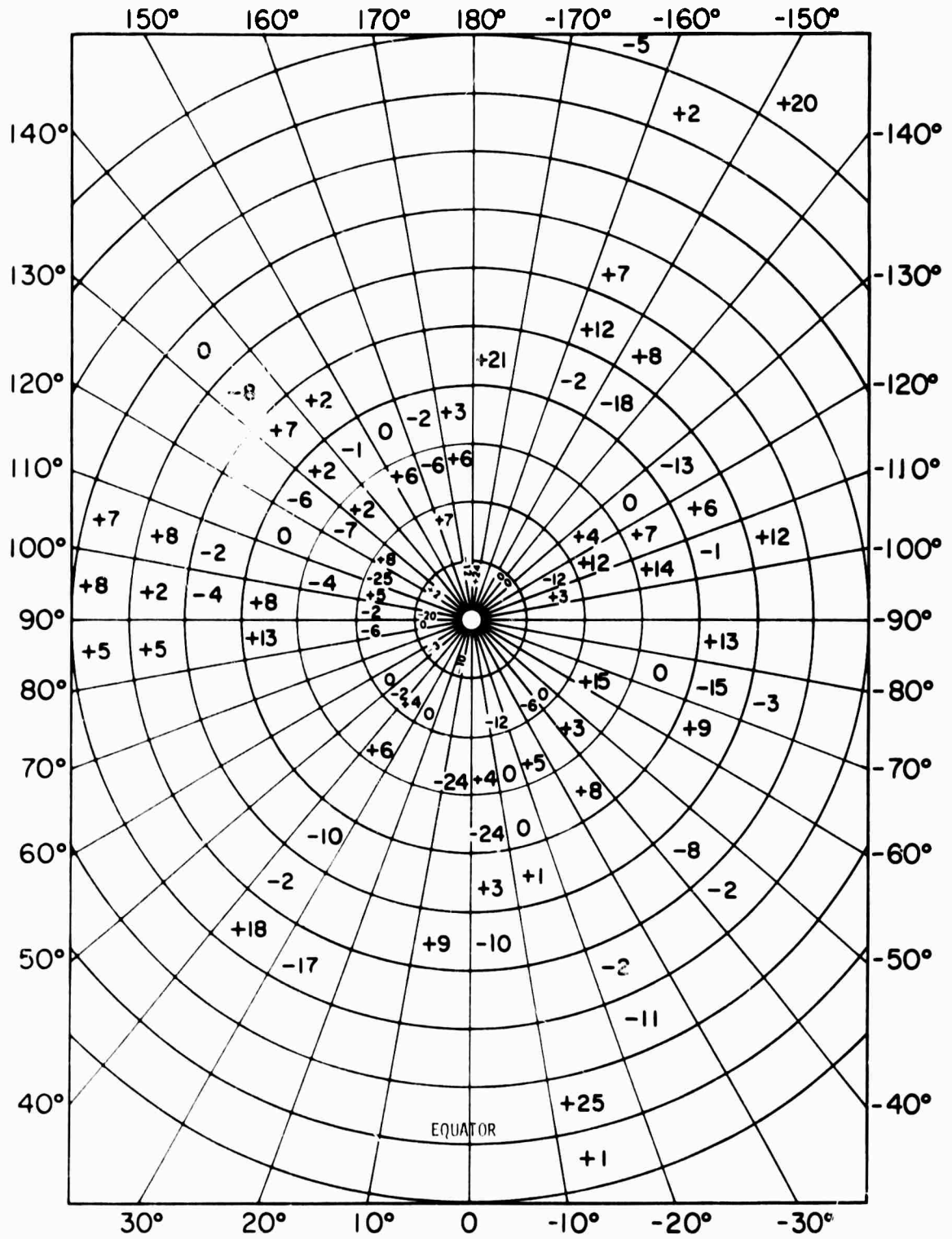


FIGURE 20. SECTORIALLY AVERAGED $\overline{\delta r}$ OF CORE.

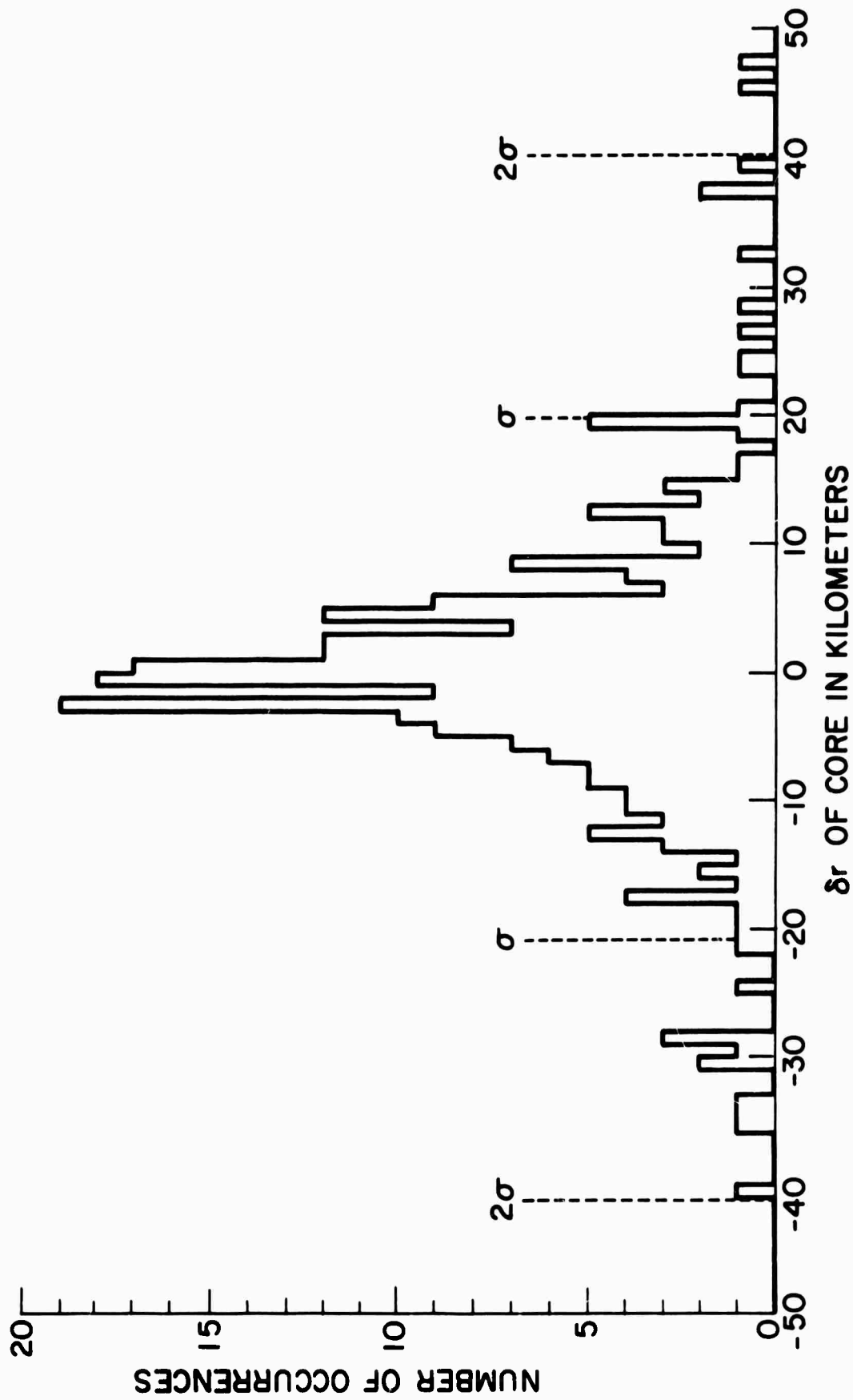


FIGURE 21. HISTOGRAM OF $\overline{\delta r}$ OF CORE (1 Km. INTERVALS).

$$H(\phi, \theta) = \sum_{n=0}^{\infty} \left[\frac{A_{n0}}{2} P_n(\cos \phi) + \sum_{m=1}^n (A_{nm} \cos m\theta + B_{nm} \sin m\theta) P_n^m(\cos \phi) \right] \quad (10)$$

whose coefficients are given by

$$A_{nm} = \frac{2n+1}{2\pi} \frac{(n-m)!}{(n+m)!} \int_0^{2\pi} \int_0^{\pi} H(\phi, \theta) P_n^m(\cos \phi) \cos m\theta \cdot \sin \phi \, d\phi \, d\theta$$

and

$$B_{nm} = \frac{2n+1}{2\pi} \frac{(n-m)!}{(n+m)!} \int_0^{2\pi} \int_0^{\pi} H(\phi, \theta) P_n^m(\cos \phi) \sin m\theta \sin \phi \, d\phi \, d\theta$$

where P_n denotes the Legendre polynomial and P_n^m the "associated Legendre polynomial" defined by

$$P_n^m(\mu) = \frac{d^m [P_n(\mu)]}{d\mu^m} \cdot \sin^m \phi, \text{ where } \mu = \cos \phi.$$

Thus the constants A_{nm} and B_{nm} can be determined by integration over the surface of the sphere. An alternate approach is to determine the A_{nm} and B_{nm} by a least squares solution to a system of linear equations, each of which has the form (10). Equation (10) can be rewritten

$$H(\phi, \theta) = \sum_{n=0}^{\infty} \sum_{m=0}^n (A_{nm} C_{nm} + B_{nm} S_{nm}) \quad (12)$$

where $C_{nm} = P_n^m(\mu) \cdot \cos(m\theta)$

and $S_{nm} = P_n^m(\mu) \cdot \sin(m\theta)$ (13)

are the so called "tesseral" surface harmonics and A_{nm} and B_{nm} are suitably chosen constants. The C_{nm} and S_{nm} have been normalized such that

$$\int_0^{2\pi} \int_0^{\pi} C_{nm}^2 \sin \phi \, d\phi \, d\theta = \int_0^{2\pi} \int_0^{\pi} S_{nm}^2 \sin \phi \, d\phi \, d\theta = 4\pi.$$

The normalizing factor, F_{nm} is $\sqrt{2n+1}$ for the zonal harmonics ($m=0$) and $\sqrt{2(2n+1) \frac{(n-m)!}{(n+m)!}}$ for the tesseral and sectoral harmonics.

Each data point defines values of ϕ , θ , and H and thus determines an equation of the form (12). The $\bar{\delta r}$ data were expressed as a series of

surface harmonics through degree (N) five. The algorithm used is a modification and extension of Pollack's [1968] program utilizing MacMillans [1930] tabulation of the tesseral harmonics through degree four in Cartesian coordinates. The program as modified can be used to determine tesseral harmonic coefficients through degree and order five and zonal harmonic coefficients to higher degrees. It also incorporates another technique, described herein as "step harmonics", found to be especially useful in the analysis of data which are not uniformly distributed on the sphere. The lack of sufficient constraints in the form of data in the equatorial regions and southern hemisphere proved to be a serious problem in the harmonic analysis. The least squares "best fit" to the observations obtained in the initial attempts resulted in some of the coefficients becoming very large. While the 4th or 5th degree series thus generated provided a slightly better fit to the data than was later obtained by the step harmonic technique, the results were unacceptable because they produced a core which protruded from the earth's surface near the south pole. Constraints were imposed in the form of artificial data points, $\overline{\delta r} = 0$, introduced at strategic locations in the southern hemisphere, but this was found to be both mathematically and psychologically unsuitable. The method of step harmonics consists of the independent determination of coefficients, a few terms at a time. The contribution of these terms is removed from the data and the residual used to compute the next set of coefficients. The coefficients computed by this method will depend upon the order of evaluation and thus will not be unique although the resulting representations of the $\overline{\delta r}$, within the limits of the data scatter and distribution of reflection points, will be similar. Since any least squares technique is highly sensitive to extreme data values, the $\overline{\delta r}$ data set was truncated at ± 20 km (approximately one standard deviation), reducing the data points to 223. First degree terms were omitted in the analysis. This is equivalent to the assumption that the surface of the core and the earth's surface are concentric. Two sets of harmonic coefficients were computed using different step sequences. These values are shown in Table 4. Set 1 was determined by first evaluating C_{00} and the second degree terms. Subsequent steps determined the third, fourth, and finally the fifth degree coefficients. The first step in the determination of coefficient set 2 was the computation of the zonal harmonic coefficients

Table 4. Harmonic Coefficients

<u>Coefficient</u>	<u>Set 1</u>	<u>Set 2</u>
A ₀₀	1.902	1.229
A ₂₀	-1.822	-1.499
A ₂₁	-1.220	-0.237
B ₂₁	1.180	0.122
A ₂₂	-2.186	-0.213
B ₂₂	-0.676	-0.349
A ₃₀	-0.137	1.338
A ₃₁	0.499	-0.214
B ₃₁	0.020	0.266
A ₃₂	0.257	-0.005
B ₃₂	0.770	-0.076
A ₃₃	-0.740	0.429
B ₃₃	0.155	0.400
A ₄₀	-0.521	-1.410
A ₄₁	0.559	-0.185
B ₄₁	-0.064	0.716
A ₄₂	-0.131	0.093
B ₄₂	0.366	0.182
A ₄₃	-1.163	-0.045
B ₄₃	-0.286	0.407
A ₄₄	0.275	-1.029
B ₄₄	0.400	-0.492
A ₅₀	-0.481	-0.365
A ₅₁	0.210	0.797
B ₅₁	-0.295	-0.376
A ₅₂	-0.502	-1.154
B ₅₂	0.098	-0.019
A ₅₃	-0.249	-1.347
B ₅₃	-0.063	-0.429
A ₅₄	0.809	1.359
B ₅₄	0.554	0.550
A ₅₅	0.656	1.614
B ₅₅	-0.164	-1.348

A_{00} , A_{20} , A_{30} , and A_{40} . Their contribution was then subtracted from the $\overline{\delta r}$ data and the resulting residuals used in the determination of the 5th degree terms. This procedure was repeated to compute the remaining fourth, third, and second degree terms. The series of spherical harmonics corresponding to sets 1 and 2 describe the existing data without introducing profound anomalies in regions where there are no data. It must be kept in mind that the principal reason for the harmonic expansion was the smoothing and interpolation of the data. The signs of A_{00} and the second degree coefficients in Table 4 are in agreement and may be representative of the gross size and shape of the core. The other terms are included only to improve the representation of the data. The rms error in this representation is approximately 7.5 kilometers for each set. The convention of positive west longitude used in the figures throughout this paper was reversed in the computation of the harmonic coefficients, rendering east longitude positive in keeping with standard practice.

An Estimate of the Shape of the Core

The values of the terms A_{20} and A_{00} , computed in the first steps of the analysis determining coefficient sets 1 and 2 show better agreement between sets than the other terms. Although obvious from rotational considerations, the oblateness of the mantle-core boundary has hitherto not been demonstrated on the basis of PcP travel times. The ellipticity of the core was determined from the A_{20} coefficient by evaluating the product $A_{20} C_{20}$ at equator and pole. The ellipticities obtained are .00176 for coefficient set 1 and .00145 for set 2. These values are notably smaller than the .00260 calculated by Bullen [1936] on the basis of P- and S-wave velocities, using the Williamson-Adams method and the Radau-Darwin approximation. Additional PcP observations are required in the equatorial regions to confirm this discrepancy.

The A_{00} coefficients in Table 4 correspond to an increase of the mean core radius of the Taggart-Engdahl Model 4 of about 1.5 kilometers.

The $\overline{\delta r}$ as defined by the coefficient sets 1 and 2 have been contoured and are shown in Figures 22 and 23 respectively. The contours overlie Figure 15 to indicate the areas where data exist. The variation in the $\overline{\delta r}$ is about 20 kilometers in each case, and the anomaly patterns are very similar. It will be shown, however, that the potential fields at the

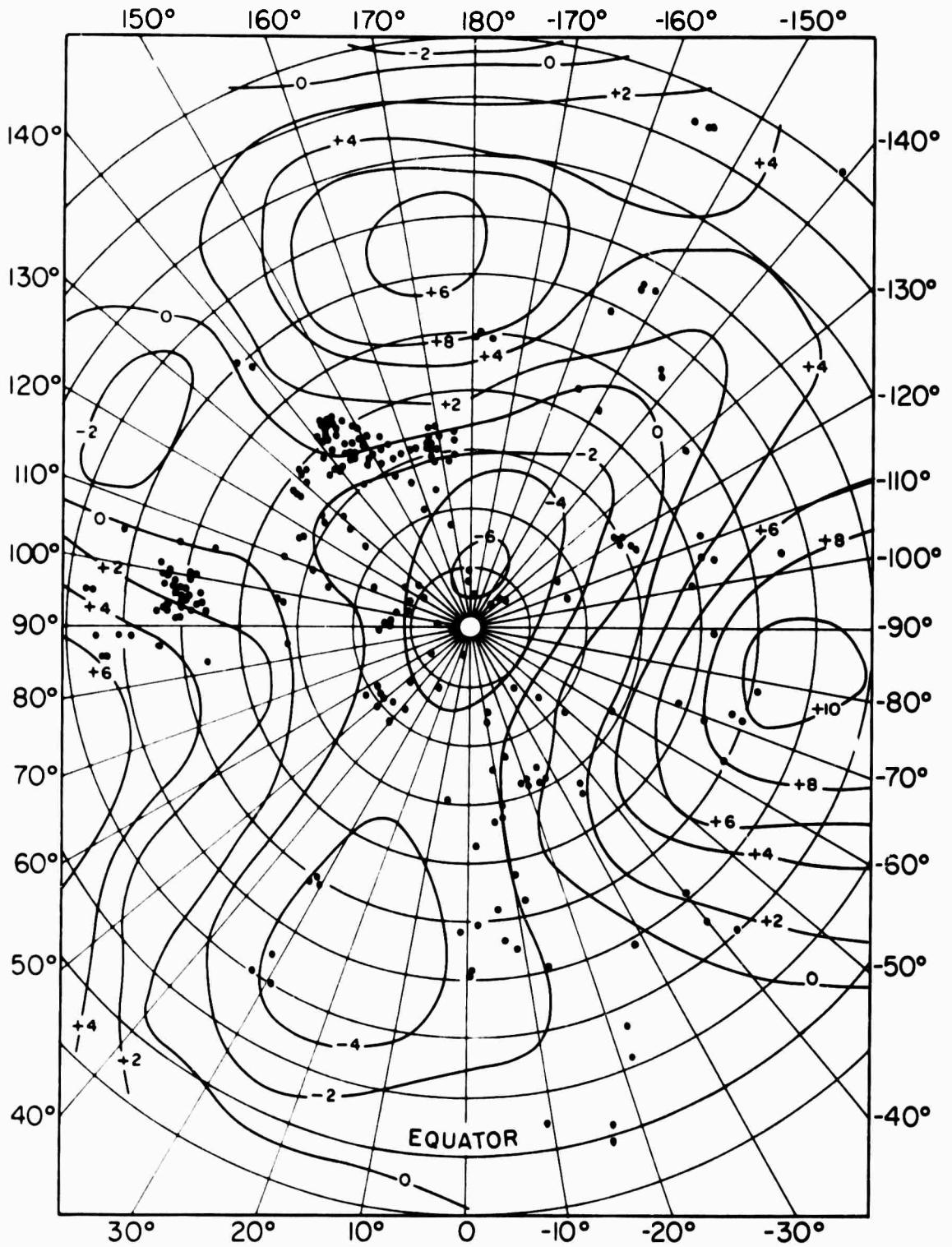


FIGURE 22. δr FROM HARMONIC EXPANSION USING COEFFICIENT SET NUMBER 1.
 (Contour interval = 2 km.)

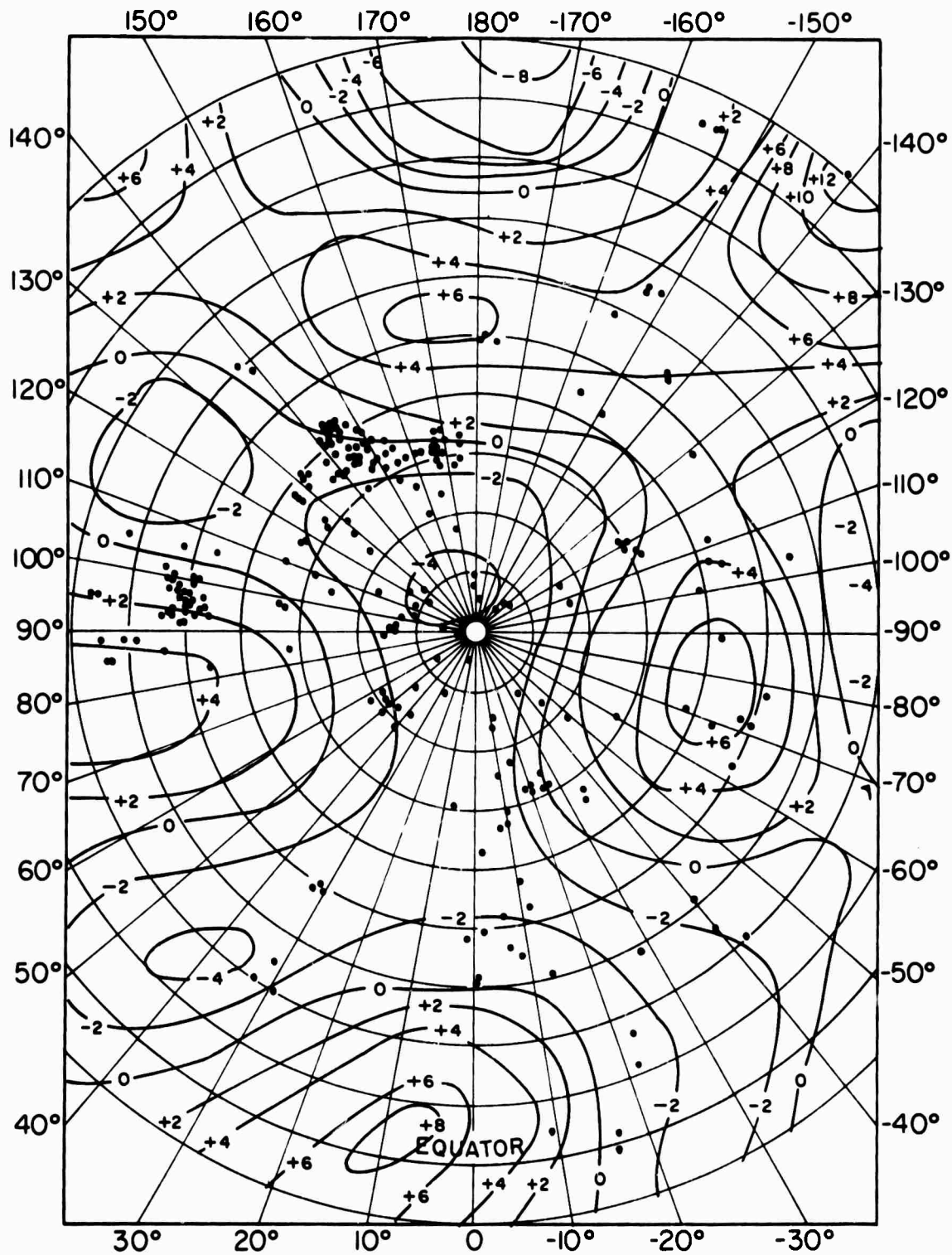


FIGURE 23. $\overline{\delta r}$ FROM HARMONIC EXPANSION USING COEFFICIENT SET NUMBER 2.
 (Contour interval = 2 km.)

surface resulting from coefficient sets 1 and 2 are quite different. The \bar{r} distributions of Figures 22 and 23 bear little resemblance to those determined by Vogel [1960] using core reflections from earthquake sources.

Computation of Geoid Heights

Because of the large density jump believed to exist at the mantle-core boundary, broad undulations on the order of kilometers should result in observable gravity variations at the earth's surface. The corresponding geoid heights may be determined by considering a surface density, q , at the mantle-core boundary, defined by

$$q(\phi, \theta) = \Delta\rho \cdot \bar{\delta r}(\phi, \theta)$$

where $\Delta\rho$ is the density contrast at the mantle-core boundary. This may be written in terms of the harmonic expansion of $\bar{\delta r}$,

$$q = \Delta\rho \sum_{n=0}^{\infty} \sum_{m=0}^n (A_{nm} C_{nm} + B_{nm} S_{nm}) .$$

Following Jeffreys [1962], the gravitational potential anomaly at the earth's surface due to $\bar{\delta r}$ is

$$\Delta W(\phi, \theta) = 4\pi G r \Delta\rho \sum_{n=0}^{\infty} \frac{1}{2n+1} \left(\frac{r}{R}\right)^{n+1} \sum_{m=0}^n (A_{nm} C_{nm} + B_{nm} S_{nm})$$

where r and R are, respectively, the radii of the core and of the earth, and G is the universal gravitational constant. The geoid height is then

$$\Delta h(\phi, \theta) = \frac{\Delta W(\phi, \theta)}{g} .$$

The hypothetical geoid heights resulting from the $\bar{\delta r}$ of Figure 22 represented by coefficient set 1, Table 4, omitting the C_{20} term and assuming a value of 4 gm/cc for $\Delta\rho$, are contoured in Figure 24. The sectoral harmonic S_{22} dominates a height distribution characterized by variations of 200 meters. The geoid heights corresponding to the $\bar{\delta r}$ of Figure 23, computed from coefficient set 2, are shown in Figure 25. The anomalies are more local in extent and smaller in amplitude than those of Figure 24.

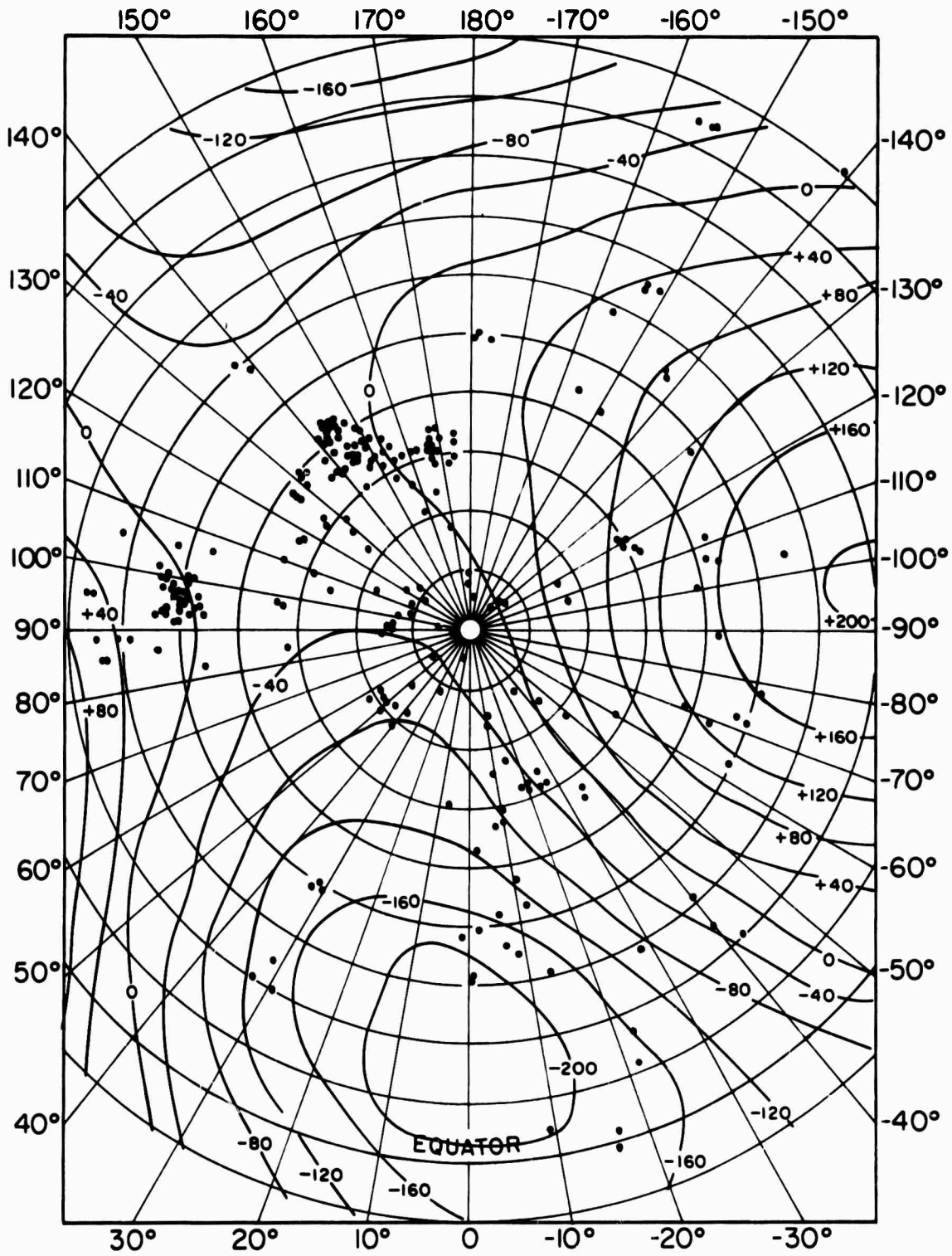


FIGURE 24. GEOID HEIGHTS COMPUTED FROM $\overline{\delta r}$ DISTRIBUTION OF FIGURE 22.
 (Contour interval = 40 meters)

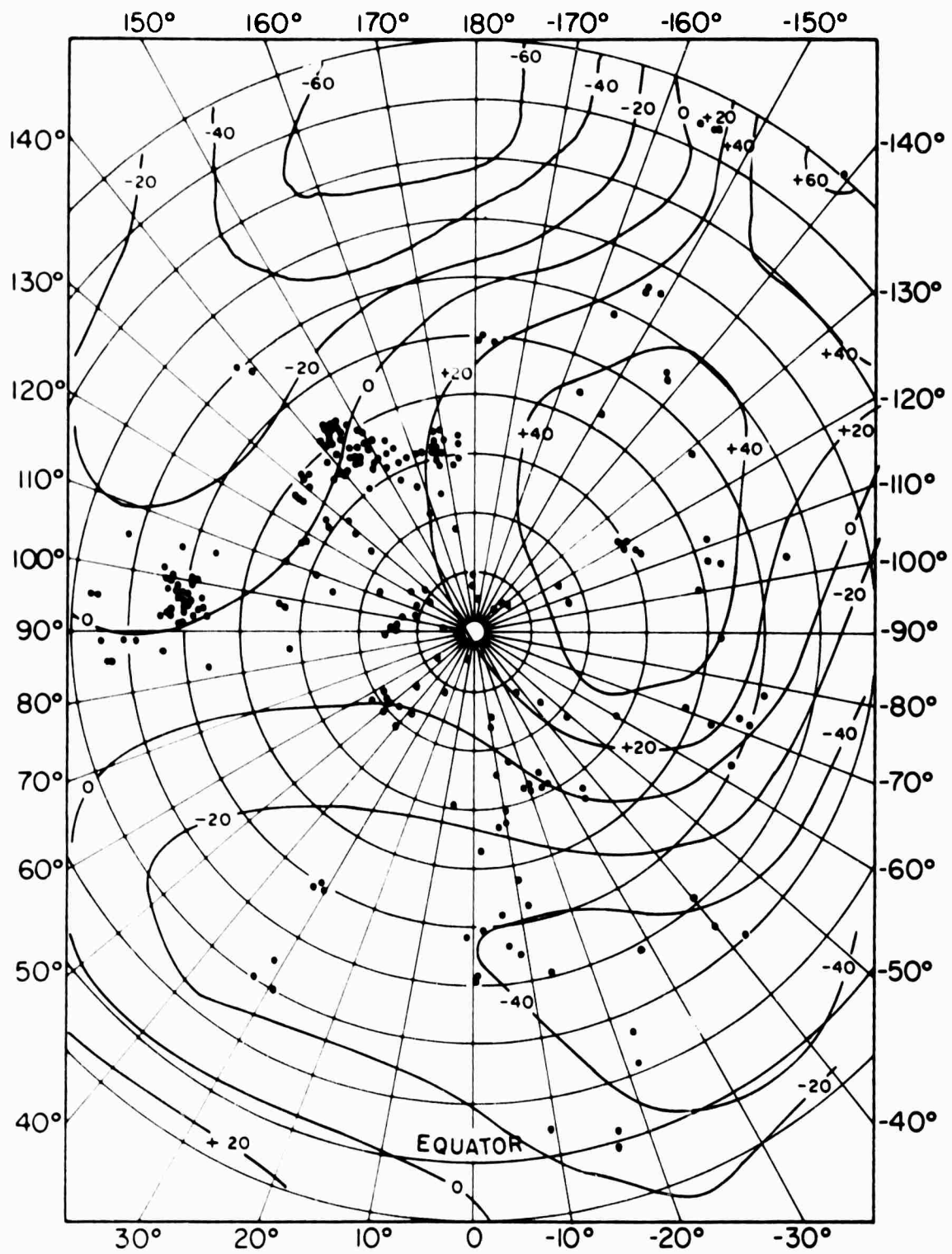


FIGURE 25. GEOID HEIGHTS COMPUTED FROM $\bar{\delta r}$ DISTRIBUTION OF FIGURE 23.
 (Contour interval = 20 meters)

Geoid heights computed by Kaula [1966] using harmonic coefficients through the 8th degree derived from observations of satellites are shown in Figure 26. The contours were transferred to the polar projection to facilitate comparison with Figures 24 and 25. While the range of values in Figures 25 and 26 is about the same, their spatial correlation is poor. Conspicuous by its absence in Figure 24 is the positive geoid anomaly centered on the Greenwich meridian at 50°N latitude. The lack of agreement could be due to many factors. Among these are:

1. The travel-time variations used in computing the $\overline{\delta r}$ may be the result of velocity variations in the mantle rather than changes in depth to the mantle-core boundary.

2. The inferred irregularities of mass distribution at the mantle-core boundary may be masked by extensive irregularities at other depths. Total or partial compensation may occur. Such compensation would have to occur with regard to the contribution of the second degree sectorial harmonics, C_{21} and S_{21} , which Jeffreys [1962] has shown must be absent in the potential since Z is the axis of greatest moment of inertia of the earth.

3. The density contrast at the mantle-core boundary may be less than the value of 4 gm/cc used in the geoid height computations. Buchbinder [1968b] has built a case for continuity of density across the boundary on the basis of an amplitude minimum and phase reversal of PcP at epicentral distances near 32°.

4. The velocity at the base of the mantle may be lower than that estimated by Taggart and Engdahl [1968]. Decreasing this velocity would tend to decrease $\overline{\delta r}$ and thus decrease the hypothetical geoid heights. Of the 84 surface focus PcP arrival times used by Taggart and Engdahl, only four were at epicentral distances greater than 65°. Although PcP travel times at shorter distances are not very sensitive to lower mantle structure, analysis of these data indicated a slight preference for a model exhibiting a gradual increase of velocity with depth in this region. Taggart and Engdahl's [1968] PcP travel time tables are based on this model with a core radius of 3477 km. The travel times tabulated in Appendix 1, some of which are taken from their

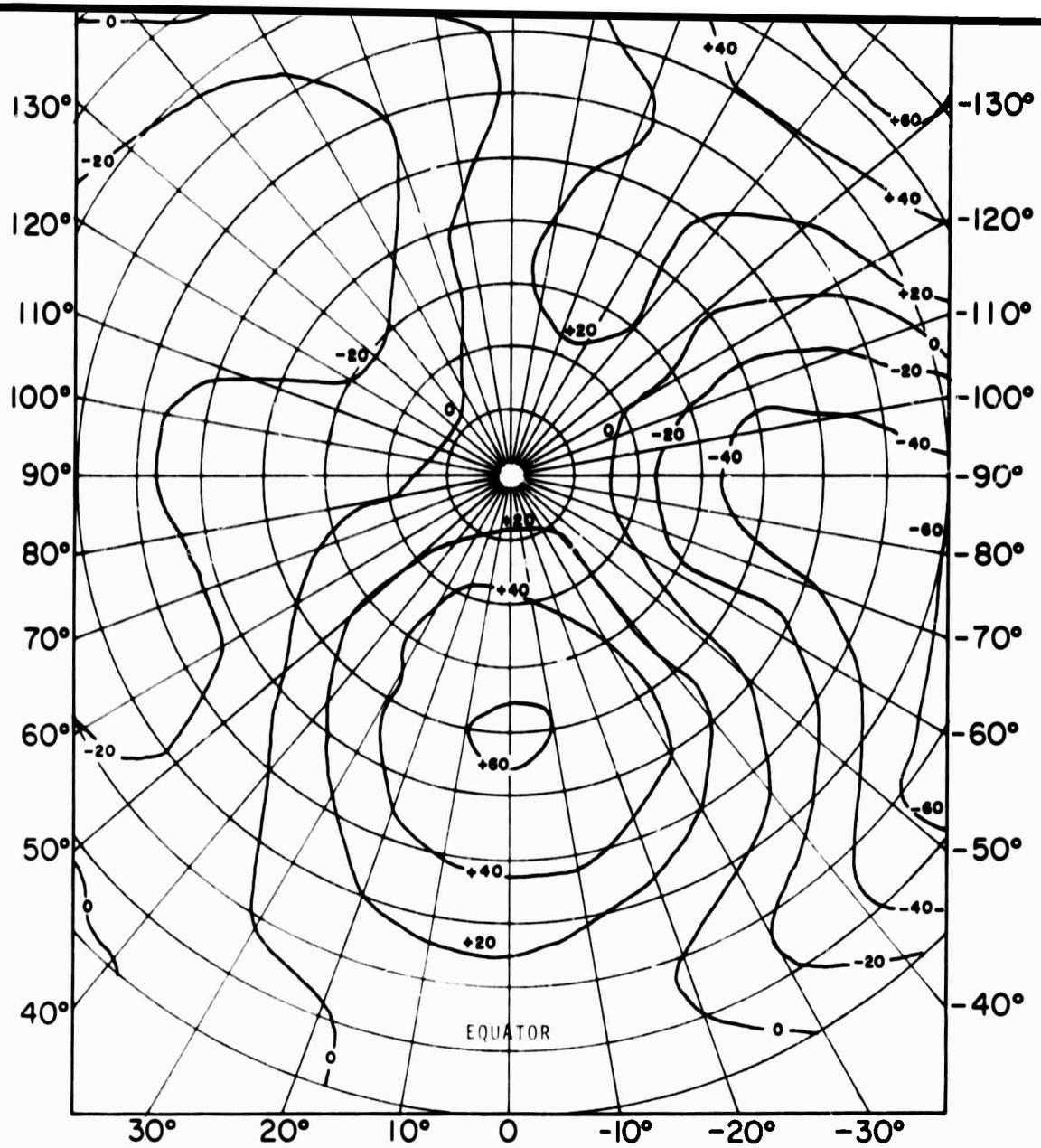


FIGURE 26. GEOID HEIGHTS COMPUTED FROM SATELLITE OBSERVATIONS (AFTER KAULA [1966]).

(Contour interval = 20 meters)

amplitude work of Sacks [1967] who interprets the shadow boundary at $\Delta = 96^\circ$ in terms of a core radius of 3550 km. This interpretation is not consistent with PcP travel times, which are sensitive to major changes in core radius. It would appear that this diffraction boundary is associated with a decrease of velocity with depth in the lowest 100 km of the mantle, rather than with the position of the mantle-core boundary. Ergin [1967] has found such a velocity decrease in the lower mantle necessary to explain the range of observations for PKK2 phases.

The sharpness of the shadow boundary at periods near one second, as determined by Sacks [1967] using earthquake data and as indicated by the data of Figure 28, implies that the amplitudes of these short-period (<1 sec) diffracted P phases are probably too small beyond about 100° to be detected.

Such short-period arrivals do exist, however, beyond 100° and have been reported to distances of 134° or more (Ergin, 1967, Lehmann, 1953). Bolt [1969] has observed that first arrivals, designated "diffracted PcP", in the distance range of 100° to 115° fall on a line of slope $dt/d\Delta$ of 4.60 seconds per degree. His lower mantle P-wave velocities, based on this slope and on PcP travel times, decrease to a value of 13.3 km/sec at the mantle-core boundary. Additional evidence of a velocity decrease at the base of the mantle may be determined from the "cutoff points" indicated by the short-period core phase travel-time data of Engdahl [1968]. The cutoff distance of PcP must be equal to twice the cutoff distance of PKKP reduced by the cutoff distance of PKKKKP. This implies PcP propagation to a distance of 124° .

Presentation of Amplitude Data

The amplitude/period (A/T) ratio of P and PcP phases and the A/T ratio PcP/P are tabulated in Appendix 1 for a number of arrivals used in the analysis of PcP and P travel times. The variation of PcP A/T (vertical component) ratios with distance is shown in Figure 27. All events have been normalized to

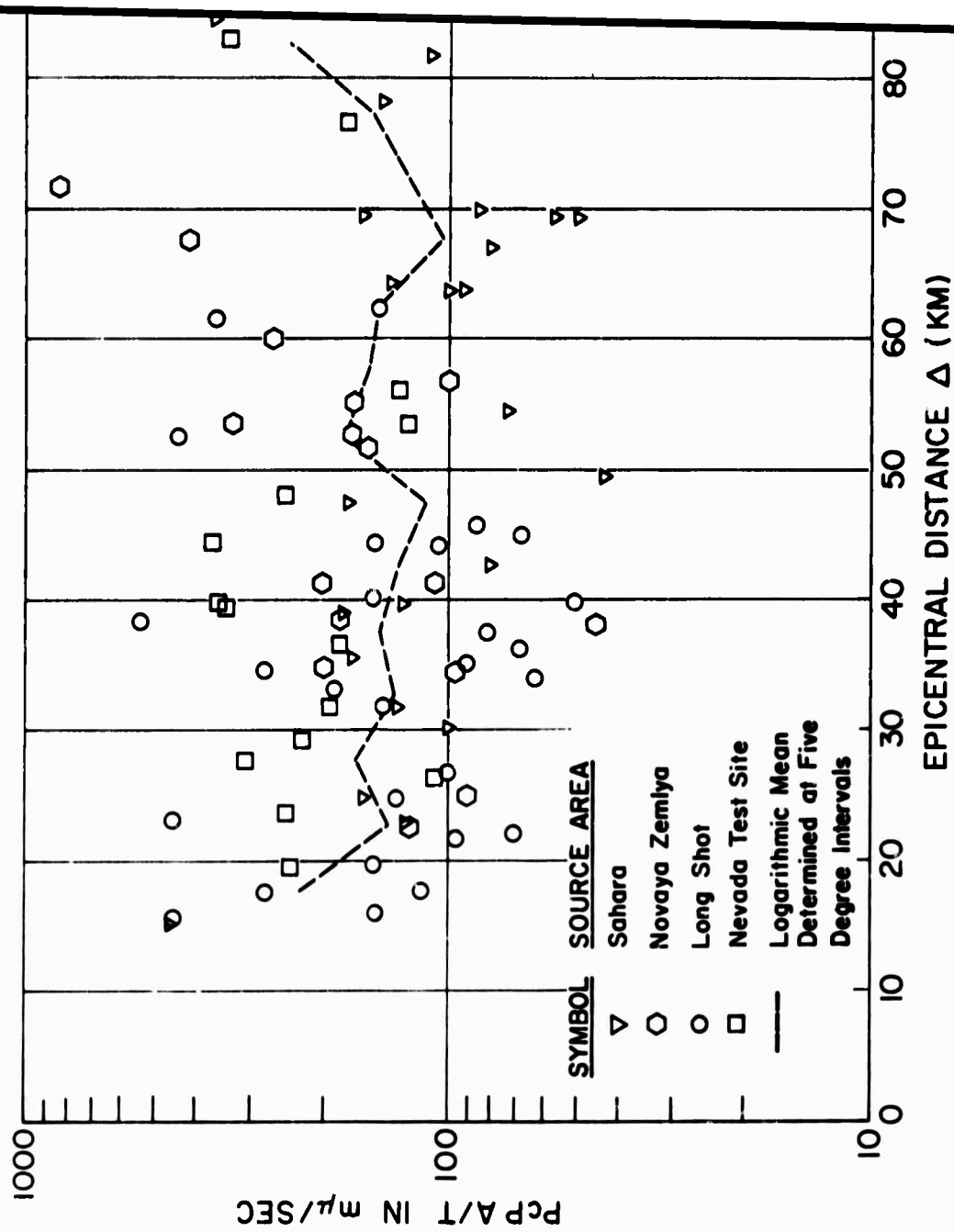
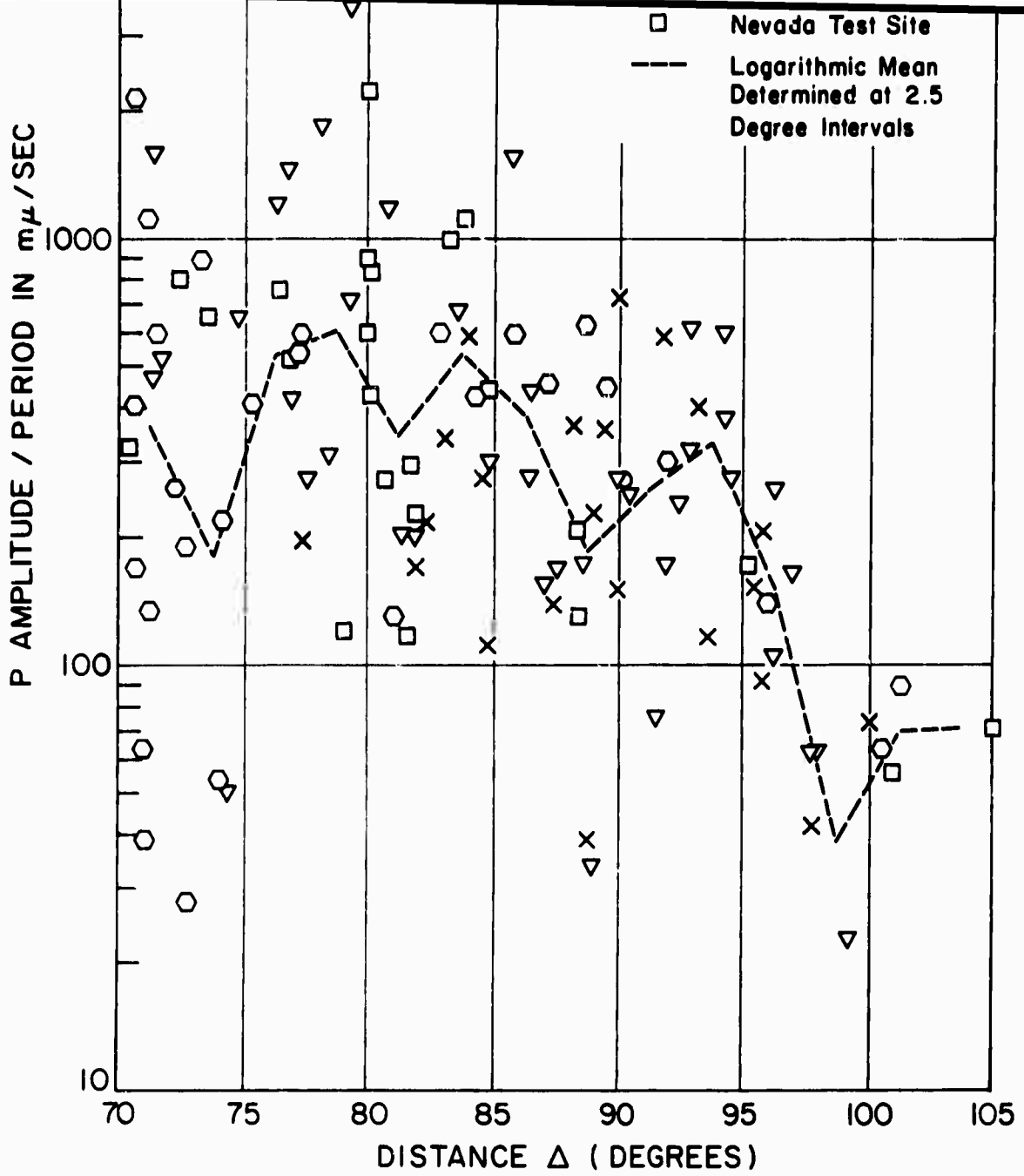


FIGURE 27. VARIATION OF VERTICAL A/T OF PcP WITH EPICENTRAL DISTANCE.

can only be estimated since the lower amplitude arrivals are either lost in the P coda or are below the threshold of detectability. The range of scatter is probably on the same order as that of P for comparable paths. The vertical amplitude/period ratio for P waves from nuclear explosions in the distance range 70° to 105° is shown in Figure 28, normalized to magnitude 6.5. Although the variation exceeds 40 decibels, the decrease of amplitude at a distance of about 96° is apparent, marking the beginning of the "shadow zone" for short-period P waves. The ratio PcP/P (vertical components) shown in Figure 29 increases somewhat with distance as indicated by the dashed logarithmic mean. The period ratio of P to PcP is shown in Figure 30 as a function of epicentral distance. The predominance of values less than unity for the Novaya Zemlya ratios is probably the most significant feature of this plot. The PcP amplitude/period ratio is presented as a function of $\overline{\delta r}$ in Figure 31. The relationship appears to be a random one, as does that of the PcP/P ratio A/T as a function of the PcP-P travel-time residual shown in Figure 32.

A Model Study of Crust and Upper Mantle Effects

The high degree of scatter in the PcP amplitude and travel-time data tends to obscure relationships due to conditions at or near the mantle-core boundary. Although lateral variations in velocity may exist in the lower mantle (Chinnery [1969]) it is probable that most of the observed data scatter is due to the inhomogeneity of the crust and upper mantle. Broad regional variations in structure produce travel-time anomalies which may be compensated by the use of source and station corrections or the PcP-P time difference. Anomalies due to more abrupt changes in structure are difficult to correct, requiring detailed knowledge of crust and upper mantle structure or empirical determination of corrections as functions of azimuth and epicentral distance. The velocity structure shown in Figures 33 and 34 is similar to the upper mantle low velocity zone proposed by



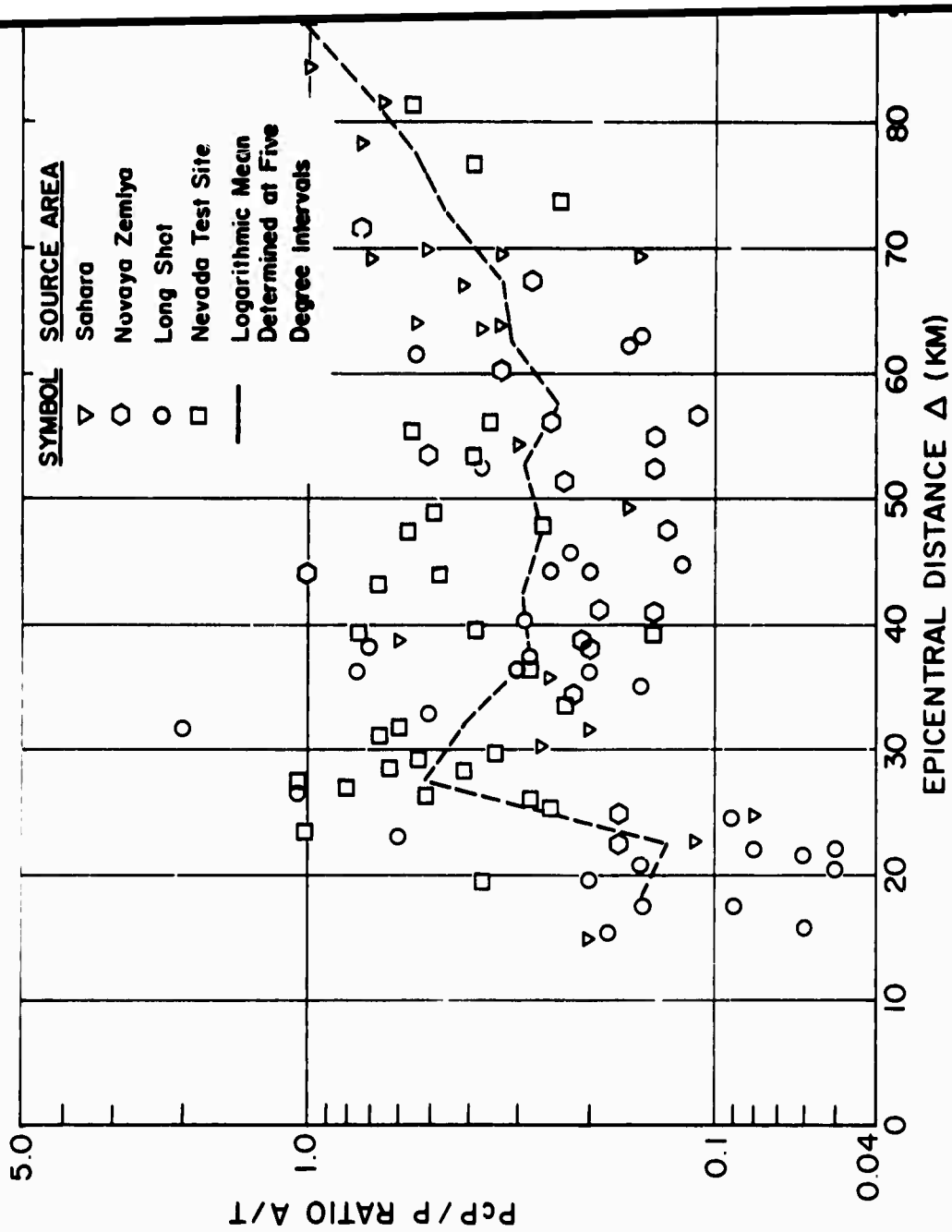


FIGURE 29. VERTICAL PCP/P RATIO A/T AS A FUNCTION OF EPICENTRAL DISTANCE.

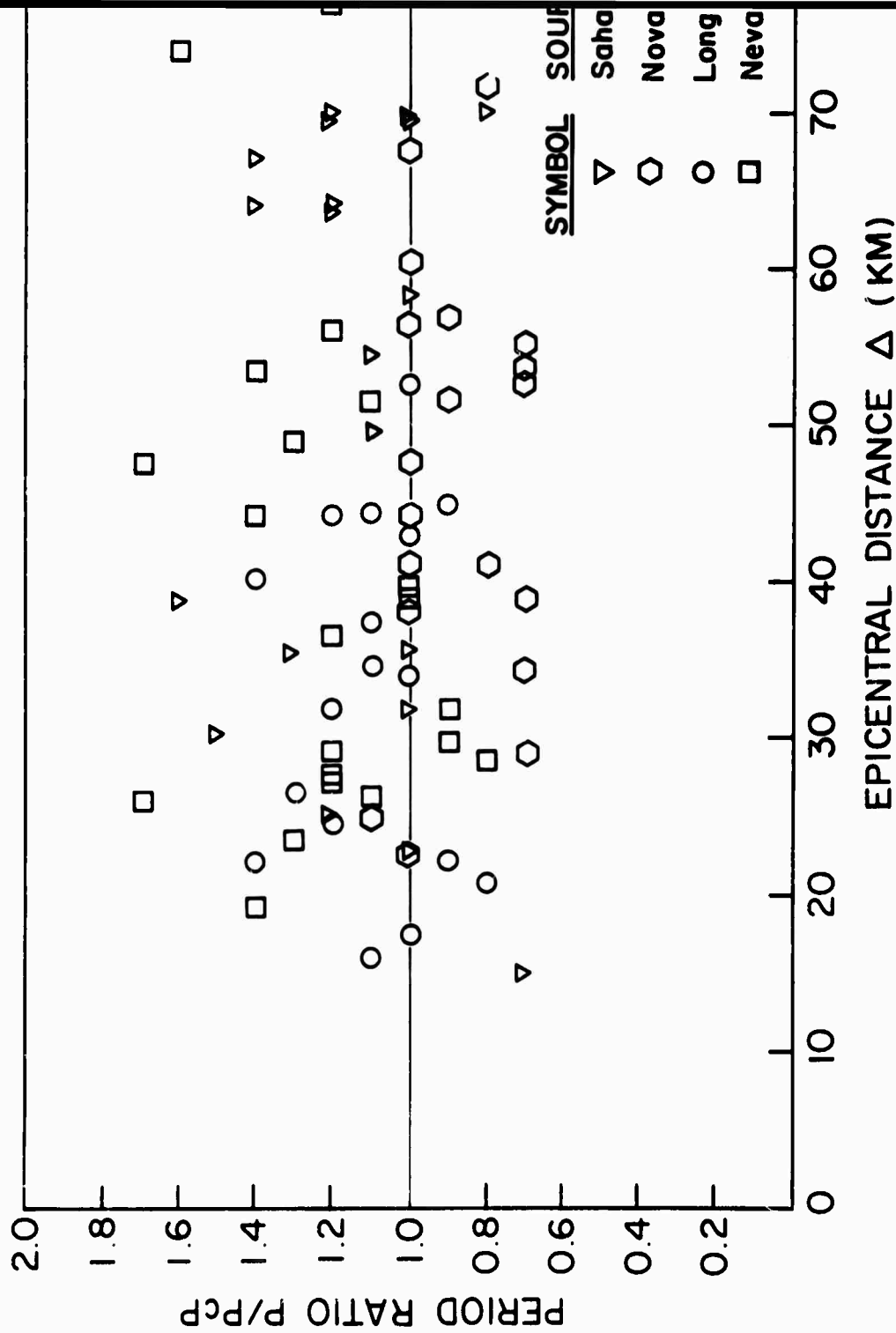


FIGURE 30. VARIATION OF PERIOD RATIO T_p/T_{PcP} WITH EPICENTRAL DISTANCE.

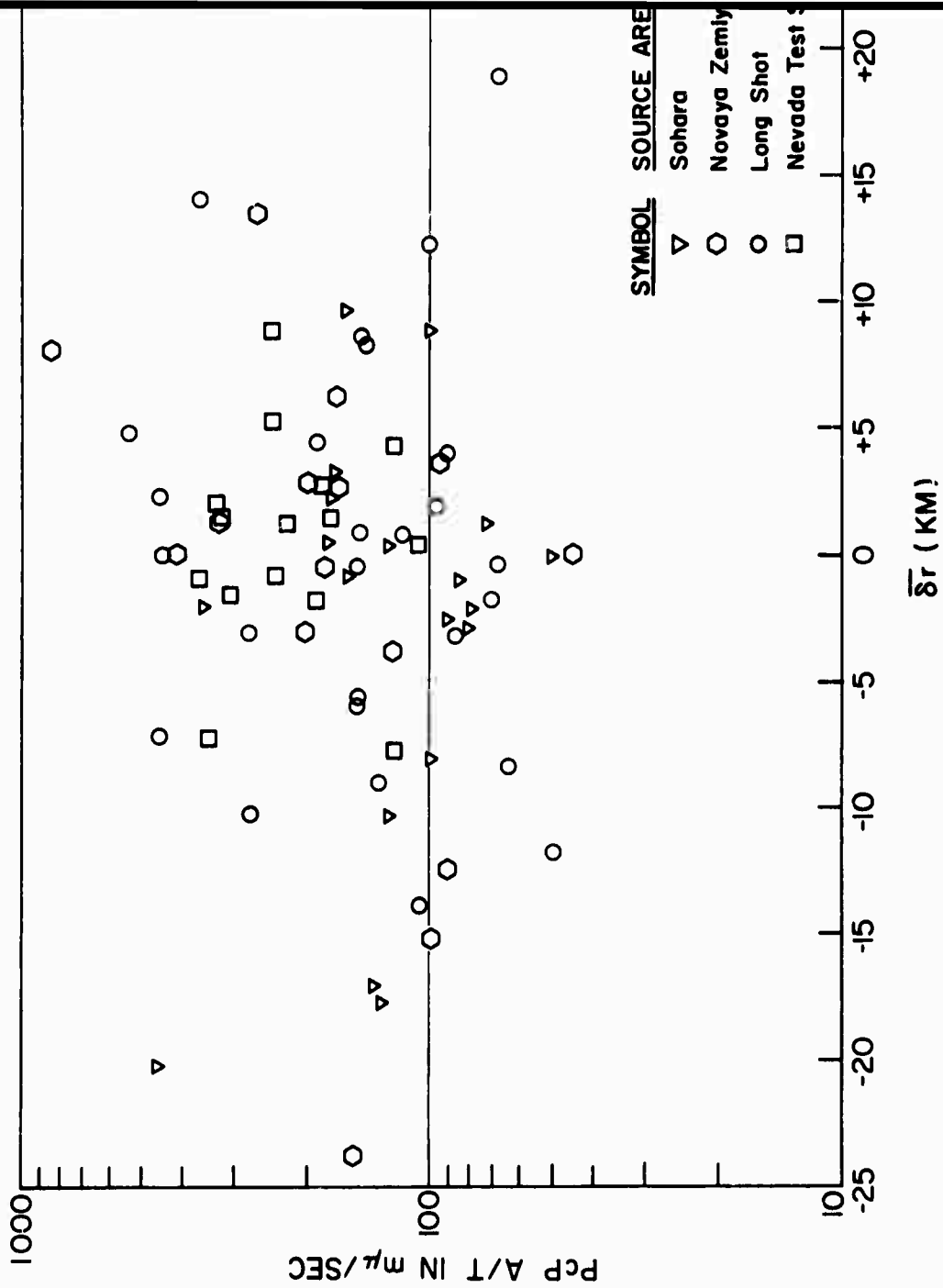


FIGURE 31. PcP A/T RATIO AS A FUNCTION OF δr .

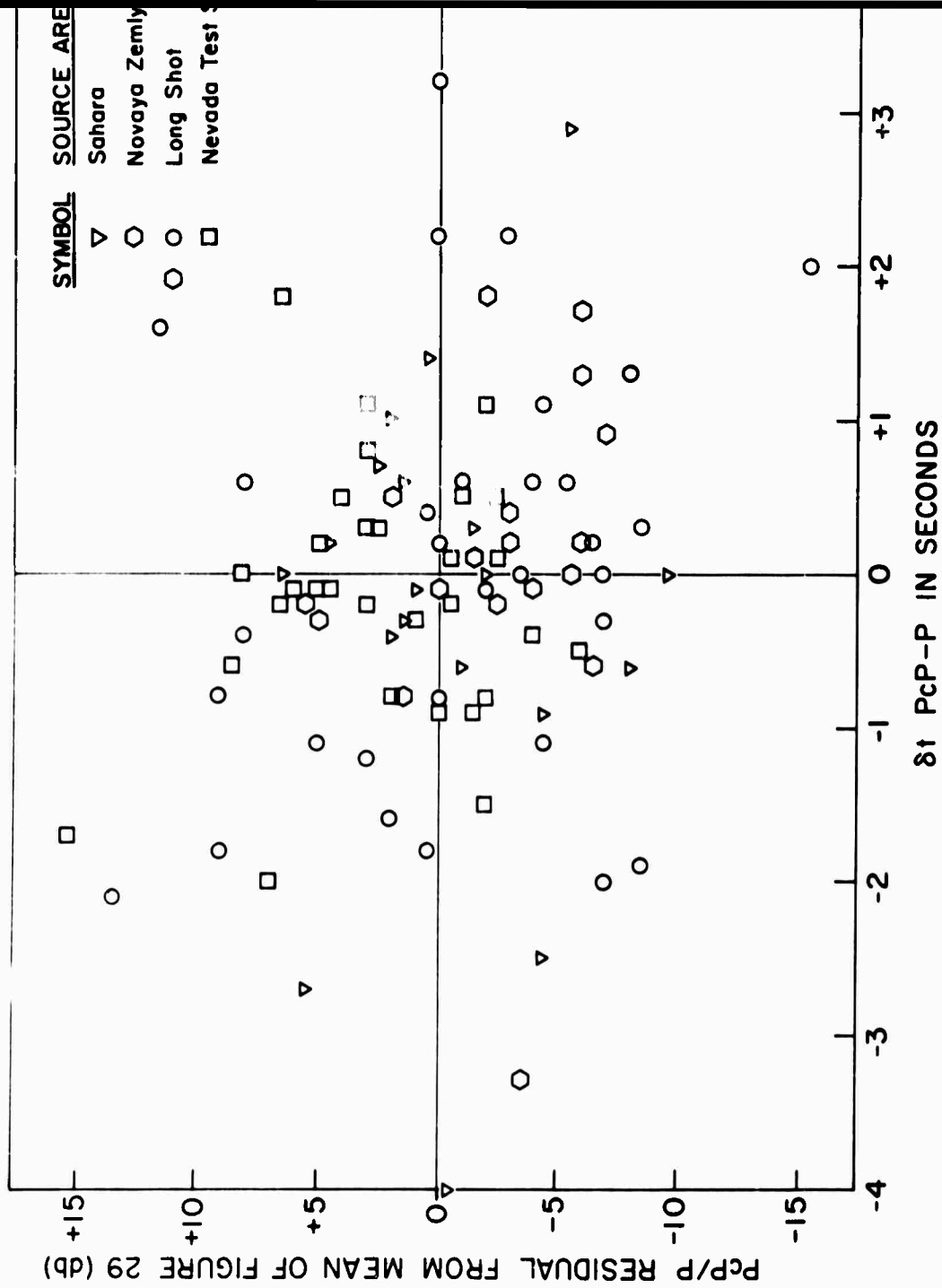


FIGURE 32. PcP/P RESIDUAL OF A/T AS A FUNCTION OF THE PcP-P TRAVEL TIME RESIDUAL.

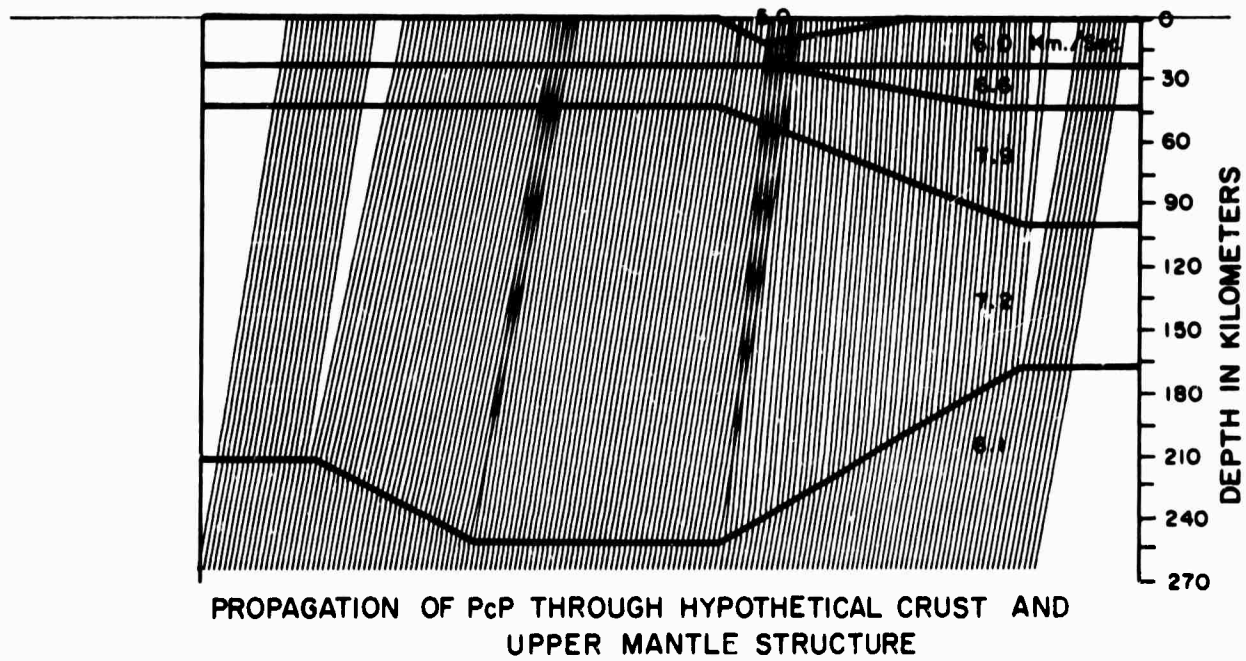
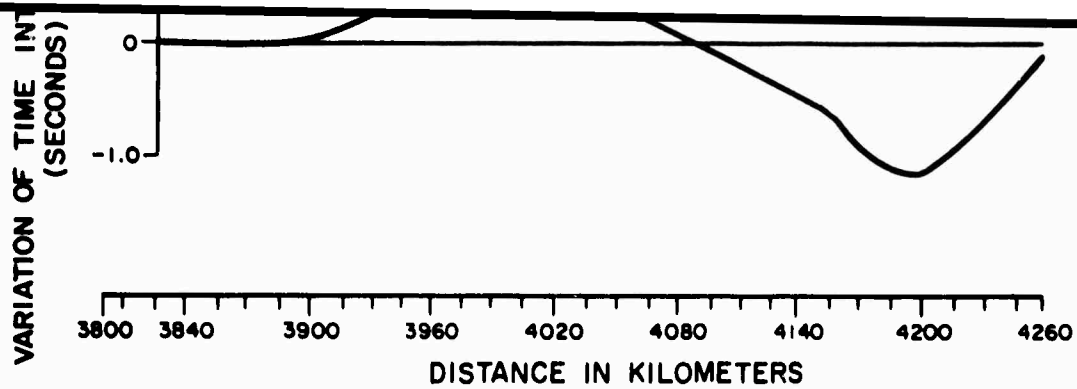


FIGURE 33. EFFECT OF VARIATIONS IN CRUST AND UPPER MANTLE STRUCTURE ON THE PcP-P TRAVEL TIME DIFFERENCE.

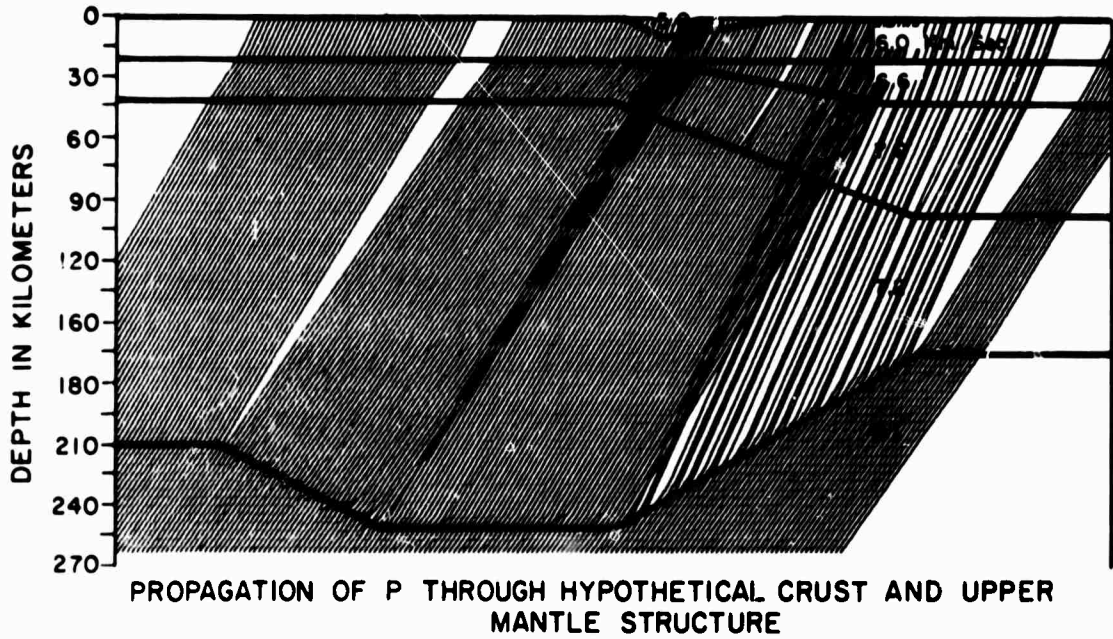
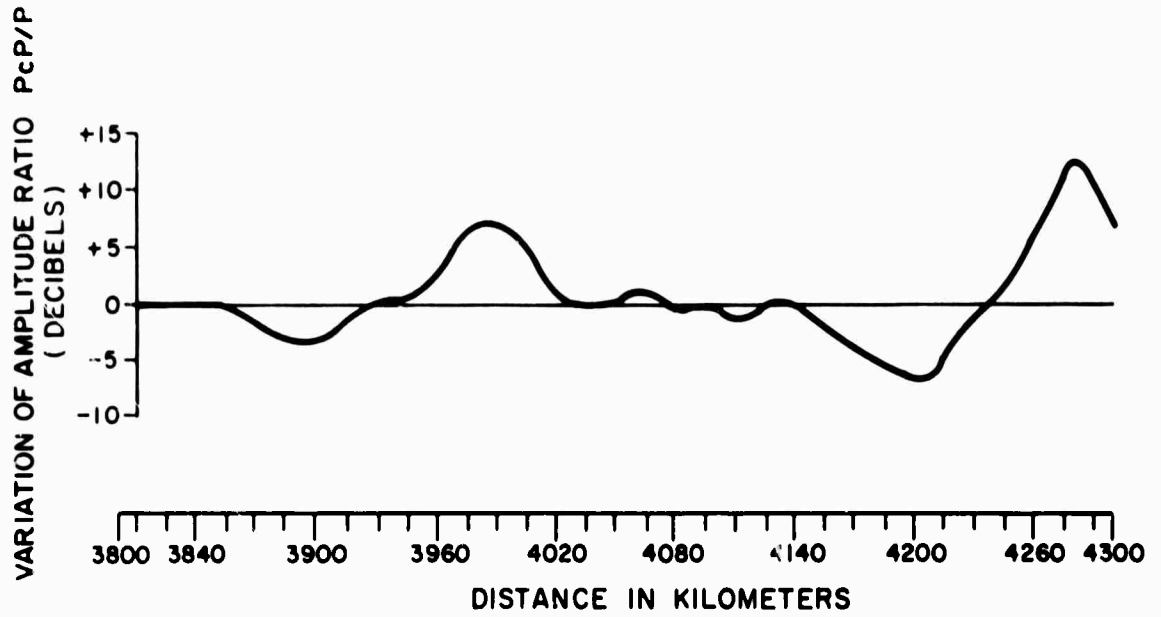


FIGURE 74. EFFECT OF VARIATIONS IN CRUST AND UPPER MANTLE STRUCTURE ON THE P_cP/P VERTICAL COMPONENT A/T RATIO.

Nuttli and Bolt [1969] to account for P-wave travel residuals at northern California stations. The lateral variations are probably the most extreme proposed anywhere with the exception of a few island arc areas. To evaluate the effect of such a model on the PcP-P time interval, PcP and P were propagated through the structure using the digital ray tracing program developed by Jackson [1968]. Plane waves and a flat earth were assumed, with a 10° angle of incidence at the base of the low velocity zone assumed for PcP (Figure 33), and 35° for P (Figure 34). These are approximately the appropriate angles at an epicentral distance of 35 degrees. Travel-time curves for PcP and P were computed from the ray travel times. The changes in the PcP-P time interval due to lateral variations of the velocity structure are shown at the top of Figure 33. It is evident from an examination of Figures 33 and 34 that there are zones of energy concentration and shadow zones. The travel-time differences of the overlapping wave fronts are generally a small fraction of the period at 1 Hz, so the arrivals will be nearly in phase. The PcP and P vertical amplitudes were taken to be proportional to the ray density at the model is shown at the top of Figure 34. A window of 48 km was used to determine the ray density, thus smoothing the amplitude variations approximate diffraction. These variations, which were found to be as large as 12 db for P and 8 db for PcP, could thus result in a variation of as much as 20 db for the ratio PcP/P. A similar crust and upper mantle structure to the north in British Columbia could account in part for the anomalous amplitudes of P and PcP observed for the Longshot event at Prince George, British Columbia, Figure 6. However, it is likely that the structure near Longshot could also contribute to the amplitude anomaly.

Summary and Conclusions

Travel times of PcP and P phases from nuclear and high explosive sources have been interpreted in terms of variations in the radius of the outer core. This interpretation results in a core which is slightly larger than that of the reference model of Taggart and Engdahl [1968] and has less ellipticity than estimated by Bullen [1936]. The distribution of data does not permit a conventional spherical harmonic analysis of the

inferred variation in core radius. A modified spherical harmonic analysis method is devised to smooth the data and to estimate the shape of the core. The variation of core radius determined from this representation is approximately 10 kilometers on the basis of terms to degree and order 5. The standard deviation of the data is approximately ± 20 kilometers, indicating the presence of variations of higher degree and order, many of which are probably due to factors other than undulation of the mantle-core boundary. Geoid heights computed from the harmonic coefficients (Set 2) do not correlate with, but are within the range of, those determined from gravity data. Analysis of PcP amplitude data shows no significant variation of amplitude with distance and an amplitude scatter on the same order as that of P. The possible contribution of an upper mantle low velocity zone of varying thickness to the amplitude and travel-time scatter is demonstrated.

Recommendations

The present study was greatly limited by the geographical distribution of events. Contained nuclear explosions and underwater high explosive shots, especially those whose zero times and locations are made known, provide a unique seismological tool for the determination of the detailed structure of the earth. One of the peaceful uses of atomic energy should be the detonation of underground explosions of approximate magnitude 6 at locations selected to provide eventual global coverage. These detonations should be announced well in advance to allow maximum participation in the recording program. Shots in the central Pacific and in the southern hemisphere are especially needed to fill the largest existing data gaps.

Additional surface-focus sources will permit refinement of source and station corrections as functions of both azimuth and epicentral distance.

The period ratio of P to PcP was found to be generally less than one for the Novaya Zemlya event of October 27, 1966. For other surface-focus events this ratio has been predominantly equal to or greater than one. Events in this region warrant further investigation to determine whether this unusual phenomenon is due to the velocity structure beneath the source or to a complex source function.

Travel times and amplitudes of short-period P waves in the distance range 90° to 140° and of PcP beyond 70° should be studied to determine in detail the velocity structure of the lowest few hundred kilometers of the

mantle and the magnitude of the density jump at the mantle-core boundary.

REFERENCES

- Bolt, B. A. [1969], "Features of the upper mantle, and the boundaries of the outer and inner core," Paper presented at the Annual Meeting of the Seismological Society of America, St. Louis, Missouri, April.
- Buchbinder, G. G. R. [1965], "PcP from the nuclear explosion Bilby, September 13, 1963," Bulletin of the Seismological Society of America, Vol. 55, No. 2, pp. 441-461, April 1965.
- Buchbinder, G. G. R. [1968a], "Properties of the core-mantle boundary and observations of PcP," Journal of Geophysical Research, Vol. 73, No. 18, pp. 5901-5923, September 15, 1968.
- Buchbinder, G. G. R. [1968b], "Amplitude spectra of PcP and P phases," Bulletin of the Seismological Society of America, Vol. 58, No. 6, pp. 1797-1820, December 1968.
- Buchbinder, G. G. R. [1969], Personal communication.
- Bufe, C. G. and D. E. Willis [1969], "Short-period teleseismic energy from Aleutian sources," Bulletin of the Seismological Society of America, October 1969 (in press).
- Bullen, K. E. [1936], "The variation of density and the ellipticities of strata of equal density within the earth," MNRAS, Geophys. Suppl., pp. 395-401, April 1936.
- Bullen, K. E. [1938], "Ellipticity corrections to earthquake waves reflected at the central core," MNRAS, Geophys. Suppl., Vol. 4, pp. 332-335, May 1968.
- Carder, D. S. [1964], "Travel times from central Pacific nuclear explosions and inferred mantle structure," Bulletin of the Seismological Society of America, Vol. 54, No. 6, Part B, pp. 2271-2294, December 1964.
- Carder, D. S., D. W. Gordon, and J. N. Jordan [1966], "Analysis of surface focus travel times," Bulletin of the Seismological Society of America, Vol. 56, No. 4, pp. 815-840, August 1966.
- Carder, D. S., D. Tocher, C. Bufe, S. W. Stewart, J. Eisler, and E. Berg, [1967], "Seismic wave arrivals from Long shot, 0° to 27°," Bulletin of the Seismological Society of America, Vol. 57, No. 4, pp. 573-590.
- Carder, D. S. [1968], Personal communication.
- Chinnery, M. [1969], "The velocity anomaly at 2000 km depth," Abstract S55, Transactions American Geophysical Union, Vol. 50, No. 4, April 1969.
- Clark, D. M. [1965], Long range seismic measurements—CHASE III, Seismic Data Laboratory Report, 124, United Electro-Dynamics, Earth Sciences Division, Teledyne, Inc., October 1965.

- Clark, D. M. [1966a], Long range seismic measurements—Longshot, Seismic Data Laboratory Report, 133, United Electro-Dynamics, Earth Sciences Division, January 1966.
- Clark, D. M. [1966b], Long range seismic measurements—CHASE IV, Seismic Data Laboratory Report, 137, United Electro-Dynamics, Earth Sciences, Division, Teledyne, Inc., February 1966.
- Cleary, J. and A. L. Hales [1966], "An Analysis of the travel times of P waves to North American stations, in the distance range 32° to 100°," Bulletin of the Seismological Society of America, Vol. 56, No. 2, pp. 467-489, April 1966.
- Cleary, J. [1967], "Azimuthal variation of the Longshot source term," Earth and Planetary Science Letters, 3, pp. 29-37.
- Dahlman, O. [1967], "Seismic records from the Longshot event obtained at the Uddeholm temporary station in Sweden," FOA 4 rapport C4281-23, February, 8 pp., Research Inst. of Nat. Defense, Stockholm 80, Sweden.
- Doyle, H. and J. Webb [1958], Department of Geology, University of Queensland, Brisbane, Australia, Personal communication 1958 obtained through the courtesy of D. S. Carder.
- Egyed, L. [1964], "The Satellite geoid and the structure of the earth," Nature, July 4, 1964, pp. 67-69, Vol. 203, No. 4940.
- Engdahl, E. R. [1968], "Seismic waves within the earth's outer core: Multiple reflection," Science, 161, pp. 263-264, July 19, 1968.
- Ergin, K. [1967], "Seismic evidence for a new layered structure of the earth's core," Journal of Geophysical Research, Vol. 72, No. 14, pp. 3669-3687, July 15, 1967.
- Gutenberg, B. and C. F. Richter [1935], "On seismic waves," (second paper), Gerlands Beitrage zur Geophysik, Vol. 43, pp. 280-360.
- Herrin, E., et al. [1968], "1968 Seismological tables for P phases," Bulletin of the Seismological Society of America, Vol. 58, No. 4, pp. 1193-1241, August 1968.
- Herrin, E. and J. Taggart [1968], "Regional variations in P travel times," Bulletin of the Seismological Society of America, Vol. 58, No. 4, pp. 1325-1337, August 1968.
- Izsak, I. G. [1964], "Tesseral harmonics of the geopotential and corrections to station coordinates," Journal of Geophysical Research, Vol. 69, No. 12, pp. 2621-2630, June 15, 1964.
- Jackson, P. L. [1968], "Two- and three-dimensional ray tracing, travel time and amplitude computation," Paper presented at the Annual Meeting of the Seismological Society of America, Tuscon, Arizona, April 13, 1968.

- Jeffreys, H. [1935], "On the ellipticity correction in seismology," MNRAS, Geophys. Suppl. Vol. 3, No. 7, 271-274.
- Jeffreys, H. [1962], The Earth, Cambridge University Press, Cambridge, 4th edition), 438 p. illus.
- Jordan, J. N. [1968], Personal communication, (Computer printouts compiled by seismology division, ESSA).
- Kanamori, H. [1967], "Spectrum of P and PcP in relation to the mantle-core boundary and attenuation in the mantle," Journal of Geophysical Research, Vol. 72, pp. 2171-2186.
- Kaula, W. M. [1966], "Tesseral harmonics of the earth's gravitational field from camera tracking of satellites," Journal of Geophysical Research, Vol. 71, No. 18, pp. 4377-4388, September 15, 1966.
- Kogan, S. D. [1960], "Travel times of longitudinal and transverse waves, calculated from data on nuclear explosions made in the region of the Marshall Islands," Izv. Geophys. Ser., 1960, pp. 371-380.
- Kogan, S. D. [1968], "Transit times and amplitude of the PcP wave in the case of surface foci," Izv., Earth Physics, No. 3, pp. 3-10.
- Lehmann, I. [1953], "On the shadow of the earth's core," Bulletin of the Seismological Society of America, Vol. 43, pp. 291-306.
- MacMillan, W. D. [1930], The Theory of the potential, Dover Publishing, Inc., New York, 469 p. illus.
- Nuttli, O. W. and B. A. Bolt [1969], "Undulations of the mantle low-velocity channel as an explanation of azimuth-dependent P wave residuals," Paper presented at the Annual Meeting of the Seismological Society of America, St. Louis, Missouri, April 1, 1969.
- Pollack, H. N. [1968], Personal communication.
- Sacks, I. S. [1967], "Diffracted P-wave studies of the earth's core. 2, lower mantle velocity, core size, lower mantle structure," Journal of Geophysical Research, Vol. 72, No. 10, pp. 2589-2594, May 15, 1967.
- Taggart, J. N. and E. R. Engdahl [1968], "Estimation of PcP travel times and the depth to the core," Bulletin of the Seismological Society of America, Vol. 58, No. 4, pp. 1293-1303, August 1968.
- Toksöz, M. N. and J. Arkani-Hamed [1967], "Seismic delay times: correlation with other data," Science, Vol. 158, pp. 783-785, November 10, 1967.
- Vogel, A. [1960], "Irregularities of the outer boundary of the earth's core on the basis of seismic waves reflected at the core," Gerlands Beitrage zur Geophysik, Vol. 69, No. 3, pp. 150-174.

APPENDIX 1
Basic Data Listed by Event

Event: Long Shot

Station	Distance (deg)	P		PcP		PcP Travel Time Reference	P		PcP		PcP A/T (mi./sec)
		Travel Time Observed (min:sec)	Travel Time Observed (min:sec)	Travel Time Observed (min:sec)	Travel Time Observed (min:sec)		Travel Time Corrected (min:sec)	Travel Time Corrected (min:sec)	A/T	A/T	
CPR	13.173	3:08.5	8:37.9	2*	3:08.7	8:39.3	.10	18.			
NOM	15.424	3:38.9	8:41.7	2*	3:39.1	8:43.1	.18	180.			
BC6	15.960	3:45.2	8:41.0	2*	3:45.4	8:42.3	.09	59.			
KDC	17.498	4:00.9	8:44.2	2*	4:01.2	8:45.5	.15	110.			
TTL	17.556	4:05.9	8:44.8	2*	4:06.2	8:46.2	.09	46.			
AMU	19.558	4:28.5	8:47.0	2*	4:28.9	8:48.3	.20	60.			
PL6	20.176	4:36.6	8:47.9	2*	4:37.1	8:49.4					
TNN	20.272	4:37.6	8:49.7	2*	4:38.0	8:51.1	.05				
MCK	20.767	4:40.6	8:49.4	2*	4:41.0	8:50.7	.11				
COL	21.686	4:49.7	8:50.2	2*	4:50.1	8:51.6	.06	38.			
BLR	22.016	4:53.6	8:52.7	2*	4:54.0	8:54.0	.08				
PX6	22.025	4:53.7	8:52.0	2*	4:54.0	8:53.2	.05	28.			
BRW	22.703	5:02.0	8:53.4	2*	5:02.5	8:55.0	.02				
HS6	23.137	5:03.3	8:53.9	2*	5:03.8	8:55.5	.50	180.			
AV6	23.863	5:13.7	8:56.6	2*	5:14.2	8:58.0					
BH-	24.683	5:20.1	8:58.5	2*	5:20.6	8:59.8	.14	53.			
WH-	26.599	5:38.1	9:02.5	2*	5:38.6	9:03.8	1.05	40.			
WL-	26.797	6:07.1	9:08.5	6	6:07.5	9:09.6	.20	13.			
SI-	31.774	6:26.7	9:15.4	6*	6:27.1	9:16.4	2.00	57.			
MAT	32.551	6:32.8	9:18.4	1	6:33.0	9:18.9					
PHC	32.937	6:36.9	9:19.5	7	6:37.3	9:20.5	.50	75.			
FL-	32.991	6:34.1	9:18.1	6*	6:34.5	9:19.2	.1	47.			
MBC	34.031	6:44.1	9:22.1	7	6:44.8	9:23.7	.23	25.			

Event: Long Shot

Station	Distance (deg)	P		PcP		PcP Travel Time Reference	P		PcP		PcP/P A/T	PcP A/T (ml/sec)
		Travel Time Observed (min:sec)	Travel Time Corrected (min:sec)	Travel Time Observed (min:sec)	Travel Time Corrected (min:sec)		Travel Time Corrected (min:sec)	Travel Time Corrected (min:sec)				
PG-	34.548	6:48.9	6:49.2	9:23.5	9:24.4	6*	6:49.2	9:24.4	4.50	110.		
CMC	35.000	6:51.9	6:52.5	9:23.3	9:24.7	1	6:52.5	9:24.7	.15	36.		
YKC	36.169	7:01.9	7:02.5	9:26.9	9:28.2	7	7:02.5	9:28.2	.20	27.		
VIC	36.222	7:03.9	7:04.3	9:28.7	9:29.6	7	7:04.3	9:29.6	.75			
KV-	36.387	7:02.9	7:03.4	9:27.9	9:29.0	6	7:03.4	9:29.0	.30	33.		
JP-	37.419	7:12.7	7:13.0	9:31.5	9:32.4	6	7:13.0	9:32.4	.28	32.		
LON	38.014	7:18.3	7:18.6	9:33.7	9:34.4	1	7:18.6	9:34.4				
PNT	38.092	7:18.6	7:19.0	9:33.9	9:34.8	6	7:19.0	9:34.8				
COR	38.206	7:21.7	7:22.1	9:35.7	9:36.5	1	7:22.1	9:36.5	.70	215.		
SEO	38.904	7:27.0	7:27.3	9:36.6	9:37.2	1	7:27.3	9:37.2				
RM6	39.365	7:28.3	7:28.6	9:37.5	9:38.4	7	7:28.6	9:38.4				
EDM	39.883	7:32.4	7:32.8	9:39.8	9:40.7	7	7:32.8	9:40.7	.05	20.		
YR-	40.148	7:37.9	7:38.2	9:41.1	9:41.8	6	7:38.2	9:41.8	.29	60.		
RES	40.298	7:35.9	7:36.6	9:38.4	9:39.9	7	7:36.6	9:39.9				
BMO	41.694	7:48.6	7:48.8	9:45.1	9:45.7	6	7:48.8	9:45.7				
HHM	41.795	7:49.6	7:49.9	9:45.1	9:45.8	8	7:49.9	9:45.8				
SW-	42.661	7:55.9	7:56.2	9:48.2	9:48.9	6	7:56.2	9:48.9				
BKS	42.694	7:57.7	7:58.0	9:49.8	9:50.4	1	7:58.0	9:50.4				
ALE	42.790	7:57.6	7:58.4	9:47.5	9:49.1	7	7:58.4	9:49.1				
BUT	43.872	8:05.5	8:05.6	9:50.5	9:51.0	8	8:05.6	9:51.0				
HL2	44.136	8:08.8	8:08.9	9:54.5	9:54.9	6	8:08.9	9:54.9	.25	60.		
HV-	44.158	8:07.1	8:07.4	9:53.9	9:54.6	6	8:07.4	9:54.6	.20	42.		
BOZ	44.642	8:11.8	8:11.9	9:55.4	9:55.9	8	8:11.9	9:55.9				
MN-	44.889	8:15.9	8:16.0	9:55.4	9:55.8	6	8:16.0	9:55.8	.12	27.		

Event: Long Shot

Station	Distance (deg)	P		PcP		PcP Travel Time Reference	P		PcP		PcP A/T (min./sec)
		Travel Time Observed (min:sec)	Travel Time Observed (min:sec)	Travel Time Corrected (min:sec)	Travel Time Corrected (min:sec)		Travel Time Corrected (min:sec)	Travel Time Corrected (min:sec)			
FFC	45.152	8:14.9	9:55.8	8:15.4	9:56.8	7	8:15.4	9:56.8			
EUR	45.591	8:21.4	9:58.5	8:21.4	9:58.8	8	8:21.4	9:58.8			
TIN	45.698	8:22.6	10:00.4	8:22.7	10:00.8	6	8:22.7	10:00.8			34.
TF-	45.820	8:22.9	9:59.9	8:23.1	10:00.3	6	8:23.1	10:00.3		.22	
KRC	45.854	8:23.5	9:59.9	8:23.7	10:00.3	6	8:23.7	10:00.3			
WDY	46.174	8:25.0	9:59.4	8:25.2	9:59.8	6	8:25.2	9:59.8			
FTC	46.614	8:29.3	10:03.1	8:29.4	10:03.4	6	8:29.4	10:03.4			
CLC	46.878	8:30.8	10:04.1	8:31.0	10:04.5	6	8:31.0	10:04.5			
LAO	47.148	8:31.1	10:04.1	8:31.4	10:04.8	6	8:31.4	10:04.8			
MWC	47.624	8:36.5	10:06.9	8:36.5	10:07.1	6	8:36.5	10:07.1			
GSC	47.703	8:37.0	10:07.0	8:37.1	10:07.4	6	8:37.1	10:07.4			
RVR	48.202	8:40.6	10:08.9	8:40.8	10:09.3	6	8:40.8	10:09.3			
BCN	48.488	8:43.7	10:09.7	8:43.9	10:10.1	8	8:43.9	10:10.1			
FGU	48.705	8:43.4	10:09.4	8:43.5	10:09.9	8	8:43.5	10:09.9			
UBO	48.968	8:46.9	10:10.9	8:47.0	10:11.3	6	8:47.0	10:11.3			
KN-	49.058	8:48.7	10:12.1	8:48.7	10:12.4	6	8:48.7	10:12.4			
HAY	49.475	8:50.4	10:13.3	8:50.6	10:13.7	6	8:50.6	10:13.7			
RG-	49.529	8:48.9	10:12.5	8:49.2	10:13.1	6	8:49.2	10:13.1			
CP-	49.669	8:52.5	10:14.2	8:52.6	10:14.5	6	8:52.6	10:14.5			
GCA	49.847	8:53.4	10:14.5	8:53.5	10:14.8	8	8:53.5	10:14.8			
RCD	50.403	8:55.9	10:16.1	8:56.1	10:16.7	1	8:56.1	10:16.7			
TFO	51.803	9:09.1	10:21.9	9:09.1	10:22.1	6	9:09.1	10:22.1			
GOL	51.866	9:09.2	10:21.4	9:09.2	10:21.6	1	9:09.2	10:21.6			

Event: Long Shot

Station	Distance (deg)	P		PcP		PcP Travel Time Reference	P		PcP		PcP/P A/T	PcP A/T (m /sec)
		Travel Time Observed (min:sec)	Travel Time Observed (min:sec)	Travel Time Corrected (min:sec)	Travel Time Corrected (min:sec)		Travel Time Corrected (min:sec)	Travel Time Corrected (min:sec)				
WN-	52.629	9:13.3	10:23.9	6	9:13.5	10:24.5				.37	175.	
WAW	57.437	9:47.6	10:41.6	7	9:48.0	10:42.3						
FIM	58.780	9:57.5	10:48.3	17	9:57.9	10:49.0				.10	35.	
WMO	59.213	10:01.0	10:49.8	6	10:01.2	10:50.2						
SV3	60.782	10:10.7	10:55.3	6	10:11.2	10:56.2						
FAY	60.844	10:15.9	10:56.7	1	10:16.1	10:57.1						
GV-	61.437	10:16.7	10:58.9	6	10:16.9	10:59.3						
DAL	61.593	10:18.4	10:59.1	6	10:18.6	10:59.5				.54	145.	
AAM	62.289	10:20.9	11:01.3	1	10:21.2	11:01.9				.16	59.	
BGM	62.289	10:21.0	11:01.8	17	10:21.3	11:02.4				.30	22.	
EN-	62.349	10:20.6	11:02.9	6	10:20.9	11:03.3						
LND	63.030	10:25.9	11:04.2	7	10:26.3	11:04.8				.15		
OXF	64.716	10:38.5	11:13.3	1	10:38.8	11:13.7						
UPP	68.064	10:57.6	11:26.2	6	10:58.3	11:27.2						
UDD	68.221	10:58.8	11:23.3	16	10:59.5	11:24.2						
CHG	69.479	11:08.8	11:32.6	1	11:08.8	11:32.7						
WRA	81.185	12:14.5	12:19.1	*	12:14.7	12:19.3						
GBA	86.654	12:43.5	12:45.8	*	12:43.4	12:45.7						

Event: Novaya Zemlya 10/27/66 05:58:00.0 73.40N 54.87E

Station	Distance (deg)	P tt Obs. (min:sec)	PcP tt Obs. (min:sec)	PcP tt Reference	P tt Corr. (min:sec)	PcP tt Corr. (min:sec)	T P (sec)	T PcP (sec)	P(A/T) (m / sec)	PcP A/T (m / sec)	PcP P A/T
KTG	22.521	5:01.0	8:54.7	*	5:01.6	8:56.7	1.1	1.1	741.	126.	.17
AKU	24.950	5:25.9	9:01.1	*	5:26.5	9:03.0	1.1	1.0	529.	90.	.17
CLL	28.360	5:54.9	9:08.7	8	5:55.4	9:10.1					
ESK	29.219	6:02.6	9:09.1	*	6:03.1	9:10.6	.8	1.1			
VKA	30.368	6:13.7	9:23.2	5	6:14.1	9:24.5					
RES	31.304	6:17.5	9:13.5	*	6:18.2	9:15.5					
STR	32.213	6:29.8	9:01.2	*	6:30.3	9:02.5					
TRI	33.374	6:39.2	9:20.2	*	6:39.7	9:20.7					
NEU	33.888	6:41.9	9:21.5	5	6:43.1	9:22.7					
BES	33.910	6:43.1	9:15.5	5	6:43.6	9:16.8					
BRW	34.141	6:47.0	9:22.8	5	6:47.8	9:24.7					
VAL	34.209	6:46.4	9:22.6	*	6:47.0	9:24.0	.8	1.1	432.	95.	.22
IST	34.703	6:50.9	9:24.4	*	6:51.4	9:25.5		1.0		200.	
FBC	38.053	7:18.2	9:33.0	*	7:18.9	9:34.7	1.1	1.1	225.	45.	.20
CIN	38.211	7:21.3	9:33.9	8	7:21.8	9:34.9					
CMC	38.857	7:26.3	9:36.4	*	7:27.0	9:38.2	.8	1.1	867.	182.	.21
BLC	41.090	7:44.6	9:43.8	*	7:45.4	9:45.5	1.0	1.0	1450.	203.	.14
COL	41.139	7:46.2	9:41.7	*	7:47.0	9:43.4	.9	1.2	563.	107.	.19
TOL	43.458	8:28.9	10:17.9	*	8:29.3	10:18.9					
YKC	44.199	8:08.9	9:54.9	*	8:09.6	9:56.5	1.1	1.1			1.0

Event: Novaya Zemlya 10/27/66. 05:58:00.0 73.40N 54.87E (Cont.)

Station	Distance (deg)	P tt Obs. (min:sec)	PcP tt Obs. (Min:sec)	PcP tt		T P (sec)	T PcP (sec)	P(A/T) (m /sec)	PcP A/T (m /sec)	PcP/P A/T
				P tt Corr. (min:sec)	Reference					
PMR	44.311	8:10.5	9:54.9	8:11.3	8	1.2	1.2	670.	154.	.23
NDI	46.296	8:27.5	10:02.6	8:27.9	5	.6	.9	1207.	169.	.14
MAL	46.508	8:28.9	10:02.6	8:29.4	5	.8	1.1	641.	327.	.51
GWC	47.603	8:34.6	10:05.7	8:35.3	*	1.2	1.2			.13
KDC	47.815	8:38.5	10:08.2	8:39.3	8					
RBA	49.730	8:53.5	10:16.7	8:54.0	5					
SIC	50.361	8:57.5	10:15.6	8:58.1	*					
PDA	51.590	9:07.9	10:23.7	9:08.5	*	1.2	1.3	670.	154.	.23
FSJ	52.456	9:14.2	10:24.1	9:14.8	*	.6	.9	1207.	169.	.14
EDM	53.413	9:20.7	10:27.5	9:21.3	*	.8	1.1	641.	327.	.51
MAT	53.514	9:21.1	10:27.0	9:21.5	5					
SHK	53.805	9:21.7	10:28.9	9:22.2	5					
SFA	54.189	9:25.9	10:30.2	9:26.5	*					
DDR	54.302	9:27.1	10:31.1	9:27.5	8					
ABU	54.331	9:27.8	10:30.7	9:28.3	5					
TSK	54.365	9:26.5	10:30.7	9:27.0	8					
SRY	54.690	9:29.5	10:32.6	9:30.0	8					
MCC	54.763	9:31.0	10:34.9	9:31.7	*					
HAL	55.058	9:32.3	10:33.8	9:32.9	*	.8	1.1	1221.	171.	.14
POO	55.909	9:38.5	10:38.0	9:38.8	*					

Event: Novaya Zemlya 10/27/66 05:58:00.0 73.40N 54.87E (Cont.)

Station	Distance (deg)	P tt Obs. (min:sec)	PcP tt Obs. (min:sec)	PcP tt		PcP/P A/T					
				Reference	Corr.						
SES	56.121	9:39.4	10:36.8	*	9:40.0	10:38.1					
PHC	56.188	9:41.0	10:37.3	*	9:41.7	10:38.5					
MNT	56.286	9:40.6	10:37.9	*	9:41.2	10:38.9	1.9	2.0			.25
OTT	56.782	9:44.4	10:41.1	*	9:45.1	10:42.2	1.1	1.2	91.	100.	.11
LF1	58.748	9:59.6	10:49.6	8	10:00.1	10:50.6					
WES	58.836	9:59.4	10:44.0	*	10:00.0	10:45.0					
LF4	58.839	9:59.2	10:49.3	*	9:59.7	10:50.2					
SCB	59.036	10:01.4	10:49.4	*	10:02.0	10:50.4					
LAO	59.505	10:04.2	10:50.7	5	10:04.7	10:51.6					
CHG	59.855	10:06.3	10:52.7	*	10:06.6	10:53.1					
TUM	59.876	10:07.7	10:54.0	5	10:08.3	10:55.1					
HKC	60.179	10:09.4	10:54.4	*	10:09.8	10:55.0	1.0	1.0	800.	264.	.33
SCP	61.626	10:19.1	11:04.4	5	10:19.6	11:05.3					
RCD	61.857	10:20.2	11:01.8	5	10:20.7	11:02.6					
KOD	64.514	10:38.6	11:14.3	5	10:38.6	11:14.3					
BAG	67.517	10:57.2	11:24.8	*	10:57.4	11:25.0	.9	.9	1479.	414.	.28
TNP	68.681	11:04.6	11:22.5	5	11:04.9	11:23.0					
SNG	71.467	11:21.5	11:41.0	*	11:21.9	11:41.4	.6	.8	1112.	834.	.75
PAS	72.634	11:28.9	11:41.9	8	11:29.4	11:42.5					

Event: Novaya Zemlya 10/27/66 05:58:00.0 73.40N 54.87E (Cont.)

Station	Distance (deg)	PcP tt				Reference	PcP tt (min:sec)	PcP tt Corr. (min:sec)	T P (sec)	T PcP (sec)	P(A/T) (m /sec)	PcP A/T (m /sec)	PcP/P A/T
		P tt Obs. (min:sec)	PcP tt Obs. (min:sec)	P tt Corr. (min:sec)	PcP tt Corr. (min:sec)								
KIP	82.944	12:28.8	12:33.5	12:29.3	*	12:33.9	12:33.9						
TRN	87.090	12:48.1	12:52.3	12:48.7	*	12:52.6	12:52.6						
PBJ	88.296	12:52.5	12:57.4	12:52.9	5	12:57.7	12:57.7						
CAR	88.594	12:54.2	12:58.6	12:54.6	*	12:58.7	12:58.7						

Event: Faultless

TUL	16.482	3:53.5	8:42.0	3:53.4	5	8:41.9	8:41.9	1.4	1.3	214.	108.	.51
ATL	26.218	5:36.8	9:04.0	5:36.7	*	9:03.9	9:03.9					
VHM	27.329	5:49.3	9:07.9	5:48.8	5	9:07.2	9:07.2					
COL	32.116	6:30.0	9:18.5	6:30.2	5	9:19.3	9:19.3					
KIP	39.666	7:36.0	9:43.5	7:35.8	*	9:43.2	9:43.2	1.1	1.1	909.	345.	.38
ADK	43.285	8:03.7	9:52.2	8:03.9	5	9:52.6	9:52.6					
BHP	44.197	8:11.5	9:56.6	8:11.2	*	9:56.1	9:56.1	1.5	1.1	800.	364.	.47
GDH	44.844	8:16.5	9:56.3	8:16.9	5	9:57.1	9:57.1					
SJG	47.913	8:40.6	10:09.2	8:40.2	*	10:08.6	10:08.6	1.4	1.4	930.	243.	.26
NOR	53.422	9:20.9	10:28.0	9:20.4	*	10:28.9	10:28.9	1.8	1.3	316.	123.	.39
TRN	56.096	9:39.0	10:38.5	9:38.6	*	10:38.1	10:38.1	1.5	1.3	404.	123.	.30
PTO	76.793	11:53.2	12:04.7	11:53.2	*	12:04.7	12:04.7	1.5	1.2	466.	175.	.38
PEL	82.992	12:27.5	12:31.3	12:27.5	*	12:31.3	12:31.3	1.5	1.5	600.	333.	.56

Event: Sahara

2/27/65 11:30:00.0 24.04N 5.01E

Station	Distance (deg)	Pc P tt		Pc P tt		Pc P tt Corr. (min:sec)	T P (sec)	T Pc P (sec)	P(A/T) (m /sec)	Pc P A/T (m /sec)	Pc P/P A/T
		P tt Obs. (min:sec)	Pc P tt Obs. (min:sec)	Reference	P tt Corr. (min:sec)						
MAL	15.020	3:29.6	8:44.1	*	3:29.6	8:43.8	.8	1.2	459.	91.7	.20
TOL	17.547	4:04.4	8:49.9	*	4:04.3	8:49.7					
TRI	22.751	5:02.4	8:55.4	*	5:02.4	8:55.4	.8	.8	227.	25.0	.11
STU	24.911	5:23.5	8:59.7	*	5:23.5	8:59.8	1.2	1.0	400.	32.0	.08
VAL	30.206	6:11.5	9:11.8	*	6:11.6	9:12.0	1.5	1.0	77.	20.0	.26
ESK	31.826	6:29.4	9:17.8	*	6:29.5	9:18.1	.9	.9	131.	26.1	.20
AAE	35.511	7:01.4	9:30.1	*	7:00.6	9:28.9	1.4	1.1			
KON	35.732	6:59.3	9:27.1	*	6:59.5	9:27.5	.9	.9	136.	33.9	.25
NUR	38.914	7:26.0	9:36.9	*	7:26.2	9:37.3	1.1	.7	61.	35.7	.59
NAI	39.829	7:38.2	9:44.4	*	7:37.6	9:43.3		1.1		25.5	
SHI	42.810	7:57.2	9:49.9	*	7:56.7	9:49.2		1.4		15.7	
KEV	47.560	8:36.0	10:06.0	*	8:36.4	10:06.6		.6		35.0	
BUL	49.570	8:52.9	10:12.7	*	8:52.4	10:11.9	1.3	1.2	54.	8.7	.16
PRE	54.364	9:27.7	10:32.1	*	9:27.3	10:31.5	.8	.7	48.	14.3	.30
NOR	58.292	9:56.0	10:48.8	*	9:56.4	10:49.5	1.0	1.0			
POO	63.826	10:33.6	11:10.5	*	10:33.0	11:09.8	1.2	1.0	49.	18.3	.37
NDI	63.967	10:33.0	11:10.3	*	10:32.6	11:09.8	1.0	.8	61.	20.0	.33
TRN	64.277	10:38.7	11:14.0	*	10:38.1	11:13.3	1.1	.8	51.	27.5	.54
SJG	66.049	10:50.0	11:19.3	*	10:49.4	11:18.6					
OGD	67.073	10:55.0	11:23.1	*	10:54.9	11:23.0	1.4	1.0	39.	16.0	.41

Event: Sahara 2/27/65 11:30:00.0 24.04N 5.01E (Cont.)

<u>Station</u>	<u>Distance</u> (deg)	<u>P tt Obs.</u> (min:sec)	<u>PcP tt Obs.</u> (min:sec)	<u>PcP tt</u> <u>Reference</u>	<u>P tt Corr.</u> (min:sec)	<u>PcP tt Corr.</u> (min:sec)	<u>T P</u> (sec)	<u>T PcP</u> (sec)	<u>P(A/T)</u> (m /sec)	<u>PcP A/T</u> (m /sec)	<u>PcP/P</u> <u>A/T</u>
CAR	69.380	11:11.2	11:32.1	*	11:10.4	11:31.3	.8	.8	16.	11.3	.70
GEO	69.411	11:10.6	11:33.5	*	11:10.4	11:33.3	1.0	1.0	67.	10.0	.15
SCP	69.530	11:12.0	11:34.7	*	11:11.8	11:34.5	1.0	.8	98.	32.5	.33
KOD	69.955	11:12.6	11:35.7	*	11:11.6	11:34.7	1.0	1.3	33.	16.9	.51
SHL	77.356	11:55.9	12:00.0	*	11:55.1	11:59.3					
CMC	78.417	12:03.1	12:13.5	*	12:03.5	12:13.9	1.3	1.4	39.	28.6	.74
LPB	81.937	12:22.2	12:24.0	*	12:21.1	12:22.9	1.2	1.0	33.	22.0	.66
ARE	84.796	12:37.8	12:40.8	*	12:36.8	12:39.9	.7	.7	71.	71.4	1.00

Event: Bilby

Station	Distance (deg)	P		PcP		PcP Travel Time Reference	P		PcP/P A/T	PcP A/T (m /sec)
		Travel Time Observed (min:sec)	Travel Time Observed (min:sec)	Travel Time Corrected (min:sec)	Travel Time Corrected (min:sec)					
EB-	19.363	4:26.8	8:49.0	3	4:26.8	8:49.3	.37	48.		
EU-	23.437	5:11.7	8:57.5	3	5:11.5	8:57.4	1.02	49.		
CPO	24.531	5:22.2	9:02.0	3	5:22.1	9:01.9				
AAM	25.360	5:28.5	9:01.8	3	5:28.5	9:01.9	.25			
ATL	26.064	5:35.9	9:03.4	3	5:35.8	9:03.2	.28			
LND	27.196	5:44.9	9:05.7	3	5:44.9	9:05.8	.80			
BL-	27.485	5:48.5	9:07.1	3	5:48.4	9:07.0	1.04	61.3		
BLA	28.283	5:56.2	9:08.8	3	5:56.4	9:08.7	.41			
CSC	28.542	5:58.4	9:09.8	3	5:58.3	9:09.7	.63			
BR-	29.107	6:03.1	9:11.1	3	6:03.0	9:11.1	.53	45.2		
SCP	29.761	6:08.2	9:12.5	3	6:08.1	9:12.5	.34			
OTT	31.169	6:20.0	9:15.5	3	6:20.0	9:15.7	.67			
DH-	31.864	6:27.0	9:18.0	3	6:26.9	9:18.0	.60	38.3		
PAL	32.720		9:20.7	3		9:20.8				
COL	33.610	6:42.3	9:22.1	3	6:42.5	9:22.8	.23			
HN-	36.563	7:08.0	9:31.1	3	7:08.0	9:31.3	.28	37.5		
HW-	38.478	7:24.9	9:38.4	3	7:24.5	9:37.9				
RES	38.734	7:27.4	9:38.3	3	7:27.8	9:39.2				
MBC	39.298	7:31.1	9:39.2	3	7:31.5	9:40.1	.14			
NP-	39.318	7:31.2	9:39.2	3	7:31.6	9:40.1	.75	67.8		

Event: Bilby (Cont.)

Station	Distance (deg)	P		PcP		PcP Travel Time Reference	P		PcP		PcP/P A/T
		Travel Time Observed (min:sec)	Travel Time Observed (min:sec)	Travel Time Corrected (min:sec)	Travel Time Corrected (min:sec)		Travel Time Corrected (min:sec)	Travel Time Corrected (min:sec)			
BHP	43.193	8:03.8	9:51.7	3	3	8:03.5	9:51.2			.67	
SJG	47.488	8:36.4	10:06.8	3	3	8:36.0	10:06.3			.57	
ALE	48.905	8:47.0	10:11.3	3	3	8:47.5	10:12.2			.49	
CAR	51.401	9:07.4	10:21.1	3	3	9:06.9	10:20.4			.23	
TRN	55.565	9:35.3	10:37.3	3	3	9:34.9	10:36.8			.56	
KEV	70.121	11:12.8	11:31.9	8	8	11:13.3	11:32.5				
SOD	72.110	11:24.7	11:41.9	8	8	11:25.2	11:42.4				
KON	73.733	11:35.3	11:52.4	3	3	11:35.6	11:52.8			.24	
NUR	77.570	11:56.9	12:04.0	8	8	11:57.3	12:04.4				
AQU	88.500	12.54.5	12:56.5	3	3	12:54.4	12:56.3			1.00	

Event: Semipalatinsk 2/13/66 04:58:00.0 49.83N 78.09E

KTG	47.223	8:34.6	10:05.0	5	5	8:35.3	10:06.3			
BAG	47.757	8:38.5	10:07.0	5	5	8:38.3	10:06.8			
GDH	56.039	9:38.8	10:36.8	5	5	9:39.5	10:38.0			
FBC	63.774	10:31.9	11:07.9	5	5	10:32.6	11:08.9			
AAM	86.869	12:45.1	12:47.0	*	*	12:45.5	12:47.3			
WIN	90.024	13:01.1	13:02.5	5	5	13:01.1	13:02.5			

Event: Semipalatinsk 1/15/65 06:00:00.0 49.92N 78.92E

<u>Station</u>	<u>Distance</u> (deg)	<u>P</u>		<u>PcP</u>		<u>PcP</u> Travel Time Reference	<u>P</u>		<u>PcP</u>	
		Travel Time Observed (min:sec)	Travel Time Observed (min:sec)	Travel Time Observed (min:sec)	Travel Time Observed (min:sec)		Travel Time Corrected (min:sec)	Travel Time Corrected (min:sec)	Travel Time Corrected (min:sec)	Travel Time Corrected (min:sec)
NDI	21.248	4:47.6	8:53.0	8	8	4:47.7	8:53.3			
QUE	21.682	4:52.2	8:54.5	8	8	4:52.1	8:54.6			
SEO	36.236		9:28.5	8	8		9:29.0			

Event: Semipalatinsk 2/26/67 03:58:00.0 49.84N 78.05E

SHI	27.607	5:51.5	9:06.1	15	15	5:51.4	9:06.2			
KEV	31.113	6:19.0	9:12.0	15	15	6:19.5	9:13.4			
MAT	44.665	8:11.3	9:54.0	15	15	8:11.5	9:54.4			
BRW	53.060	9:17.0	10:25.0	15	15	9:17.7	10:26.3			
TNN	58.938	10:00.2	10:49.7	15	15	10:00.8	10:50.7			

Event: Bravo

UGL	41.960	7:52.3	9:47.1	4	4	7:52.3	9:47.0			
SEM	77.932	11:58.0	12:08.5	4	4	11:57.9	12:08.4			

Event: Romeo

KAB	61.751	10:20.9	11:01.6	4	4	10:20.8	11:01.5			
IRK	63.193	10:29.4	11:06.6	4	4	10:29.3	11:06.5			

Event: Navajo

<u>Station</u>	<u>Distance</u> (deg)	<u>P</u>		<u>PcP</u>		<u>P</u>	<u>PcP</u>	
		<u>Travel Time</u> <u>Observed</u> (min:sec)	<u>Travel Time</u> <u>Observed</u> (min:sec)	<u>Travel Time</u> <u>Reference</u>	<u>Travel Time</u> <u>Corrected</u> (min:sec)		<u>Travel Time</u> <u>Corrected</u> (min:sec)	<u>Travel Time</u> <u>Corrected</u> (min:sec)
MAT	34.825	6:51.6	9:25.1	10	6:51.4	9:24.6		
COL	62.121	10:21.3	11:01.4	10	10:21.5	11:01.6		
EUR	73.949	11:38.2	11:52.3	9	11:37.5	11:51.6		

Event: Koa

CTA	35.251	6:56.7	9:27.5	11	6:56.3	9:26.6		
WAT	61.051	10:13.9	10:57.2	9	10:13.6	10:56.7		

Event: Oak

MAT	32.866		9:19.9	9		9:19.4		
CTA	35.148	6:55.5	9:27.4	11	6:55.1	9:26.5		
KRP	50.853	9:02.6	10:19.5	9	9:02.5	10:19.2		
COL	63.326		11:06.0	9		11:06.2		
EUR	76.518	11:53.3	12:05.3	9	11:52.6	12:04.6		

Event: Poplar

Station	Distance (deg)	P		PcP		PcP Travel Time Reference	P		PcP	
		Travel Time Observed (min:sec)	Travel Time Observed (min:sec)	Travel Time Corrected (min:sec)	Travel Time Corrected (min:sec)		Travel Time Corrected (min:sec)	Travel Time Corrected (min:sec)		
MAT	34.729		9:25.0	9		9:24.5				
CTA	36.702	7:08.5	9:32.5	11		7:08.1				
KRP	50.281	9:00.0	10:19.8	9		8:59.9				
COL	62.140		11:02.8	9						11:03.0
EUR	74.029	11:38.6	11:52.6	9		11:37.9				11:51.9

Event: Chase III

UBO	27.530	5:49.4	9:07.4	14		5:49.2				9:07.3
TFO	29.985	6:11.9	9:14.3	12		6:11.7				9:14.0
TUC	30.204	6:13.3	9:13.9	8		6:13.1				9:13.7
HL2	30.952	6:20.1	9:16.4	14		6:20.0				9:16.4
EUR	32.519		9:20.9	8						9:20.7
BMO	32.984	6:37.6	9:20.9	14		6:37.5				9:21.0
MN-	34.381	6:50.2	9:26.2	14		6:50.0				9:26.1
NP-	43.988	8:10.1	9:56.3	14		8:10.6				9:57.3
COL	50.095	8:56.6	10:16.2	8		8:57.1				10:16.8

Event: Chase IV

Station	Distance (deg)	P		PcP		PcP Travel Time Reference	P		PcP	
		Travel Time Observed (min:sec)	Travel Time Observed (min:sec)	Travel Time Observed (min:sec)	Travel Time Observed (min:sec)		Travel Time Corrected (min:sec)	Travel Time Corrected (min:sec)		
RK-	19.346	4:26.0	9:02.5	13	4:26.1	9:03.0				
WMO	19.693	4:30.9	8:59.3	13	4:30.8	8:59.2				
UBO	27.462	5:49.6	9:08.0	13	5:49.6	9:07.9				
TFO	29.913	6:11.7	9:14.5	13	6:11.5	9:14.3				
SG-	31.133	6:22.9	9:18.2	13	6:22.6	9:18.0				
EUR	32.451	6:34.2	9:21.3	8	6:33.9	9:21.1				
BMO	32.921	6:36.7	9:25.5	13	6:36.6	9:25.6				
MN-	34.312	6:50.1	9:26.8	13	6:49.9	9:26.7				

PcP TRAVEL TIME REFERENCES

*Readings made or verified by this author

1. Taggart, J. and E. R. Engdahl [1968], "Estimation of PcP travel times and the depth to the core," Bull. Seis. Soc. Am., 58, 4, 1293-1303.
2. Carder, D. S., D. Tocher, C. Bufe, S. W. Steward, J. Eisler, and E. Berg [1967], "Seismic wave arrivals from Longshot, 0° to 27°," Bull. Seis. Soc. Am., 57, 4, 573-590.
3. Buchbinder, G. G. R. [1965], "PcP from the nuclear explosion BILBY, September 13, 1963," Bull. Seis. Soc. Am., 55, 2, 441-461.
4. Kogan, S. D. [1960], "Travel times of longitudinal and transverse waves, calculated from data on nuclear explosions made in the region of the Marshall Islands," Izv. Geophys. Ser., 371-380, (Mudge, R. B., trans.).
5. Computer printout of P and PcP travel times and P amplitudes compiled by Seismology Division, Coast and Geodetic Survey, Rockville, Md., and obtained through the courtesy of J. N. Jordan.
6. Clark, D. M. [1966], Long Range seismic measurements—LONGSHOT, Seismic Data Laboratory Report, 133, United Electro-Dynamics, Earth Sciences Division, Teledyne, Inc., January.
7. Buchbinder, G. G. R. [1968], "Properties of the core-mantle boundary and observations of PcP," J. Geophys. Res., 73, 18, 5901-5923.
8. Earthquake data reports, Coast and Geodetic Survey, Rockville, Md.
9. Carder, D. S., Personal communication.
10. Carder, D. S. [1964], "Travel times from central Pacific nuclear explosions and inferred mantle structure," Bull. Seis. Soc. Am., 54, 6, 2271-2294.
11. Doyle, H. and J. Webb, Department of Geology, University of Queensland, Brisbane, Australia, personal communication [1958] obtained through the courtesy of D. S. Carder.
12. Clark, D. M. [1965], Long Range seismic measurements—CHASE III, Seismic Data Laboratory Report, 124, United Electro-Dynamics, Earth Sciences Division, Teledyne, Inc., October.
13. Clark, D. M. [1966], Long Range seismic measurements—CHASE IV, Seismic Data Laboratory Report, 137, United Electro-Dynamics, Earth Sciences Division, Teledyne, Inc., February.

14. Buchbinder, G. G. R., Personal communication.
15. Bulletin Mensuel, Union Geodesique et Geophysique Internationale, Bureau Central International de Seismologie (B.C.I.S.), 38 Boulevard de'Anvers, Strasbourg, France, February 1967.
16. Dahlman, O. [1967], Seismic records from the LONGSHOT event, report issued by the Research Institute of National Defense, Stockholm, Sweden, February.
17. Bufe, C. and Willis, D. [1969], "High-Frequency teleseismic energy from Aleutian sources," Bull. Seis. Soc. Am., October, (in press).

Note: Amplitude and period data included is generally from the same author as the travel-time data. Most of the Longshot values of PcP A/T and the PcP/P ratio A/T are read from amplitude-distance plots prepared by D. S. Carder (personal communication).

APPENDIX 2

Sample Output of Distance Program With
Reflection Point and Ellipticity Parameters

EVENT FAULTLESS

LATITUDE		38.634 DEGREES		0.0 MINUTES		0.0 SECONDS					
LONGITUDE		116.215 DEGREES		0.0 MINUTES		0.0 SECONDS					
ELEVATION		885. METERS									
STA. CODE	DISTANCE DEGREES	EPI. TO STA.	AZIMUTH	SIA.	TU EPI.	LATITUDE	LONGITUDE	REFLECTION POINT AZIMUTH	S2	H SUM KM.	SO+0.4SA+S1
TUL	16.482	53.2	285.6	37.53	105.82	99.6	-0.038	-1.31	-0.076		
AAM	24.955	71.1	272.5	41.43	100.39	98.7	-0.105	-3.64	-0.211		
ATL	20.218	91.6	290.6	36.92	99.74	101.7	-0.028	-0.44	-0.032		
VHM	27.329	136.0	325.3	28.10	105.50	142.0	0.112	4.16	0.239		
COL	32.116	335.2	129.5	52.57	127.24	212.8	-0.297	-11.55	-0.657		
KIP	39.666	256.6	54.9	31.57	139.01	243.4	0.059	3.18	0.172		
AUK	43.285	308.2	83.2	49.16	142.52	250.3	-0.239	-7.21	-0.431		
BHP	44.197	122.2	317.9	24.77	95.69	133.1	0.158	5.50	0.319		
GDM	44.844	26.7	260.7	57.32	97.72	139.4	-0.375	-12.73	-0.743		
SJG	47.913	100.7	306.0	30.61	68.59	116.6	0.074	3.96	0.214		
MOR	53.422	10.4	285.9	64.38	105.40	160.9	-0.480	-14.99	-0.890		
TRN	56.096	104.5	309.5	27.15	85.45	121.6	0.125	5.29	0.296		
PTO	76.793	47.7	305.9	54.50	63.83	92.7	-0.330	-3.21	-0.282		
PEL	82.992	142.9	325.7	2.97	92.62	151.8	0.331	-0.34	0.116		

APPENDIX 3
Residuals and Reflection Point Coordinates

Event: Long Shot, $A_i = -.5$ sec

Station	Distance (deg)	PcP		Corrected PcP		PcP-P		δr PcP (km)	δr PcP Corrected (km)	δr PcP-P (km)	Reflection Point		$\frac{\delta r}{r}$ (km)
		Travel Time Residual (sec)	Aj (sec)	Travel Time Residual (sec)	Travel Time Residual (sec)	North Latitude	West Longitude						
CPR	13.173	- .3	- .1	+ .3	- 1.5	+ 2.1	- 2.1	+ 10.7	56.66	174.41	+ 4.3		
NOM	15.424	+ .6	- .1	+ 1.2	- 1.8	- 4.3	- 8.6	+ 13.0	58.06	174.53	+ 2.2		
BC6	15.960	- 1.1	- .1	- .5	- 1.9	+ 7.9	+ 3.6	+ 13.7	55.45	169.43	+ 8.6		
KDC	17.498	- .2	- .3	+ .6	+ 2.2	+ 1.5	- 4.4	- 10.1	55.24	167.77	-10.2		
ITL	17.556	+ .3	- .1	+ .9	- 1.1	- 2.2	- 6.7	+ 8.1	57.60	170.35	+ .7		
AMU	19.558	- 1.0	- .2	- .3	- 1.2	+ 7.4	+ 2.2	+ 8.9	57.10	167.34	+ 5.6		
PL6	20.176	- 1.0	0	- .5	- 2.6	+ 7.5	+ 3.8	+ 19.5	60.70	174.47	+11.6		
TNN	20.272	+ .5	+ .1	+ .9	- .8	- 3.8	- 6.8	+ 6.0	58.97	169.25	- .4		
MCK	20.767	- .8	+ .1	- .4	+ .4	+ 6.0	+ 3.0	- 3.0	58.39	167.66	0		
COL	21.686	- 1.6	- .6	- .5	0	+ 12.2	+ 3.8	0	59.03	167.52	+ 1.9		
BLR	22.016	+ .2	+ .1	+ .6	+ 1.1	- 1.5	- 4.6	- 8.4	58.48	166.31	- 6.5		
PX6	22.025	- .6	- .3	+ .2	+ .3	+ 4.6	- 1.5	- 2.3	58.24	165.99	- 1.9		
BRW	22.703	- .2	- .1	+ .4	- .7	+ 1.5	- 3.0	+ 5.3	61.70	172.68	+ 1.2		
HS6	23.137	- .7	- .5	+ .3	+ 1.6	+ 5.3	- 2.3	- 12.2	59.52	166.46	- 7.2		
AV6	23.863	+ .3	- .2	+ 1.0	0	- 2.3	- 7.7	0	60.73	167.74	- 3.8		
BH-	24.683	+ .4	- .1	+ 1.0	+ 1.3	- 3.1	- 7.8	- 10.1	57.96	162.82	- 9.0		
WH-	26.599	0	- .1	+ .6	+ .5	0	- 4.8	- 4.0	58.01	160.89	- 4.4		
WL-	26.797	- 2.0	- .4	- 1.1	- 1.8	+ 16.8	+ 9.2	+ 15.1	58.36	157.90	+12.2		
SI-	31.774	- .5	- .2	+ .2	- 2.1	+ 4.3	- 1.7	+ 18.1	56.02	155.07	+ 8.2		
MAT	32.551	- .2	- .7	+ 1.0	- .7	+ 1.7	- 8.7	+ 6.1	45.64	-156.01	- 1.3		
PHC	32.937	+ .6	+ .5	+ .6	- 1.6	- 5.2	- 5.2	+ 13.9	54.00	153.90	+ 4.4		
MBC	34.031	+ .7	- .1	+ 1.3	+ .6	- 6.2	- 11.4	- 5.3	66.27	164.95	- 8.4		
PG-	34.548	- .1	- .5	+ .9	- .2	+ .9	- 8.0	+ 1.8	56.20	152.60	- 3.1		
CMC	35.000	- 1.2	- .1	- .6	- .3	+ 10.7	+ 5.3	+ 2.7	63.37	156.95	+ 4.0		
YKC	36.169	- 1.2	- .8	+ .1	0	+ 10.8	- .9	0	61.16	153.17	- .4		

Event: Long Shot, $A_i = -.5$ sec

Station	Distance (deg)	PcP		Corrected PcP		PcP-P		$\frac{\delta r}{\text{PcP}}$ (km)	$\frac{\delta r}{\text{PcP}}$ Corrected (km)	Reflection Point		$\frac{\delta r}{\text{PcP-P}}$ (km)
		Travel Time Residual (sec)	A_i (sec)	Travel Time Residual (sec)	Travel Time Residual (sec)	North Latitude	West Longitude					
VIC	36.222	+ .2	+ .2	+ .5	- .4	- 1.8	- 4.6	+ 3.6	+ 3.6	53.44	151.17	- .5
KV-	36.367	- 1.0	- .7	+ .2	+ 3.2	+ 9.1	- 1.8	- 29.1	- 29.1	58.22	151.37	- 15.4
JP-	37.419	- .6	- .5	+ .4	+ .2	+ 5.6	- 3.7	- 1.9	- 1.9	56.27	150.02	- 2.8
LON	38.014	- .4	0	+ .1	- .1	+ 3.8	- .9	+ .9	+ .9	52.79	149.79	0
PNT	38.092	- .3	- .2	+ .4	+ 1.0	+ 2.8	- 3.8	- 9.4	- 9.4	54.34	149.46	- 6.6
COR	38.206	+ 1.1	+ 1.0	- 1.6	+ .6	- 10.5	+ 15.2	- 5.7	- 5.7	51.52	149.98	+ 4.8
SEO	38.904	- .5	- .2	+ .2	+ 3.5	+ 4.8	- 1.9	- 33.6	- 33.6	47.35	- 149.74	- 17.8
RM6	39.365	- .8	+ .1	- .4	+ 1.3	+ 7.8	+ 3.9	- 12.6	- 12.6	56.49	148.28	- 4.4
EDM	39.883	- .1	0	+ .4	+ 2.0	+ 1.0	- 3.9	- 19.6	- 19.6	57.12	147.85	- 11.8
YR-	40.148	+ .4	0	+ .9	- .8	- 4.0	- 8.9	+ 7.9	+ 7.9	50.13	148.93	- .5
RES	40.298	- 2.1	- .2	- 1.4	- .6	+ 20.8	+ 13.9	+ 5.9	+ 5.9	68.12	158.06	+ 9.9
BMO	41.694	- .9	- .4	0	0	+ 9.2	0	0	0	52.49	146.80	0
HMM	41.795	- 1.1	+ .1	- .7	- .5	+ 11.2	+ 7.1	+ 5.1	+ 5.1	54.70	146.22	+ 6.1
SW-	42.661	- 1.0	- .2	- .3	+ .6	+ 10.3	+ 3.1	- 6.2	- 6.2	55.32	145.38	- 1.6
BKS	42.694	+ .5	+ .8	+ .2	+ .3	- 5.2	- 2.1	- 3.1	- 3.1	48.32	147.78	- 2.6
ALE	42.790	- 1.1	- .1	- .5	- .9	+ 11.4	+ 5.2	+ 9.4	+ 9.4	72.01	169.20	+ 7.3
BUT	43.872	- 3.0	+ .1	- 2.6	- 1.0	+ 31.8	+ 27.6	+ 10.6	+ 10.6	53.80	144.61	+ 19.1
HL2	44.136	+ .3	+ .3	+ .5	+ .6	- 3.2	- 5.4	- 6.4	- 6.4	52.30	144.82	- 5.9
HV-	44.158	- .3	- .2	+ .4	+ 2.2	+ 3.2	- 4.3	- 23.5	- 23.5	55.41	144.05	- 13.9
BOZ	44.642	- .4	- .3	+ .4	+ .8	+ 4.3	- 4.3	- 8.6	- 8.6	53.75	143.96	- 6.4
MN-	44.889	- 1.6	+ .4	- 1.5	- 2.0	+ 17.3	+ 16.2	+ 21.6	+ 21.6	49.18	145.55	+ 18.9
FFC	45.152	- 1.6	- .1	- 1.0	+ .9	+ 17.4	+ 10.9	- 9.8	- 9.8	59.70	143.17	+ .6
EUR	45.591	- 1.0	+ .2	- .7	- 1.3	+ 10.9	+ 7.6	+ 14.2	+ 14.2	50.04	144.55	+ 10.9
TIN	45.698	+ .6	+ .4	+ .7	- .1	- 6.6	- 7.7	+ 1.1	+ 1.1	48.48	145.28	- 3.3
TF-	45.820	- .2	+ .4	- .1	- .6	+ 2.2	+ 1.1	+ 6.6	+ 6.6	47.27	145.90	+ 3.8

Event: Long Shot, $\Delta t = -.5 \text{ sec}$

Station	Distance (deg)	PcP		Corrected PcP		PcP-P		δr PcP		δr PcP Corrected		δr PcP-P		Reflection Point		δr (km)
		Travel Time Residual (sec)	Aj (sec)	Travel Time Residual (sec)	Travel Time Residual (sec)	Travel Time Residual (sec)	Travel Time Residual (sec)	δr PcP (km)	δr PcP (km)	δr PcP Corrected (km)	δr PcP-P (km)	North Latitude	West Longitude			
KRC	45.854	-.6	+1.1	-1.2	-.7	+6.6	+13.2	+7.7	47.38	145.80	+10.4					
WDY	46.174	-2.1	+ .5	-2.1	-1.4	+23.3	+23.3	+15.5	47.70	145.35	+19.4					
FTC	46.614	+ .1	+ .5	+ .1	-.3	-1.1	-1.1	+3.4	47.33	145.23	+1.2					
CLC	46.878	+ .1	+ .4	+ .2	+ .4	-1.1	-2.2	-4.5	47.94	144.64	-3.4					
LAO	47.148	-.3	0	+ .2	+1.2	+3.4	-2.3	-13.6	55.20	141.45	-8.0					
MMC	47.624	+ .2	+ .3	+ .4	+ .5	-2.3	-4.6	-5.7	47.07	144.58	-5.2					
GSC	47.703	+ .2	+ .4	+ .3	+ .6	-2.3	-3.4	-6.8	47.80	144.06	-5.1					
RVR	48.202	+ .3	+ .2	+ .6	+ .9	-3.5	-6.9	-10.4	47.05	144.13	-8.6					
BCN	48.488	0	+ .9	-.4	-.2	0	+4.6	+2.3	48.45	143.04	+3.4					
FGU	48.705	-.9	-.1	-.3	+ .8	+10.4	+3.5	-9.3	51.83	141.18	-2.9					
UBO	48.968	-.6	+ .1	0	0	+7.0	0	0	51.50	141.11	0					
KN-	49.058	+ .1	+ .7	-.1	-.2	-1.2	+1.2	+2.3	49.30	142.11	+1.8					
HAY	49.475	0	+ .5	0	+ .8	0	0	-9.4	47.17	143.03	-4.7					
RG-	49.529	-.6	+ .2	-.3	+1.6	+7.1	+3.5	-18.9	54.98	139.40	-7.7					
CP-	49.669	+ .1	+ .3	+ .3	+ .4	-1.2	-3.5	-4.7	46.56	143.28	-4.1					
GCA	49.847	0	+ .6	-.1	+ .2	0	+1.2	-2.4	49.48	141.37	-.6					
RCD	50.403	-.3	+ .3	-.1	+1.8	+3.6	+1.2	-21.8	54.49	138.77	-10.3					
TFO	51.803	-.1	+ .6	-.2	-.5	+1.3	+2.5	+6.3	48.17	140.53	+4.4					
GOL	51.866	-.9	+ .3	-.7	-.7	+11.3	+8.8	+8.8	51.93	138.49	+8.8					
WN-	52.629	-.7	+ .3	-.5	+ .5	+9.0	+6.4	-6.4	54.67	136.76	0					
WAW	57.437	-1.3	-.5	-.3	0	+19.1	+4.4	0	60.33	130.87	+2.2					
FIM	58.780	0	-.3	+ .8	+1.0	0	-12.2	-15.3	59.36	129.72	-13.8					
WMO	59.213	-.5	-.7	+ .7	+ .1	+7.8	-10.9	-1.6	50.76	132.91	-6.2					
SV3	60.782	-.9	-.4	0	+ .7	+14.5	0	-11.3	67.62	127.23	-5.6					
FAY	60.844	0	-.7	-.2	-3.3	0	+3.2	+53.1	52.40	130.61	+28.2					
GV-	61.437	-.1	+ .3	+ .1	-.2	+1.6	-1.6	+3.3	50.16	131.40	+ .8					
DAL	61.593	-.8	+ .3	-.6	-1.1	+13.2	+9.9	+18.2	50.19	131.25	+14.0					

Event:

Station	Distance (deg)	PcP		Corrected PcP		PcP-P		Δr PcP (km)	Δr PcP Corrected (km)	Δr PcP-P (km)	Reflection Point		$\bar{\delta r}$ (km)
		Travel Time Residual (sec)	Aj (sec)	Travel Time Residual (sec)	Travel Time Residual (sec)	North Latitude	West Longitude						
BGM	62.289	- .7	0	- .2	+ 1.0	+ 11.8	+ 3.4	- 16.8	57.92	126.75	+ .8		
AAM	62.289	- 1.2	0	- .7	+ .6	+ 20.2	+ 11.8	- 10.1	57.92	126.75	- 6.7		
EN-	62.349	+ .3	- .3	+ 1.1	+ 2.3	- 5.0	- 18.5	- 38.6	53.61	128.66	-28.6		
LND	63.030	- 1.2	+ .1	- .8	+ .2	+ 20.6	+ 13.8	- 3.4	58.90	125.66	+ 5.2		
OXF	64.716	+ .7	0	+ 1.2	- .9	- 12.7	- 21.7	+ 16.3	52.70	127.08	- 2.7		
UPP	68.064	+ .2	- .6	+ 1.3	+ 2.7	- 4.0	- 26.1	- 54.3	82.47	-131.85	-40.2		
UDD	68.221	- 3.2	- .1	- 2.6	- 1.3	+ 64.6	+ 52.5	+ 26.3	83.48	-137.57	+39.4		
CHG	69.479	- .3	+ .4	+ .6	+ .6	+ 6.4	- 12.7	- 12.7	42.01	-129.32	-12.7		
WRA	81.185	- 4.0	+ .1	- 3.4	- 1.8	+144.8	+123.1	+ 65.2	16.87	-152.03	+94.2		
GBA	86.654	- 1.7	+ .4	- .8	- .2	+ 78.0	+ 36.7	+ 9.2	44.16	-113.39	+23.0		

Event: Novaya Zemlya, 10/27/66 05:58:00.0 73.40N 54.87E A1 = -.3

Station	Distance (deg)	PcP		Corrected PcP		PcP-P		δr PcP (km)	δr PcP Corrected (km)	δr PcP-P (km)	Reflection Point		δr (km)
		Travel Time Residual (sec)	Aj (sec)	Travel Time Residual (sec)	Travel Time Residual (sec)	North Latitude	West Longitude						
KTG	22.521	+ 1.9	+ .9	+ 1.3	+ .5	- 14.4	- 9.9	- 3.8	75.52	- 12.83	- 29.8		
AKU	24.950	+ 3.1	- .2	+ 3.6	+ .4	- 24.2	- 28.1	- 3.1	73.06	- 10.78	- .6		
*CLL	28.360	+ 2.0	0	+ 2.3	+ 1.6	- 16.4	- 18.9	- 13.1	63.56	- 25.85	- 30.6		
ESK	29.219	+ .5	0	+ .8	- .1	- 4.2	- 6.6	+ .8	66.76	- 15.43	- 2.6		
VKA	30.368	+11.6	+ .1	+11.8	+ 9.8	- 99.1	- 99.1	- 82.3	61.84	- 27.66	- 4.0		
RES	31.304	0	- .2	+ .5	+ 2.8	0	- 4.3	- 23.8	85.64	13.94	+ 6.6		
STR	32.312	-15.5	+ .1	-15.3	-16.7	+133.3	+131.6	+143.6	62.57	- 21.53	- 8.6		
TRI	33.374	- .5	+ .5	- .7	- 1.0	+ 4.4	+ 6.1	+ 8.7	60.73	- 25.41	- 2.7		
NEU	33.888	0	+ .2	+ .1	+ .6	0	- .9	- 5.3	61.84	- 20.63	- 2.0		
BES	33.910	- 5.9	- .4	- 5.2	- 5.6	+ 51.9	+ 45.8	+ 49.3	62.04	- 19.96	+11.4		
BRW	34.141	+ 1.1	- .1	+ 1.5	- .6	- 9.7	- 13.2	+ 5.3	84.91	-140.53	0		
VAL	34.209	+ .4	+ .6	+ .1	- .1	- 3.5	- .9	+ .9	65.76	- 9.16	- 5.4		
IST	34.703	+ .5	+ .4	+ .4	- .2	- 4.5	- 3.6	+ 1.8	57.60	- 36.03	- 30.6		
FBC	38.053	- .3	- .6	+ .6	+ .2	+ 2.8	- 5.6	- 1.9	78.58	28.54	+ .7		
*CIN	38.211	- .5	0	- .2	- 1.7	+ 4.8	+ 1.9	+ 16.2	55.92	- 35.11	- 2.8		
CMC	38.857	+ .7	- .1	+ 1.1	- .2	- 6.7	- 10.5	+ 1.9	86.70	87.61	+ 2.8		
BLC	41.090	+ .9	0	+ 1.2	+ .2	- 8.8	- 11.8	- 2.0	82.75	57.39	+12.8		
COL	41.139	- 1.4	- .4	- .7	- 3.3	+ 14.0	+ 7.0	+ 33.0	84.00	-177.73	+ .7		
TOL	43.458		+ .2		+ 1.1			- 11.6	59.23	- 10.97	- 21.0		
YKC	44.199	+ 1.5	- .8	+ 2.6	+ 1.9	- 16.1	- 27.4	- 20.3	84.13	98.20	- 19.2		
*PMR	44.311	+ 1.1	0	+ 1.4	+ .7	- 11.8	- 15.0	- 7.5	82.39	177.60	+73.4		
NDI	46.296	+ 1.0	+ .3	+ 1.0	- .2	- 11.1	- 11.1	+ 2.2	51.30	- 71.76	- 13.7		
MAL	46.508	+ .5	+ .2	+ .6	- .6	- 5.6	- 6.7	+ 6.7	57.70	- 10.17	+ 1.6		
GMC	47.603	+ .2	0	+ .5	+ 1.7	- 2.3	- 5.7	- 19.4	76.33	48.48	+ 8.6		
*KDC	47.815	+ 2.1	- .3	+ 2.7	+ 1.2	- 23.9	- 30.8	- 13.7	80.22	177.68	+ 7.1		

Event: Novaya Zemlya, 10/27/66 05:58:00.0 73.40N 54.87E AI = -.3

Station	Distance (deg)	PcP		Corrected PcP		PcP-P		δr PcP (km)	δr PcP Corrected (km)	δr PcP-P (km)	Reflection Point		δr (km)
		Travel Time Residual (sec)	Aj (sec)	Travel Time Residual (sec)	Travel Time Residual (sec)	North Latitude	West Longitude						
RBA	49.730	+ 3.1	+ .5	+ 2.9	+ 2.1	+ 2.1	- 36.9	- 34.5	- 25.0	- 7.83	56.58	- 7.83	- 6.8
SIC	50.361	0	- .2	+ .5	- .4	- .4	0	- 6.1	+ 4.8	39.91	72.27	39.91	-15.6
PDA	51.590	+ 3.2	+ .7	+ 2.8	+ 1.8	+ 1.8	- 40.0	- 35.0	- 22.5	7.01	60.50	7.01	-16.0
FSJ	52.456	+ .7	0	+ 1.0	- .6	- .6	- 9.0	- 12.8	+ 7.7	123.40	80.48	123.40	- 2.9
EDM	53.413	+ .5	0	+ .8	- .2	- .2	- 6.6	- 10.5	+ 2.6	102.95	79.51	102.95	-90.7
MAT	53.514	- 1.1	- .7	- .1	- .9	- .9	+ 13.3	+ 1.3	+ 11.8	-119.41	60.26	-119.41	-14.0
SHK	53.805	0	+ .3	0	+ 1.3	+ 1.3	0	0	- 17.2	+137.6	58.58	+137.6	+7.4
SFA	54.189	+ .2	0	+ .5	- .1	- .1	- 2.7	- 6.7	+ 1.3	46.45	71.48	46.45	- 3.1
*DDR	54.302	+ .2	0	+ .5	- .2	- .2	- 2.7	- 6.7	+ 2.7	-120.37	60.11	-120.37	-47.6
ABU	54.331	- .5	+ .3	- .5	- 1.2	- 1.2	+ 6.7	+ 6.7	- 2.7	-121.12	59.09	-117.49	0
*TSK	54.365	- .5	0	- .2	+ .2	+ .2	+ 6.7	+ 2.7	- 20.4	112.95	60.34	-121.12	- 3.8
*SRY	54.690	+ .3	0	+ .6	+ .2	+ .2	- 4.1	- 8.1	0	39.95	59.93	-120.53	+ 9.0
MCC	54.763	+ 2.7	0	+ 3.0	+ 1.5	+ 1.5	- 36.7	- 40.8	+ 2.8	100.08	79.17	112.95	- 4.3
HAL	55.058	+ .3	+ .7	- .1	0	0	- 4.1	+ 1.4	+ 18.5	129.33	69.20	129.33	- 6.9
POO	55.909	+ .8	+ .7	+ .4	0	0	- 11.3	- 5.6	+ 1.4	50.40	46.14	50.40	+20.0
SES	56.121	- .5	0	- .2	- .2	- .2	+ 7.1	+ 2.8	- 13.1	52.85	77.97	52.85	-11.6
PHC	56.188	- .3	+ .5	- .5	- 1.3	- 1.3	+ 4.3	+ 7.1	- 4.6	91.72	78.59	91.72	-24.0
MNT	56.286	- .3	0	0	- .1	- .1	+ 4.3	0	+ 75.0	49.21	71.12	49.21	-11.2
OTT	56.782	+ 1.1	- .6	+ 2.0	+ .9	+ .9	- 16.0	- 29.0	- 9.2	94.49	71.38	94.49	- 4.4
*LF1	58.748	+ 1.9	0	+ 2.2	+ .3	+ .3	- 29.1	- 33.8	+ 13.9	57.77	76.02	57.77	0
WES	58.836	- 4.1	+ .9	- 4.7	- 4.9	- 4.9	+ 62.7	+ 71.9	+ 17.2	93.61	69.28	93.61	-12.6
LF4	58.839	+ .9	0	+ 1.2	+ .6	+ .6	- 13.8	- 18.4	+ 6.3	47.50	76.19	47.50	-22.2
SCB	59.036	+ .4	0	+ .7	- .9	- .9	- 6.2	- 10.8	+ 7.9		71.09	71.09	
LAO	59.505	- .3	0	0	- 1.1	- 1.1	+ 4.7	0			75.77	75.77	
CHG	59.855	- .4	+ .4	- .5	- .4	- .4	+ 6.3	+ 7.9			47.50	47.50	

Event: Novaya Zemlya, 10/27/66 05:58:00.0 73.40N 54.87E AI = -.3

Station	Distance (deg)	PcP		Corrected PcP		PcP-P		Δr PcP (km)	Δr PcP Corrected (km)	Δr PcP-P (km)	Reflection Point		Δr (km)
		Travel Time Residual (sec)	Aj (sec)	Travel Time Residual (sec)	Travel Time Residual (sec)	North Latitude	West Longitude						
TUM	59.876	+ 1.6	+ .6	+ 1.3	+ .1	- 25.1	- 20.4	+ 1.6	+ 1.6	76.75	121.31	- 9.4	
HKC	60.179	+ .4	+ .8	- .1	- .8	- 6.4	+ 1.6	+ 12.7	+ 12.7	50.49	-101.20	+ 7.2	
SCP	61.626	+ 5.0	- .1	+ 5.4	+ 3.8	- 82.5	- 89.1	- 62.7	- 62.7	69.47	57.35	- 75.9	
RCD	61.857	+ 1.5	+ .3	+ 1.5	0	- 24.9	- 24.9	0	0	74.22	89.91	- 12.4	
KOD	64.514	+ 2.1	+ .4	+ 2.0	+ 1.2	- 37.6	- 35.8	- 21.5	- 21.5	42.12	- 72.42	- 28.6	
BAG	67.517	+ .4	0	+ .7	+ .1	- 7.8	- .1	- 2.0	- 2.0	48.15	-105.92	- 7.8	
TNP	68.681	- 6.5	+ .4	- 6.6	- 6.9	+133.9	+136.0	+142.1	+142.1	72.16	112.73	+139.0	
SNG	71.467	+ .1	0	+ .4	- .3	- 2.3	- 9.2	+ 6.9	+ 6.9	41.79	- 90.33	- 1.2	
*PAS	72.634	- 3.6	+ .4	- 3.5	- 4.7	+ 87.8	+ 85.4	+114.7	+114.7	70.23	114.51	+100.0	
KIP	82.944	+ 2.8	+1.1	+ 2.0	- .3	-110.3	- 78.8	+ 11.8	+ 11.8	61.82	170.76	- 33.5	
TRN	87.090	+ 3.5	+ .4	+ 3.4	+ 1.5	-162.8	-158.1	- 69.8	- 69.8	51.94	44.64	-114.0	
PBJ	88.296	+ 3.3	+ .6	+ 3.0	+ 2.9	-160.7	-146.1	-141.2	-141.2	59.69	84.06	-143.6	
CAR	88.594	+ 3.0	- .3	+ 3.6	+ 2.3	-147.3	-176.8	-112.9	-112.9	52.72	50.56	-144.8	

*Used event: Novaya Zemlya, 11/7/68 10:02:07.1 73.405N 54.859E AI = -.3

Event: Sahara, 2/27/65 11:30:00.0 24.04N 5.01E AI = 0.0

Station	Distance (deg)	PcP		Corrected PcP		PcP-P		δr PcP (km)	δr PcP Corrected (km)	δr PcP-P (km)	Reflection Point		δr (km)
		Travel Time Residual (sec)	Aj (sec)	Travel Time Residual (sec)	Travel Time Residual (sec)	North Latitude	West Longitude						
MAL	15.020	+ 1.9	+ .2	+ 1.7	+ 3.9	- 13.7	- 12.2	- 28.1	30.30	- 0.60	- 20.2		
TOL	17.547	+ 3.9	+ .2	+ 3.7	- 1.2	- 28.5	- 27.0	+ 8.8	31.87	- 0.87	- 9.1		
TRI	22.751	+ .1	+ .5	- .4	+ .3	- .8	+ 3.0	- 2.3	34.78	- 8.81	+ .4		
STU	24.911	- .1	- .3	+ .2	0	+ .8	- 1.6	0	36.26	- 6.80	- .8		
VAL	30.206	- .6	+ .6	- 1.2	- .9	+ 5.0	+ 10.1	+ 7.6	38.06	1.14	+ 8.8		
ESK	31.826	+ 1.2	0	+ 1.2	+ 2.9	- 10.3	- 10.3	- 24.9	39.58	- 1.85	- 17.6		
AAE	35.511	+ 1.5	+1.1	+ .4	- 1.3	- 13.5	- 3.6	+ 11.7	17.13	- 22.56	+ 4.0		
KON	35.732	- .5	+ .2	- .7	0	+ 4.5	+ 6.3	0	41.71	- 6.66	+ 3.2		
NUR	38.914	- .4	- .3	- .1	0	+ 3.8	+ 1.0	0	42.50	- 11.88	+ .5		
NAI	39.829	+ 2.7	0	+ 2.7	- .6	- 26.5	- 26.5	+ 5.9	11.75	- 21.64	- 10.3		
SHI	42.810	- 1.1	- .6	- .5	+ .9	+ 11.4	+ 5.2	- 9.4	28.89	- 28.29	- 2.1		
KEV	47.560	- .1	+ .2	- .3	- .1	+ 1.1	+ 3.4	+ 1.1	47.18	- 11.03	+ 2.2		
BUL	49.570	- 2.1	- .5	- 1.6	- 2.5	+ 24.8	+ 18.9	+ 29.5	1.98	- 16.98	+ 24.2		
PRE	54.364	- .3	- .2	- .1	- .1	+ 4.0	+ 1.3	+ 1.3	- 0.87	- 16.55	+ 1.3		
NOR	58.292	+ 2.4	- .6	+ 3.0	+ 1.6	- 36.2	- 45.3	- 24.2	52.95	- 2.05	- 34.8		
POO	63.826	+ .4	+ .7	- .3	+ .6	- 7.0	+ 5.3	- 10.6	25.13	- 40.16	- 2.6		
NDI	63.967	- .2	+ .3	- .5	+ 1.4	+ 3.5	+ 8.9	- 24.8	31.35	- 40.28	- 8.0		
TRN	64.277	+ 2.1	+ .4	+ 1.7	+ .2	- 37.4	- 30.3	- 3.6	20.34	29.55	- 17.0		
SJC	66.049	+ .1	- .3	+ .4	- 1.6	- 1.9	- 7.5	+ 30.1	25.20	31.38	+ 11.3		
OGD	67.073	+ .2	- .5	+ .7	- .4	- 3.8	- 13.4	+ 7.7	39.46	30.29	- 2.8		
CAR	69.380	- 1.1	- .3	- .8	- 2.7	+ 23.3	+ 17.0	+ 57.2	20.88	32.47	+ 37.1		
GEO	69.411	+ .7	+ .1	+ .6	- .6	- 14.8	- 12.7	+ 12.7	38.81	32.09	0		
SCP	69.530	+ 1.4	- .1	+ 1.5	- .6	- 29.8	- 32.0	+ 12.8	39.99	31.75	- 9.6		
KOD	69.955	- .2	+ .4	- .6	+ .7	+ 4.3	+ 13.0	- 15.1	20.79	- 42.79	- 1.0		

Event: Sahara, 2/27/65 11:30:00.0 24.04N 5.01E AI ≈ 0.0

Station	Distance (deg)	PcP		Corrected PcP		PcP-P		δr PcP (km)	δr PcP Corrected (km)	δr PcP-P (km)	Reflection Point		$\overline{\delta r}$ (km)
		Travel Time Residual (sec)	Aj (sec)	Travel Time Residual (sec)	Travel Time Residual (sec)	North Latitude	West Longitude						
SHL	77.356	7.2	- .5	6.7	- 6.5	219.6	204.4	198.3	32.30	- 48.12	+201.4		
CMC	78.417	2.8	- .1	2.9	+ 1.0	89.6	92.8	32.0	59.14	19.39	- 62.4		
LPB	81.937	3.5	+ .4	3.9	- 4.0	132.0	147.0	150.8	4.64	32.56	+148.9		
ARE	84.796	.9	+ .5	.4	- .3	38.3	17.0	12.8	4.79	34.33	- 2.1		

Event: Bilby AI = +.9

Station	Distance (deg)	PcP		Corrected PcP		PcP-P		δr PcP		δr PcP Corrected		δr PcP-P		Reflection Point		δr (km)
		Travel Time Residual (sec)	Aj (sec)	Travel Time Residual (sec)	Travel Time Residual (sec)	Travel Time Residual (sec)	Travel Time Residual (sec)	δr PcP (km)	δr PcP (km)	δr PcP Corrected (km)	δr PcP-P (km)	North Latitude	West Longitude			
EB-	19.363	+ .4	-.7	+ .2		0		- 3.0	- 1.5	- 1.5	0	43.61	106.89	- .8		
EU-	23.437	+ .8	+ .5	- .6		- 1.7		- 6.2	+ 4.6	+ 4.6	+ 13.1	35.56	101.57	+ 8.8		
CPO	24.531	+ 2.9	-.7	+ 2.7		+ .5		- 22.6	- 21.1	- 21.1	- 3.9	37.12	100.65	-12.5		
AAM	25.360	+ .9	0	0		+ .5		- 7.1	0	0	- 4.0	40.63	100.46	- 2.0		
ATL	26.064	+ .6	0	- .3		- .8		- 4.8	+ 2.4	+ 2.4	+ 6.4	36.11	99.82	+ 4.4		
LND	27.196	+ .6	+ .1	- .4		+ .2		- 4.9	+ 3.2	+ 3.2	- 1.6	41.19	99.39	+ .8		
BL-	27.485	+ 1.1	-.3	+ .5		- .1		- 8.9	- 4.1	- 4.1	+ .8	38.54	98.75	- 1.6		
BLA	28.283	+ .8	0	- .1		- .9		- 6.6	+ .8	+ .8	+ 7.3	38.31	98.24	+ 4.0		
CSC	28.542	+ 1.3	+ .3	+ .1		- .8		- 10.7	- .8	- .8	+ 6.6	36.64	98.19	+ 2.9		
BR-	29.107	+ 1.2	+ .3	0		- .3		- 10.0	0	0	+ 2.5	39.80	97.81	+ 1.2		
SCP	29.761	+ .9	-.1	+ .1		+ .5		- 7.6	- .8	- .8	- 4.2	40.33	97.46	- 2.5		
OTT	31.169	+ .5	-.6	+ .2		+ .5		- 4.3	- 1.7	- 1.7	- 4.3	42.83	97.20	- 3.0		
DH-	31.864	+ .9	+ .1	- .1		+ .3		- 7.7	- .9	- .9	- 2.6	41.32	96.25	- 1.8		
PAL	32.720	+ 1.4	-.1	+ .6				- 12.2	- 5.2	- 5.2		40.79	95.58	- 5.2		
COL	33.610	+ .9	-.6	+ .6		- .4		- 7.9	- 5.3	- 5.3	+ 3.5	51.80	126.96	- .9		
HN-	36.563	+ .7	+ .2	- .4		- .2		- 6.4	+ 3.6	+ 3.6	+ 1.8	43.99	93.79	+ 2.7		
HW-	38.478	+ 1.5	+ .7	- .1		+ .1		- 14.3	+ 1.0	+ 1.0	- 1.0	29.84	137.53	0		
RES	38.734	+ 2.2	-.2	+ 1.5		- .8		- 21.1	- 14.4	- 14.4	+ 7.7	55.91	110.72	- 3.4		
MBC	39.298	+ 1.2	-.1	+ .4		- .5		- 11.6	- 3.9	- 3.9	+ 4.9	56.52	116.78	+ .5		
NP-	39.318	+ 1.2	0	+ .3		- .6		- 11.6	- 2.9	- 2.9	+ 5.8	56.53	116.79	+ 1.4		
BHP	43.193	- .4	-.1	- 1.2		- 2.0		+ 4.2	+ 12.6	+ 12.6	+ 21.0	23.95	95.85	+16.8		
SJC	47.488	- .2	-.3	- .8		- .2		+ 2.3	+ 9.0	+ 9.0	+ 2.3	29.77	88.79	+ 5.6		
ALE	48.905	+ .7	-.1	- .1		- .1		- 8.1	+ 1.2	+ 1.2	+ 1.2	60.94	109.14	+ 1.2		
CAR	51.401	- .3	-.3	- .9		- 1.5		+ 3.7	+ 11.2	+ 11.2	+ 18.6	25.69	88.78	+14.9		
TRN	55.565	+ .2	+ .4	- 1.1		+ 1.8		- 2.8	+ 15.3	+ 15.3	- 25.0	26.29	85.68	- 4.8		

Event: Bilby Ai = +.9

Station	Distance (deg)	PcP		Corrected PcP		PcP-P		Reflection Point			
		Travel Time Residual (sec)	Aj (sec)	Travel Time Residual (sec)	Travel Time Residual (sec)	Travel Time Residual (sec)	North Latitude	West Longitude	\bar{r} (km)		
KEV	70.121	- 3.0	+ .2	- 4.1	- 3.1	+ 65.4	+ 89.4	+ 67.6	69.91	94.16	+ 78.5
SOD	72.110	- 1.5	- .2	- 2.2	- 1.7	+ 35.3	+ 51.7	+ 40.0	70.29	90.53	+ 45.8
KON	73.733	+ 2.0	+ .2	+ .9	+ 1.3	- 51.0	- 23.0	- 33.2	65.98	76.71	- 28.1
NUR	77.570	- 3.2	- .3	- 3.8	- 3.3	+ 98.2	+116.7	+101.3	70.44	79.09	+109.0
AQU	88.500	+ 1.0	+ .4	- .3	+ .1	- 49.1	+ 14.7	- 4.9	62.55	55.92	+ 4.9

Event: Faultless Ai = +.4

TUL	16.482	- 2.3	- .6	- 2.6	- 4.7	+ 16.8	+ 19.0	+ 34.3	37.53	105.82	+ 26.6
ATL	26.218	+ 1.0	0	+ .1	- .2	- 8.0	- .8	+ 1.6	36.92	99.74	+ .4
VHM	27.329	+ 1.8	+ .6	+ .3	- 1.6	- 14.6	- 2.4	+ 13.0	28.10	105.50	+ 5.3
COL	32.116	+ 1.6	- .1	+ .8	+ .1	- 13.8	- 6.9	- .9	52.57	127.24	- 3.9
KIP	39.666	+ 3.2	+1.1	+ 1.2	+ .3	- 31.0	- 11.6	- 2.9	31.57	139.01	- 7.2
ADK	43.285	+ .7	+ .2	- .4	- .5	- 7.4	+ 4.2	+ 5.3	49.16	142.52	+ 4.8
BHP	44.197	+ 1.1	- .1	+ .3	- .1	- 11.8	- 3.2	+ 1.1	24.77	95.69	- 1.0
GDH	44.844	+ .1	- .1	- .7	- 1.7	- 1.1	+ 7.6	+ 18.4	57.32	97.72	+ 13.0
SJG	47.913	+ .6	- .3	0	- .9	- 6.8	0	+ 10.3	30.61	88.59	+ 5.2
NOR	53.422	+ .7	- .6	+ .4	+ .8	- 9.2	- 5.2	- 10.5	64.38	105.40	- 7.8
TRN	56.096	- .4	+ .4	- 1.7	+ 1.1	+ 5.6	+ 24.0	- 15.5	27.15	85.45	+ 4.2
PTO	76.793	+ .6	- .1	- .2	+ .1	- 17.8	+ 5.9	- 3.0	54.56	63.83	+ 1.4
PEL	82.992	+ .2	+ .5	- 1.2	+ 1.1	- 7.9	+ 47.3	- 43.3	02.57	92.62	+ 2.0

Event: Sempalatinsk, 2/13/66 04:58:00.0 49.83N 78.09E AI = -.3

Station	Distance (deg)	PcP		Corrected PcP		PcP-P		δr PcP (km)	δr PcP Corrected (km)	δr PcP-P (km)	Reflection Point		$\overline{\delta r}$ (km)
		Travel Time Residual (sec)	Aj (sec)	Travel Time Residual (sec)	Travel Time Residual (sec)	North Latitude	West Longitude						
KTG	47.223	+ .9	+ .9	+ .3	- .8	- 10.2	- 3.4	+ 9.0	68.36	- 48.67	+ 2.8		
BAG	47.757	- .8	0	- .5	- 1.6	+ 9.1	+ 5.7	+ 18.2	34.76	-103.65	+ 12.0		
GDH	56.039	- .1	- .1	+ .3	- .2	+ 1.4	- 4.2	+ 2.8	73.90	- 45.13	- .7		
FBC	63.774	- .4	- .6	+ .5	+ .1	+ 7.0	- 8.8	- 1.8	77.43	- 36.50	- 5.3		
AAM	86.869	- 1.0	0	- .7	- .7	+ 46.1	+ 32.3	+ 32.3	80.52	- 1.86	+ 32.3		
WIN	90.024	+ .6	-1.0	+ 1.9	+ .2	- 31.0	- 98.2	- 10.3	15.61	- 41.68	- 54.2		

Event: Sempalatinsk, 1/15/65 06:00:00.0 49.92N 78.92E AI = -.3

NDI	21.248	+ 1.0	+ .3	+ 1.0	- .2	- 7.5	- 7.5	+ 1.5	39.13	- 77.94	- 3.0
QUE	21.682	+ 1.0	+ .1	+ 1.2	+ .6	- 7.6	- 9.1	- 4.6	40.02	- 72.06	- 2.2
SEO	36.236	- .4	- .2	+ .1		+ 3.6	- .9		46.12	-105.57	- .9

Event: Sempalatinsk, 2/26/67 03:58:00.0 49.84N 78.05E AI = -.3

SHI	27.607	+ .1	- .6	- .2	- 3.2	- .8	+ 1.6	+ 25.9	40.32	- 63.58	+ 13.8
KEV	31.113	- 1.6	+ .2	- 1.5	- 1.9	+ 13.6	+ 12.8	+ 16.2	61.89	- 60.70	+ 14.5
MAT	44.665	- 2.3	- .7	- 1.3	+ .2	+ 24.8	+ 14.0	- 2.2	47.09	-111.73	+ 5.9
BRW	53.060	- .8	- .1	- .4	- .1	+ 10.4	+ 5.2	+ 1.3	72.72	-107.77	+ 3.2
TNN	58.938	+ 1.2	+ .1	+ 1.4	+ .2	- 18.4	- 21.4	- 3.1	73.46	-118.59	- 12.2

Event: Western Pacific Events

Station	Distance (deg)	PcP		Corrected PcP		PcP-P		δr PcP (km)	δr PcP Corrected (km)	δr PcP-P (km)	Reflection Point		\bar{r} (km)
		Travel Time Residual	Aj (sec)	Travel Time Residual	(sec)	Travel Time Residual	(sec)				North Latitude	West Longitude	
Event: Bravo Ai = +.4													
UGL	41.960	- .6	+ .7	- 1.7	- .7	+ 6.1	+ 17.3	+ 7.1	- 155.98	+ 12.2	30.75	- 133.64	+ 5.8
SEM	77.932	- .5	- .3	- .6	+ .5	+ 15.7	+ 18.8	- 15.7	- 133.64	+ 7.1	38.58	- 142.47	+ 5.8
Event: Romeo Ai = +.1													
KAB	61.751	+ .4	+ .2	+ .1	- .8	- 6.6	- 1.7	+ 13.2	- 143.21	+ 10.4	35.13	- 142.47	+ 10.4
IRK	63.193	- .3	+ .2	- .6	- .6	+ 5.2	+ 10.4	+ 10.4	- 142.47	+ 10.4	35.54	- 142.47	+ 1.6
Event: Navajo Ai = +1.1													
MAT	34.825	- .4	- .7	- .8	- 1.1	+ 3.6	+ 7.1	+ 9.8	- 153.15	+ 8.4	24.57	- 179.13	+ 8.4
COL	62.121	- .7	- .4	- 1.4	- .5	+ 11.7	+ 23.4	+ 8.4	- 179.13	+ 15.9	40.18	- 179.13	+ 15.9
EUR	73.949	- .1	+ .2	- 1.4	- 1.5	+ 2.6	+ 36.3	+ 38.9	160.78	+ 37.6	31.47	160.78	+ 37.6
Event: KOA Ai = +.5													
CTA	35.251	0	+ .1	- .6	- .8	0	+ 5.4	+ 7.2	- 154.40	+ 6.3	- 4.22	- 154.40	+ 6.3
WAT	61.051	- 1.4	0	- 1.9	- .5	+ 22.8	+ 31.0	+ 8.2	- 140.57	+ 19.6	- 10.07	- 140.57	+ 19.6
Event: Oak Ai = +.5													
MAT	32.866	- .5	- .7	- .3	- .6	+ 4.5	+ 2.7	+ 2.7	- 151.34	+ 2.7	24.41	- 151.34	+ 2.7
CTA	35.148	+ .3	+ .1	- .3	- .6	- 2.7	+ 2.7	+ 5.3	- 154.35	+ 4.0	- 4.26	- 154.35	+ 4.0
KRP	50.853	+ .4	+ .3	- .4	- .2	- 4.9	+ 4.9	+ 2.4	- 168.10	+ 3.6	- 13.19	- 168.10	+ 3.6
COL	63.326	- 1.0	- .4	- 1.1	- .2	+ 17.3	+ 19.0	- 5.9	- 176.74	+ 19.0	40.45	- 176.74	+ 19.0
EUR	76.518	+ 1.7	+ .2	+ 1.0	+ .2	- 49.8	- 29.3	- 5.9	162.75	- 17.6	32.04	162.75	- 17.6

Event: Western Pacific Events

Station	(ueg)	PCP		Corrected PCP		PCP-P		δr PCP		δr PCP Corrected		δr PCP-P		Reflection Point		$\overline{\delta r}$ (km)
		Travel Time	Residual	Travel Time	Residual	Travel Time	Residual	(km)	(km)	(km)	(km)	North Latitude	West Longitude			
Event: Poplar Al5																
MAT	34.729	- .5	- .7	- .3		+ 4.5	+ 2.7	24.58	-153.08	+ 2.7						+ 2.7
CTA	36.702	.7	+ .1	+ .1		- 6.4	- .9	- 4.23	-155.96	- 2.8						- 2.8
KRP	50.281	+ 2.7	+ .3	+ 1.9		- 32.4	- 22.8	-13.11	-169.85	- 13.8						- 13.8
COL	62.140	+ .7	- .4	+ .6		- 11.7	- 10.0	40.20	-179.05	- 10.0						- 10.0
EUR	74.029	- .2	+ .2	- .9		+ 5.2	+ 23.4	31.51	160.85	+ 19.5						+ 19.5

Event: CHASE III Ai = +1.4

Station	Distance (deg)	PCP		Corrected PCP		PCP-P		5r PCP (km)	5r PCP Corrected (km)	5r PCP-P (km)	Reflection Point	
		Travel Time Residual * Aj (sec)	Residual (sec)	Travel Time Residual (sec)	Travel Time Residual (sec)	North Latitude	West Longitude				5r (km)	
UBO	27.530	- .1	+ .1	- .2	- .4	+ .8	+ 1.6	+ 3.2	39.92	91.52	+ 2.4	
TFO	29.985	+ .5	+ .6	- .1	- .4	- 4.2	+ .8	+ 3.4	37.00	93.16	+ 2.1	
TUC	30.204	- .3	+ .3	- .6	- .6	+ 2.5	+ 5.0	+ 5.0	35.96	93.12	+ 5.0	
HL2	30.952	+ .4	+ .3	+ .1	- .1	- 3.4	- .9	+ .9	41.95	93.41	0	
EUR	32.519	+ .4	+ .2	+ .2	- 1.1	- 3.5	- 1.7	+ 9.6	40.04	94.82	- 1.7	
BMO	32.984	- .6	- .4	- .2	0	+ 5.2	+ 1.7	0	42.87	94.53	+ 5.6	
MN-	34.381	+ .6	+ .4	+ .2	- 4.0	- 5.3	- 1.8	+ 42.4	39.72	96.06	- .9	
NP-	43.988	+ 1.6	0	+ 1.6	- 4.0	- 17.0	- 17.0	+ 2.4	58.02	84.27	+ 12.7	
COL	50.095	- .5	- .4	- .1	- .2	+ 6.0	+ 1.2		56.24	98.31	+ 1.8	

Event: CHASE IV Ai = +2.1

RK-	19.346	+12.1	- .8	+12.8	+13.9	- 89.5	- 95.5	-102.9	44.23	82.94	- 99.2
WMO	19.693	+ 7.7	- .7	+ 8.4	+ 8.7	- 57.8	- 63.0	- 65.3	36.88	86.71	- 64.2
UBO	27.462	0	+ .1	- .1	- .7	0	+ .8	+ 5.7	39.91	91.61	+ 3.2
TFO	29.913	+ .3	+ .6	- .3	- .4	- 2.5	+ 2.5	+ 3.4	36.99	93.20	+ 3.0
SG-	31.133	+ .8	0	+ .8	- .2	- 6.8	- 6.8	+ 1.7	37.84	94.05	- 2.6
EUR	32.451	+ .3	+ .2	+ .1	- .3	- 2.6	- .9	+ 2.6	40.03	94.87	+ .8
BMO	32.921	+ 3.5	- .4	+ 3.9	+ 4.3	- 30.5	- 33.9	- 37.4	42.86	94.58	- 35.6
MN-	34.312	+ .7	+ .4	+ .3	+ .3	- 6.2	- 2.6	- 2.6	39.71	96.10	- 2.6

* Includes Ai

DOCUMENT CONTROL DATA - R & D

(Security classification of title, body of abstract and indexing annotation must be entered when the overall report is classified)

1 ORIGINATING ACTIVITY <i>(Corporate author)</i> Willow Run Laboratories of the Institute of Science and Technology, The University of Michigan, Ann Arbor, Michigan		2a. REPORT SECURITY CLASSIFICATION UNCLASSIFIED	
		2h. GROUP	
3 REPORT TITLE AN ESTIMATE OF THE CONFIGURATION OF THE SURFACE OF THE EARTH'S CORE FROM THE CONSIDERATION OF SURFACE FOCUS PcP TRAVEL TIMES			
4 DESCRIPTIVE NOTES <i>(Type of report and inclusive dates)</i> Scientific Final, Part 3			
5 AUTHOR(S) <i>(First name, middle initial, last name)</i> Charles G. Bufe			
6 REPORT DATE September 1970		7a. TOTAL NO OF PAGES xii + 99	7h. NO. OF REFS 43
8a. CONTRACT OR GRANT NO AF 49(638)-1759		9a. ORIGINATOR'S REPORT NUMBER(S) 8071-33-F ₂	
8b. PROJECT NO 8652		9b. OTHER REPORT NO(S) <i>(Any other numbers that may be assigned this report)</i> AFOSR-70-2392TR	
8c.			
8d.			
10 DISTRIBUTION STATEMENT This document has been approved for public release and sale; its distribution is unlimited.			
11 SUPPLEMENTARY NOTES TECH, OTHER		12 SPONSORING MILITARY ACTIVITY AF Office of Scientific Research (SRPG) 1400 Wilson Boulevard Arlington, Virginia 22209	
13 ABSTRACT Travel times of PcP and P phases from nuclear and high explosive sources are interpreted in terms of variations in the radius of the earth's outer core. This interpretation favors a core which is slightly larger and has less ellipticity than the Taggart-Engdahl reference model. Other interpretations in terms of lateral variation in mantle velocity are possible. Because of the geographic distribution of events and stations, only the northern hemisphere of the core is represented. A modified spherical harmonic analysis method is used to smooth the data and to estimate the shape of the core. The variation of core radius determined from this representation of data truncated at one standard deviation is approximately ± 10 kilometers on the basis of terms to degree and order 5. Variations in geoid height resulting from the inferred variations in core radius do not correlate with, but are of the same order of magnitude as, those determined from satellite observations. PcP amplitude/period shows little variation with epicentral distance. The PcP phase is generally shorter in apparent period than the P phase. This relationship is reversed, however, for arrivals from the Novaya Zemlya event of October 27, 1966. Ray tracing techniques are used to estimate the perturbation of the PcP-P time interval and PcP/P amplitude ratio produced by a hypothetical upper mantle low velocity zone of varying thickness.			

14 KEY WORDS	LINK A		LINK B		LINK C	
	ROLE	WT	ROLE	WT	ROLE	WT
PcP travel times Earth's core Spherical harmonic analysis Travel-time residuals Upper mantle velocity variations						